Stochastic Orebody Modelling and Stochastic Long-Term Production Scheduling for an Iron Ore Deposit, in Northern Quebec

By:

MARIA NATALIA VALLEJO GARCIA

Department of Mining and Materials Engineering,

McGill University, Montreal

December, 2016

A thesis submitted to McGill University as partial fulfillment of the requirements of the degree of Master of Engineering.

DEDICATION

I would like to dedicate this work to my parents, William Vallejo and Elda Lucia Garcia and to my brother Juan Pablo Vallejo.

Family is not defined only by last names or by blood; it is defined by **commitment** and by **love**. *God* blessed me with this beautiful and supportive family.

You are my rock, my compass, my lighthouse, and my north.

You are my beginning and my end.

All because of you and only for you, my only love, my family.

ACKNOWLEDGEMENTS

First of all, I would like to thank God for having me to enjoy his blessings and love during this beautiful experience.

I would like to thank my supervisor Dr. Roussos Dimitrakopoulos for welcoming me to the COSMO Laboratory, for his invaluable guidance and support during my master's degree.

Thanks to all the beautiful human beings who have accompanied me during my formation years, the one who have gone, the ones who remain, the ones to come.

Thanks to Mr. David Londoño, my angel on earth, his help, friendship and counsel are always an asset in my life.

I also would like to thank two amazing women and colleagues, Fernanda del Castillo and Amina Lamghari, I cannot imagine my life during these years without your immeasurable support, friendship and love.

Thanks to all my colleagues in COSMO Lab, for your help, patience and support during all this time; including Luis, Ashish, Adrien, Sean, Ilnur, Ryan, Ray, Denis, Tom, Linquing, Cosmin, Veronique, Amir Joao, Renaud, and Deborah; you were key parts of the process.

All this work could not have happened without the support of the COSMO Laboratory of McGill University, and the New Millennium Iron Corp (NML) for providing the data of the KéMag deposit and conceding the permission to use it in this thesis, especial thanks to Mr. Michael Spleit who collaborated with his technical assistance during this process.

The work in this thesis was funded from the National Science and Engineering Research Council of Canada (NSERC), Collaborative R&D Grant CRDPJ 411270-10 with AngloGold Ashanti, Barrick Gold, BHP Billiton, De Beers, Newmont Mining and Vale. This work was also funded from The Fonds de recherche du Québec – Nature et technologies (FRQNT), Fond FRQ-NT MI-181547.

CONTRIBUTION OF AUTHORS

The author of this thesis is the primary and sole author of this thesis.

Professor Roussos G. Dimitrakopoulos was the supervisor of the author's Masters of Engineering program and participated in the technical editing of all the related work and future publications.

ABSTRACT

The process of mine planning, from prospection of orebody deposits defining its extension, location and value, until obtaining minerals and their extraction sequence in time, requires mathematical optimization to determine the size and grade (grades) of the deposit and finally define a proper mine schedule to obtain the maximum earnings from it, at the lowest possible cost, in order to fulfill the business targets.

In general, a mining project passes through a set of stages in order to evaluate its viability. One of these stages is the "feasibility stage" where the gathered information from mining studies is used to determine the economics and practical aspects of the ore deposit. This identifies, early on, whether further investment in estimation and engineering studies are required, and identifies areas for further work and development.

The KéMag iron ore deposit owned by New Millennium Limited in northern Quebec, Canada, is in feasibility stage. The KéMag iron ore deposit is a taconite type, where the iron content is present as finely dispersed magnetite between 20 and 35 % iron (Fe) in a sedimentary rock interlayered with quartz, chert, and carbonate.

Traditional mine planning uses estimation methods to model orebodies, estimate reserves, and optimize the mine planning, and production schedule. The result is a single estimated orebody model which is an input to spatially model attributes of interest. Commonly, this process ignores the presence of geological uncertainty causing most of the mine plans and forecasts to be biased and unrealistic. In many instances, the profit expectations and mine production are not met causing financial depletion, loss of credibility, and risking the business itself.

In order to overcome the above-mentioned problems, geological uncertainty can be modeled, measured and managed through stochastic geological modelling to represent the uncertainty of the attributes of the orebody to quantify geological uncertainty by generating equally probable scenarios of the orebody (realizations).

This thesis focuses on a set of methodologies to develop a whole process of stochastic orebody modelling and stochastic strategic mine planning for the KéMag deposit, aiming to generate a

modelling and optimization methodology that integrates geological uncertainty and manages risk in the mine schedule. This mathematical framework has been successfully implemented in the last two decades allowing modelling and integration of geological uncertainty to mine design, production scheduling and valuation of mining projects. From the application, several cases have shown an increment on the value of the production schedules up to 25%, and a reduction of deviation from production targets from 9% to 0.2%.

Other case studies have also shown that stochastic pit limits can be about 15% larger adding then, 10% to Net Present Value in comparison with the conventional framework results, suggesting that through the use of strategic stochastic mine a better utilization of natural resources is also achieved.

For the KéMag deposit a set of fifteen realizations of nine lithological units (layers) were simulated using *WAVESIM* which is a multiple point simulation method combined to an image compression procedure to allow faster simulations. The orebody simulations obtained through *WAVESIM* serve as geological boundaries to integrate the variability of the four grades of interest using *DBMAFSIM* this method allows the simulation of correlated variables directly at block support using min/max autocorrelation factors MAF. The final result is a series of equally probable representations of the deposit that incorporate both grade and tonnage uncertainty. These simulations of the KéMag deposit were validated in terms of histograms, variograms (low order statistics) and high-order statistics through 3rd order cumulants maps for the boundary limits only.

Geological uncertainty can then, be managed by directly incorporating stochastic simulations within the mine scheduling framework. To achieve this, one flexible method for long-term production scheduling based on Stochastic Integer Programming (SIP) was applied with an acceleration methodology based on a heuristic algorithm called Topological Sort Algorithm (TSA) to reduce the computational time required to solve the problem of production scheduling. The result of the stochastic mine planning framework is a single schedule robust enough to account for geological uncertainty of the KéMag deposit giving valuable information for the conceptual stage of the project, in terms of silica content, iron production and expected cash flows per year.

RÉSUMÉ

La planification minière est une procédure divisée entre la prospection du minerai, son obtention et sa séquence d'extraction. Elle requiert une optimisation mathématique pour déterminer la taille et la teneur de minerai dans un gisement, et aussi pour définir un plan d'extraction qui maximise les revenus et minimise les couts dans le but de satisfaire au mieux les cibles économiques.

Généralement, un projet minier doit passer à travers d'une série d'étapes pour évaluer sa viabilité. Une de ces étapes est celle de préfaisabilité. À ce moment, l'information accumulée est utilisée pour déterminer la praticabilité et les retours économiques du gisement minier. Ceci permet d'identifier, aussitôt, les lieux possibles de développement, et si des investissements supplémentaires sont nécessaires pour effectuer des estimations et des études techniques.

Le gisement de fer KéMag appartenant à New Millennium Ltd dans le nord du Québec au Canada est à une étape de préfaisabilité. Le gisement de fer KéMag est de type taconite. La taconite est un fer qui se présente sous forme de magnétite finement dispersée entre 20 et 35% dans une roche sédimentaire entrelacé de quartz, de chert et de carbonate.

La planification minière traditionnelle utilise des méthodes d'estimation pour modéliser les gisements miniers, estimer les réserves et optimiser la planification et le calendrier de production. Le résultat est un modèle unique du gisement minier qui sert d'entrée pour un cadre technique servant à modéliser spatialement les attributs d'intérêt. Fréquemment, cette procédure ignore la présence d'incertitude géologique rendant la plupart des plans d'extraction et des prédictions peu réalistes et partiellement biaisés. Dans plusieurs cas, les attentes en termes de production et de profit monétaire ne sont pas remplies causant un épuisement financier et une perte de crédibilité en plus de risquer la survie de l'entreprise.

Dans le but d'atténuer les risques mentionnés précédemment, l'incertitude géologique peut être modélisée, mesurée et contrôlée à travers des méthodes stochastiques géostatistiques pour représenter l'incertitude des attributs du gisement minier. Ainsi, il est possible de quantifier l'incertitude géologique en générant des scénarios équiprobables des gisements miniers (réalisations). Cette thèse explore une série de méthodes pour développer un modèle stochastique du gisement minier et de planification minière spécifiquement pour le gisement KéMag.

L'approche vise à générer une stratégie de modélisation et d'optimisation qui intègre l'incertitude géologique et la gestion du risque dans la planification minière. Ce cadre mathématique a déjà été implémenté avec succès dans les deux dernières décennies permettant la modélisation et l'intégration de l'incertitude géologique au design de mines, à la coordination de la production et à l'évaluation de projets miniers. Par son application, plusieurs cas ont montré une augmentation de la valeur de leur calendrier de production par 25% et une réduction de l'écart par rapport à leur cible de production entre 0.2 et 9%.

Des études de cas démontrent que les contours finaux stochastiques des mines à ciel ouvert pourraient être 15% plus langé menant à une augmentation de 10% de leur valeur actuelle nette comparativement à ce qui est prédit par les résultats des approches conventionnelles. Cette constatation démontre une utilisation plus efficace des ressources naturelles par l'emploi d'une approche stochastique de planification minière.

Pour le gisement minier de KéMag, une série de quinze réalisations (gisements miniers) de neuf unités (couches) lithologiques a été simulé en utilisant la méthode *WAVESIM*. *WAVESIM* est une méthode de simulation à points multiples combinée à une procédure de compression d'image permettant une accélération des simulations. Les simulations de gisement minier obtenu par *WAVESIM* servent de frontières géologiques pour l'intégration de la variabilité des quatre éléments d'intérêt à partir de *DBMAFSIM*, une méthode permet la simulation de variables corrélées directement au support de block en utilisant des facteurs min/max d'autocorrélation(MAF).

Le résultat final est une série de représentations équiprobable du gisement minier incluant les incertitudes reliées à la teneur de minerai et au tonnage. Ces simulations du gisement minier de KéMag ont été validées à l'aide d'histogrammes, de variogrammes (statistiques d'ordre inférieur) et de statistiques d'ordre supérieur à partir de cartes de cumulants d'ordre 3 pour les limites aux frontières.

L'incertitude géologique peut être contrôlée en incluant directement des simulations stochastiques au sein du cadre de planification minière. Pour ce faire, une méthode flexible pour la planification de la production à long-terme basée sur la programmation stochastique en nombres entiers (*Stochastic Integer Programming* (SIP)) a été appliquée avec une méthode d'accélération

heuristique appelée *Topological Sort Algorithm* (TSA) pour réduire le temps de calcul de la solution. Le résultat du cadre de planification minier stochastique est une unique cédule assez robuste pour prendre en considération l'incertitude géologique du gisement KéMag. De plus, d'importantes informations pour l'étape de conception du projet sont fournies, incluant le contenu en silicium, la production de fer et les revenus annuels attendus.

TABLE OF CONTENTS

LIST OF FIGURES

CHAPTER 1

INTRODUCTION

1.1 Overview

Advanced computational technologies and data processing has been used in the mining industry for more than three decades to model and optimize mineral resources, in a framework known as "mine planning". Mine planning is crucial to optimize mine designs and production scheduling aiming to maximize the economic value of the mining assets from prospection and exploration until the mine closure.

Traditionally, mine planning optimizes mine design and production schedule using a single deterministic representation of geological model as input. This representation is considered a smooth representation of the reality, which is generally generated using geostatistical estimation methods, defining the value of a block as an average of all possible grades in different locations of the deposit taken separately.

Conventional mine planning considers the economic valuation of a mined block as a linear function that is usually calculated prior to the mine optimization in order to define ore and waste blocks. Moreover, these optimization methods are based on a single deterministic orebody model which can produce misleading results because it does not account for the likely deviation from the model in reality.

In the last decade, new methodologies and algorithms have been developed to overcome the shortcomings of the conventional mine planning framework. These new methodologies enable the explicit management of the uncertainty, through a conditional simulation orebody modelling to produce a set of equally probable orebody representations (simulations) that denotes the distribution and spatial correlations of the attributes of interest.

With the development of simulation methods, the impact of geological uncertainty in ore reserve calculations, ultimate pit definition and production scheduling can be readily measured and managed through a set of equally probable simulations. This set of simulations is used as input for

the mining optimization. This procedure is developed to not only maximizing the NPV of the mine, but also minimizing deviations from production targets. These goals are achieved by incorporating grade uncertain into the mine production schedule formulation in the form of stochastic mine planning and production scheduling.

1.2 Goals and objectives

Integrating uncertainty into mine design and production scheduling is a recent framework that has consistently demonstrated the ability to not only reduce the levels of risk of not meeting production targets, but also increases the economic value of the mining operation.

The goal of this thesis is to show a complete stochastic orebody modelling and to develop a stochastic mine production schedule for an iron deposit. To demonstrate the applicability of these novel methodologies for mine optimization while integrating uncertainty, using exactly the same input data (e.g. drillholes) as the conventional modelling and mine planning framework. By integrating geological uncertainty directly in the mine planning process, it is, possible to manage the risk related to the various products and elements in the mine production scheduling.

In order to achieve this goal, the related objectives are outlined as follows:

i. Review traditional deterministic or conventional mine planning frameworks, as well as stochastic mine planning frameworks, and outline their inherent limitations and applicability in the mining industry.
ii. Review the literature on geostatistical simulations, from two-point based methodologies to newer approaches such as high-order simulation methods.
iii. Review the literature on mine production scheduling, from simple mixed integer programing problems, to stochastic integer programing adapted to optimize mining complexes.
iv. Apply the stochastic mine planning framework to the KéMag iron ore deposit in northern Quebec by:
    a. Modelling the iron ore deposit, firstly using multiple point simulation methods to simulate boundaries and volume uncertainty (lithologies) and then jointly-simulate directly at block support a set of correlated variables (grades).

b. Then, making use of the set of orebody simulations obtained in a), obtain a stochastic long-term production schedule applying a heuristic algorithm to solve the stochastic integer program model of the mine production scheduling problem.

v. Draw conclusions from the study and recommendations for future work.

1.3 Thesis outline

This thesis is organized according to the following chapters:

Chapter 1: Introduction, goals, objectives and outline of this thesis.

Chapter 2: Compilation and review of technical literature to the state of the art related to stochastic orebody modelling and stochastic mine planning.

Chapter 3: Description of the methodologies applied for i) stochastic orebody modelling using *WAVESIM* and *DBMAFSIM,* and ii) for stochastic mine planning of an iron deposit with an SIP formulation. All this aiming for the stochastic optimization of a multi-element, life-of-mine production schedule solved in conjunction with a heuristic algorithm to minimize risk of deviation from production targets and to maximize the expected discounted cash flows of the mine.

Chapter 4: Application of the methods descripted in Chapter 4 to the KéMag iron ore deposit in northern Quebec.

Chapter 5: Conclusions and future work

CHAPTER 2

LITERATURE REVIEW

2.1 Introduction

Mining is a production activity related to the extraction of valuable minerals from the earth (orebody, deposit). In general, an orebody is any single mineral or combination of minerals occurring in a mass, or deposit, of economic interest (CRIRSCO definitions, 2013).The economic valuation of orebodies is affected by factors such as geological uncertainty, mining and transporting methods, market price fluctuations, environmental factors among others. Mining companies require technologically advanced tools and methodologies to increase profits, improve mining methods, and enhance the use of the natural resources/reserves to meet the economic expectations of the stakeholders.

Generally, the process of orebody modelling ignores the presence of geological uncertainty causing most of the mine plans and forecasts to be unrealistic. In many instances, the expectations in terms of profit and mine production are not met causing financial depletion, loss of credibility, among other factors risking the business itself. These unwanted factors, happen because mine planning process is based on inputs with an inherent uncertainty; one of the key risks in a mining project is geological uncertainty.

Traditional mine planning is a step-wise framework that uses estimation methods to model orebodies. The result of these estimation techniques is a single model consisting of the expected mineral content for a block of material in the deposit which is a smooth representation of the reality given the average-weight nature of the estimation process. This grade averaging produces an unfavourable effect called “smoothing effect” (Dimitrakopoulos, 1988). Smoothing effect is present in any estimated orebody model, as it is in the case of a Kriged model, where geological uncertainty is not taken into account.

The technical literature (Godoy, 2003; Ramazan and Dimitrakopoulos, 2007; Menabde *et al*., 2007; Leite and Dimitrakopoulos, 2007; Albor and Dimitrakopoulos, 2010) has shown that the risk of not meeting production targets and expected Net Present Value ((NPV) - financial indicator)

is increased due the smoothing effect of commonly used estimation methods on a non-linear transfer function. Thus, a single estimated model as representation of the deposit does not provide means for decision making in a robust way, as is required for optimization models for mine planning. Therefore, the integration of the uncertainty into the mine planning process is required.

It is important to mention that majority of the available optimization models for mine production scheduling are linear formulations that use a single estimated model and a fixed destination criterion based in the material content. The economic valuation of mineral deposits is a non-linear transfer function. However, conventional frameworks calculate the economic value of a block of material as a linear function to classify a block either ore or waste. This classification is done before the optimization. The most common criteria used in the mining industry is the so-called cut-off grade (COG). In general, a cut-off grade is defined as the minimum amount of valuable material that one metric ton of material must contain before this material is sent to the processing plant (Rendu, 2013).

Geological uncertainty can be modeled, measured and managed and quantified through stochastic geostatistical methods. This is achieved by generating equally probable scenarios of the orebody (realizations).These scenarios are key to a better understanding of geological characteristics of ore deposits. Risk can be quantified through the integration of uncertainty into the decision-making. This yields a mine design and production schedule with higher value and better risk management. Risk management ensures that the mining operation is capable of meeting production targets over time. (Leite, 2008, 2014; Dimitrakopulos, 2011).

The availability of uncertainty modelling techniques leads to the development of new scheduling approaches integrating the modelled geological uncertainty into the mine planning process. This concept is expanded to even more general overview of the mining business when integrating global optimization of mining complexes. For this optimization important factors such as blending requirements, different processing streams, transportation systems, and product sales are included into the optimization simultaneously. (Whittle, 2010; Montiel and Dimitrakopoulos, 2014; Goodfellow and Dimitrakopoulos, 2014a).

2.2 Overview of strategic mine planning under uncertainty

It is inarguable that there are many sources of uncertainty when dealing with orebody modelling and mine planning. However, among all of them geological uncertainty is seen as the main reason why mining projects do not meet their expectations (Vallee, 2000; Baker and Giacomo, 2001; Dimitrakopulos *et al*., 2002; Ramazan and Dimitrakopulos, 2004). The use of conditional simulation to generate orebody models, which can further be used to analyse risk in mining projects was firsts proposed by Ravenscroft (1992). In his work, the application of a probabilistic assessment of geological uncertainty in production scheduling uses a set of stochastic simulations. In this method, a production schedule is evaluated separately for each scenario, which provides a range of values for the quantities and qualities of mined material in each period. The methodology provides a better understanding of the production scheduling but does not include ore variability into the production scheduling optimization.

Based on Ravenscroft's approach, Dimitrakopoulos *et al*. (2002) tested the performance of a conventional production schedule by evaluating the schedules obtained for a set of 50 stochastic simulations. The results showed that the annual mine production for the given "optimal" production schedule was different for each one of the 50 simulations, creating a range of possible cash flows with only 20% of them meeting the expectations of the estimated NPV. There was also a 95% probability of the project to return a lower NPV than the predicted using the estimated orebody model. These results show that there is a low probability of the single estimation of being accurate. This methodology is recognized as a risk analysis of the estimated expectations of the project but it does not manage the risk itself.

Later, some methods to implement strategic mine planning with stochastic schedule were developed to include a set of equally probable scenarios of the orebody as input for the optimization. The goal is not only maximizing the NPV of the project, but also minimizing deviations from production targets. These goals are achieved by incorporating grade uncertainty into the mine production schedule formulation. For example, Godoy and Dimitrakopoulos (2004) obtain promising results. Herein, the authors proposed a novel optimization approach to effectively integrate grade uncertainty into the optimization of long-term production scheduling in open pit

mines using a combinatorial optimization technique called "simulated annealing" proposed by Gemand and Gemand (1984) and based on the Metropolis (1953) algorithm.

To generate a final optimal schedule using simulated annealing, a suboptimal configuration (i.e. an initial mine sequence) is continuously perturbed until it matches some pre-defined characteristics as coded into an objective function (Kirkpatrick *et al*., 1983). In mine planning, the objective function is usually a measure of the difference between the desired ore and waste production and those of a candidate mining sequence. Each perturbation is accepted or rejected based on whether it improves or not the value of the objective function.

The approach by Godoy and Dimitrakopoulos (2004) was applied in a gold deposit and it returned a schedule with a NPV increment of 28% in comparison with the obtained using the traditional scheduling approach where grade uncertainty is not taken into account. The same study also shows that the stochastic approach leads to substantially reducing the project risk by lowering potential deviation from production targets in the order of 13%.

A key contributor to these improvements is that the stochastic (risk-integrating) approach can discriminate the "upside potential" of the metal content and hence distinguish economic value of a mining block from its "downside risk". This idea led Dimitrakopoulos *et al*., (2007) to introduce a more systematic approach to selecting an open pit mine design amongst a set of designs. This is done by a quantification of the upside potential and the downside risk for key project performance indicators, such as the periodical discounted cash flow and the amount of ore tonnes and metal production. In this work, the reference point that defines upside versus downside potential is the Minimum Acceptable Return (MAR) of the investment, which usually differs from the "expected value" also known as "average value".

The same year, Leite and Dimitrakopoulos (2007) implemented Godoy's methodology in a copper deposit. The stochastic approach generated a Life of Mine (LOM) schedule with a 26% higher NPV than the conventional schedule, also, in concordance with Godoy's findings the risk analysis showed that the stochastic schedule has low chances to deviate from production targets. Leite's work at that time did not include the definition of pit limits nor optimization of pushbacks in the proposed stochastic optimization approach. Then, to include uncertainty in the selection of the

ultimate pit, Albor (2009) extended Godoy's work to the inclusion of an optimization for pit limits. One of the most important findings, after the application of this extension in a copper deposit, was that a set of only ten (10) schedules was needed in order to meet production targets. However, more than ten did not add any benefit.

In his work, Albor (2009) also found that selecting a different ultimate pit from the available pit shells and using simulated annealing to schedule the material resulted in a 10% higher NPV in comparison with the NPV obtained from the optimized schedule for conventional pit limits. Thanks to these results it was confirmed that stochastic pit limits are larger than the ones obtained through conventional optimization. Explicitly in this case the stochastically optimized pit limits shown to be 17% larger in total tonnage. This means that the stochastic scheduling process can return mine schedules that can retrieve more metal, hence more value from the same orebody, improving the utilization of the mineral resource.

The successful application of these approaches and other cases were summarized by Dimitrakopulos (2011). Here, the author recaps ten years of research in the integration of two elements: stochastic simulation and stochastic optimization. These elements provide an extended mathematical framework that allows modelling and direct integration of orebody uncertainty to mine design, production planning, and valuation of mining projects and operations.

Stochastic mine planning workflow is graphically represented in Figure 1. It shows that, instead of a single orebody model as an input to the optimization for mine design and an assessment of individual key project indicators, a set of equally probable models of the deposit can be used. These orebody models are conditional to the same available data and their statistical characteristics are constrained to reproduce all available information, and represent equally probable models of the actual and unknown spatial distribution of the elements of interest.

Godoy and Dimitrakopoulos (2011) present a framework for geological risk analysis that quantifies the impact of grade uncertainty in four different cases to show the availability of multiple equally probable models of a deposit enables the mine planning process to assess the sensitivity of pit design and long-term production scheduling. The results are mine sequences with

substantially higher NPV, larger pit limits, and longer LOM with more ore material. But the problem related to the a-priori destination policy of where to send a block remains.

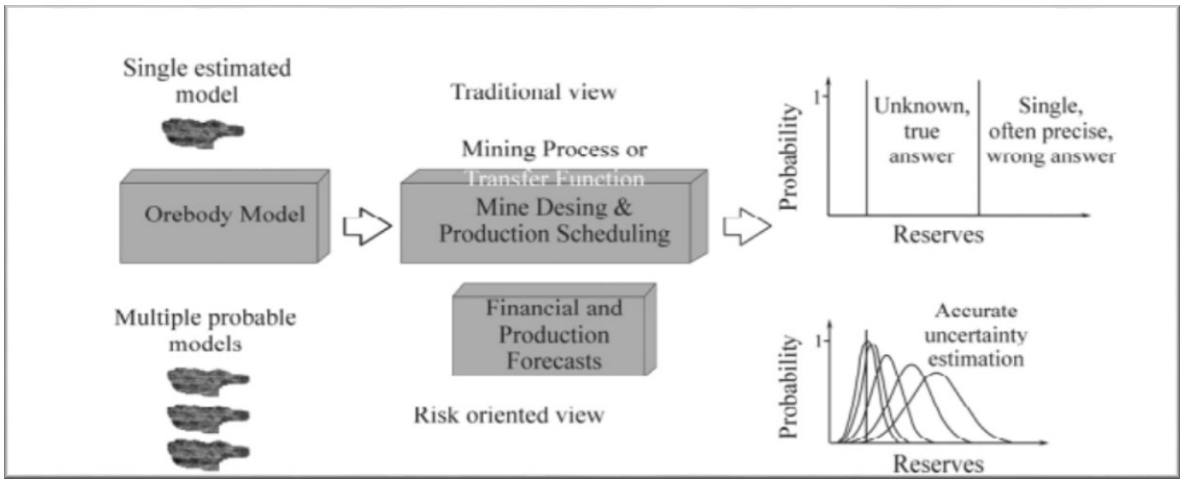

Figure 1. Traditional (deterministic or single model) view and practice versus risk-integrating (stochastic) approach to mine modelling, from reserves to production planning and life-of-mine scheduling, and assessment of key project indicators. (Dimitrakopulos, 2011).

The formulations previously mentioned, assume a classification of ore and waste material using a cut-off grade (COG) policy. COG introduced by Lane (1988) is one of the most popular types of destination policies in the mining industry, herein the decision of where to send a block after being extracted is decided based on the metal content (grade) being above or below a threshold. COG is usually calculated by comparing cost and benefits, where a single parameter such as minimum metal content, is sufficient to define the cut-off grade (Rendu, 2013).

By specifying the destination of the material a priori, this fixed ore-waste classification can result in low-grade material sent for processing first, thus deferring, the processing of higher-grade ore that may be readily available. Moreover, these models ignore the impact that the aggregate of blocks have on the mining capacity and in the production constraints that are imposed in the processing streams of the mining complex.

Then, moving forward with the advances in stochastic mine production scheduling the models developed over the last years are often oversimplified. These formulations are designed to optimize

a single mine with a single output production stream (e.g. mill, crusher). Consequently, when a mine complex is considered, those methods are limited to provide only local optimum results. Then, a more global approach was introduced (Goodfellow and Dimitrakopoulos, 2013, 2014a, 2014b; Montiel and Dimitrakopoulos 2014). The idea is then have the optimization guided to optimize entire mining complexes. This means considering not only mining and production scheduling, but also all the activities constituting a mining operation; including blending, several processing streams, transportation, product manufacture and sales, to maximize the economic value over the life of a resource (mineral, material) in the supply chain.

Past attempts for global asset optimization have been studied (Whittle, 2007; Whittle, 2009). This optimization aims to optimize mining supply chains, starting with the decisions of what material extract from different mines in a given period and how efficiently use the resources of the supply chain to maximize the value of the extracted material. This approach ignores the inherent effect that geological uncertainty has on the product value and on the operational feasibility of the supply chain. In this approach the optimization of when (production period) and where (location), extract certain material and how to maximize its value is performed independently. The optimization is performed separately because solving them jointly often exceeds the capabilities of the currently available mining tools (Whittle, 2010).Therefore, when a mining complex is considered the obtained results applying this approach are sub-optimal solutions for the supply chain.

Stochastic mine planning frameworks are useful tools when optimizing complex supply chains because it allows the dynamic evaluation (simulation) of the impact that a set of decisions have on a mining complex, finally, it attempts to improve these decisions through the use of a stochastic optimizer. Montiel and Dimitrakopoulos (2013) presented a heuristic method which is an approach to problem solving that employs a practical mathematical methodology that cannot guarantee optimal or perfect solutions, but is usually sufficient for the immediate goals. The authors applied a heuristic algorithm in the solution of the stochastic integer programming to generate mine production schedules accounting for multiple metals or attributes, multiple rock types, stockpiles and processing options (operating modes) for a single mine.

The methodology mentioned above, was applied to a copper deposit. The study showed a reduction of the deviations from production targets from 9% to 0.2% while increasing the expected NPV by

30% when compared with the obtained using conventional methods. In this work, the authors also proved in coherence with Albor's (2009) work, that there are not significant additional benefits from increasing the number of simulations used in the optimizer after 10 simulations.

When more than a single mine is required to be optimized (e.g. multi-pit optimization) the problem becomes large in size and exigent in terms of computational requirements. To overcome this, Goodfellow and Dimitrakopoulos (2014a) proposed a two-stage stochastic mining complex optimization model that can accommodate non-linear aspects of the supply chain and also does not require simplifying assumptions to generate high-quality solutions. The first stage of the optimization decides the production schedules for the mines along with the destination policies. In the second the processing stream decisions resolve how to best use the processing streams and destinations in order to maximize the value of the material that has been extracted. The authors applied a hybrid metaheuristic comprised of particle swarm optimization and a modified simulated annealing optimizer, in a fashion that the particle swarm optimizes the destination policies and processing streams and the simulated annealing optimizes the long-term production schedule and processing stream flow. Goodfellow and Dimitrakopoulos (2014a) tested this methodology on a copper-gold mining complex and experimental results showed that a maximum of 3.5% reduction in risk of not meeting production targets is obtained while returning a 14.2% higher NPV in comparison with the conventional solution.

Later, Montiel and Dimitrakopoulos (2015) presented a mining complex optimization approach to include in the optimization different features such as, multi pits, several material types, stockpiles, process destinations, various operating configurations of the metallurgical plant, transportation systems, and final products. This approach uses a heuristic algorithm based on simulated annealing where an initial scheduling solution is fed into a three-stage hierarchy perturbation cycles. In the outermost cycle, perturbations occur on the block scale, modifying the periods and destinations of each block. In the second level, perturbations to the operational alternatives at each given destination are made. In the third level, perturbations are made to the proportion of output material transported using the available transportation systems.

The implementation of Montiel's method in a multi-pit copper operation allowed the reduction of the average deviations from production targets from 18% to 1%. Although NPV forecasts for the

base case obtained through conventional methods are not considered meaningful given its large deviations from capacities and blending targets, the solution generated by implementing this method generates an increase of 5% of the project's NPV, showing the ability of the method to generate a higher NPV with less risk.

Optimization of mining complexes demonstrates that when incorporating geological uncertainty the solutions generated outperform solutions obtained using conventional deterministic approaches, which consider a single smooth representation of a deposit. These models return a mine schedule as a solution and destination policies that are robust enough to account for geological uncertainty, avoiding the use of a-priori cut-off grade policies. Also, optimization of mining complexes define the sequence of extraction of the mining blocks in different pits, and transportation systems used to transport the processed material to their final destinations.

After this overview of strategic stochastic mine planning, the following sections describe the literature review first for the stochastic orebody modelling (Section 2.3) and then for the stochastic mine planning (Section 2.4). These elements provide a framework that allows modelling and direct integration of orebody uncertainty to mine design.

2.3 Stochastic orebody simulation

Simulation of spatially correlated categorical and continuous variables as rock types and metal grades of mineral deposits respectively is a challenging task. The optimization of entire mining complexes demonstrates the importance of modelling geological uncertainty. Spatial uncertainty is typically modeled by generating multiple realizations (scenarios) of a given attribute through a process known as geostatistical simulation. In orebody modelling, the location and the connectivity of the material grades, especially the high ones, must be well understood to perform a successful mine optimization and scheduling. This is possible through geostatistical simulation.

2.3.1 Two point simulation methods

The traditional geostatistical framework relies on two-point statistics in the form of a covariance or a variogram model to model orebodies. (Journel, 1974; David, 1977; David, 1988 ; Goovaerts, 1997). Two-point statistics, namely the variograms, are an important structural

parameter but does not contain all the structural information of the random function model. Therefore, second-order spatial statistical techniques are not enough to model some complex structures in mineral deposits as curvilinear geometries, typical in mineral deposits. It means that these methods are limited in their ability to describe connectivity and incorporate complex shapes or geometries that are inherent to mineral deposits (Journel, 2007).

Two-point geostatistical simulation relies on the sequential simulation framework proposed by Rosenblatt (1952) and Kolmogorov (1956). In this approach, for each node to be simulated, a Conditional Cumulative Probability Function (*ccdf*) has to be generated considering the initial hard data set (e.g. drillhole database) and previously simulated nodes.

To do that the simplest case of sequential simulation follows the following steps:

1. Define a random path to visit the nodes to be simulated in a defined grid.

2. Generate a *ccdf* for a given node.

3. Draw a value from the *ccdf* in step 2. (Since the *ccdf* can be generated for all the nodes in the grid, one at a time, it is possible to randomly draw a value for each of them)

4. Include the draw value (simulated node) as conditional data.

5. Repeat step 2, 3, 4 until all nodes in the grid are simulated.

6. Repeat steps 1 to 5 to generate more realizations.

Two of the most used geostatistical simulations techniques are Sequential Gaussian Simulation (SGS) (Goovaerts, 1997; Isaaks, 1990) and Sequential Indicator Simulation (SIS) (Journel, 1989; Journel, 1994). SGS is a commonly used method requiring the *ccdf* to follow a Gaussian distribution. To achieve this, the initial data is transformed to standard normal scores. The mean and variance is estimated using Kriging. With these two parameters, the normal distribution is built to define the *ccdf* for any given node. The simulation is complete when all nodes are simulated, then the simulated values are back-transformed to the original data space.

An equivalent method to SGS is the simulation through Lower-Upper (LU) decomposition (Davis, 1987). The method also follows a Gaussian distribution, both methods require computation of a covariance matrix, which depending on the size of the data, can be difficult to process in terms of computational requirements. In LU decomposition, the covariance matrix is decomposed in lower and upper triangular matrices using the so-called Cholesky decomposition. Afterwards, the realizations are generated by multiplying the lower triangular matrix with a vector of independent and normally distributed random numbers. In LU decomposition, each row of the resulting vector corresponds to one node in the simulation grid. Thus, if LU is implemented row by row the method is equivalent to the SGS.

To overcome the computational requirements problems of SGS and LU decomposition Dimitrakopoulos and Luo (2004) proposed a Generalized Sequential Gaussian Simulation (GSGS) which is conceived as a hybrid of both methods stated above. GSGS preforms the simulation grouping nodes and simulating the groups through LU instead than simulating node by node as is in SGS. In this method, the random path is defined to visit a group of nodes at a time giving flexibility to deal with large grids in a more efficient way.

Given that the natural distribution of geological data is unknown, the mentioned methods above suppose that the data follows a Gaussian distribution. To deal with this assumption, the Sequential Indicator Simulation SIS generates a *ccdf* by defining a set of threshold values using Indicator Kriging. In general, the simulations obtained through SIS rely on strict stationary assumptions and reproduce well the continuity of extreme values (that is, high grades- or-low grades). This is extremely important because high grades drive the profitability of mining projects, it guides the mining sequence in a process colloquially known as “high-grading” (Whittle and Rozman, 1991). Finally, SIS has as drawbacks the fact that is computationally extensive and that is challenging in the requirement of the interpretation of variograms at high cut offs.

All these methods mentioned above have an additional complication related to the output files of the simulations. The simulations are generated at a point support but mine planning tasks such as resources assessment, pit optimization, and production scheduling are done at a block support, requiring the output of the simulations to be averaged to fit the block sizes. The block size is usually related to the Selective Mining Unit (SMU) (Switzer and Parker, 1975). This reblocking

process implies the approximation of the block values by a linear average of the contained point values. When the point-block relation is linear, as in the case of metal grades in a mineral deposit, the procedure is simple and does not require any prior assumption about the distribution of the block values. In general, this process works well when the process is performed over a single representation of the deposit. However, as was mentioned before, risk assessment applications call for the use of multiple equally probable realizations. Thus, under these circumstances, the computational performance in terms of processing time and storage becomes a limiting factor.

Aiming to solve these limitations, Godoy (2002) introduced a simulation method which generates realizations directly at a block support. The method termed *DBSIM* works as similar as *GSGS*, herein a group of nodes is simulated using LU; then those nodes are averaged to obtain the value for the determined block size, and after the averaging process the nodes values are discarded, keeping only the block values as results of the simulation and stored for further conditioning. The method leads to substantial gains in computational efficiency that makes it suitable for simulating very large grids with up to 10^8 nodes (Godoy 2003).

To compare the efficiency of the method, Benndorf and Dimitrakopoulos (2007) performed a study between *GSGS* and *DBSIM* in a simulation of a single variable. The former took 7% less time than *GSGS* to run, and only required 1% of the computer memory when compared with *GSGS*. Regardless the successful application of *DBSIM*, the methodology is limited to simulate only a single variable. Then, a method to simulate a set of multiple correlated variables a framework accounting for keeping the spatial correlation is required. To jointly simulate a set of multiple spatially correlated continuous variables, a viable alternative to co-simulation frameworks is to transform the initial set of spatially correlated attributes into a new set of uncorrelated (orthogonal) factors. These factors are independently modelled and simulated, and finally back-transformed to the original space of the multivariate dataset, aiming the reproduction of their cross correlations.

Factor decorrelation was first introduced in multivariate geostatistics through a strategy based on Principal Component Analysis (PCA) (David, 1988). Although this methodology is simple, it can only guarantee that the factors are uncorrelated at lag (distance) zero.

Aiming to find factors that are uncorrelated not only for lag zero but also at any other distance. Desbarats and Dimitrakopoulos (2000) introduced Minimum/Maximum Autocorrelation Factors (MAF) (Switzer and Green, 1984) for geostatistical simulations, relying on the linear model of corregionalization (LMC) for the multivariate random field. Then, MAF is able to provide a set of factors uncorrelated at any lag. The efficiency of joint-simulation with MAF is enhanced when the simulations are done directly on a block support scale.

Then, Boucher and Dimitrakopoulos (2009) introduced the concept of MAF combined with *DBSIM* for geostatistical simulations. The methodology transforms a set of correlated variables into uncorrelated factors which can be independently simulated and then back transformed preserving the original correlation of the data. The algorithm termed *DBMAFSIM* was successfully applied by Boucher and Dimitrakopoulos (2012) in an iron ore deposit in Western Australia. The authors demonstrate that the method is practical and able to reproduce the spatial correlations between multiple elements, the method also minimizes the information stored by retaining only the block values, a procedure that significantly speeds up the simulation process while reducing the size of the output files and requirements of memory allocation.

One of the advantages of *DBMAFSIM* is that it overcomes the lack of preservation of extreme values connectivity because the approach does not require a reblocking post-processing. The simultaneous simulation of internal points of each block preserves the connectivity better than point-by-point approaches which usually uses a path to randomly visiting internal nodes at random way generating then poor relations of extreme values. Therefore, approaches such as *DBMAFSIM* provides a substantial advantage because the connectivity of high-valued blocks is important for the mine planning and production scheduling (Godoy, 2004). The application of *DBMAFSIM* in mineral deposits has shown to work well in reproducing the statistical, spatial continuity and cross continuity of multiple correlated variables as is presented in several studies (Lopez *et al*., 2011; Goodfellow *et al*., 2012; de Freitas and Dimitrakopoulos, 2014).

Simulation of spatially correlated continuous and categorical variables as rock types and metal grades of mineral deposits is a challenging task. Limitations of variogram-based simulation methods as the mentioned in this literature review are discussed in Journel (2005) and Journel (2007). Curvilinear geometries, typical in mineral deposits are not properly modelled through these

methods. Two-point statistics methods are not enough to model some crucial features inherent to mineral deposits, such as non-linear relations and spatial connectivity of extreme values. An example of the mentioned limitations is presented in Figure 2. From there it can be seen that structures with very different spatial patterns can share very similar variograms, despite having different levels of connectivity.

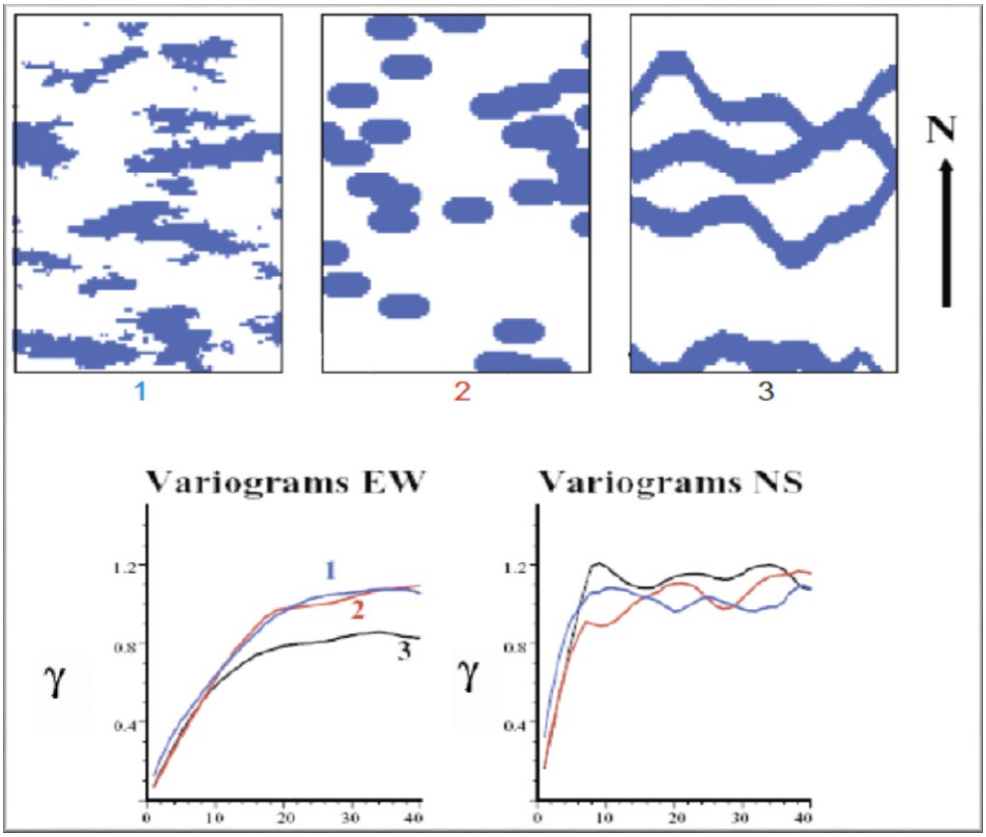

Figure 2. Different patterns, same variograms (Journel, 2007).

2.3.2 Multiple point simulation methods

To address the limitations of two-point statistical techniques Journel (1989) and Guardiano and Srivastava (1993) introduced in the form of multiple point models, the so-called high-order spatial statistics for geostatistical studies. High-order statistics are functions that use the third or higher statistically power of a sample to capture high-order relations between points from an image. This image, known as Training Image (TI), is a depction of a database of geological

patterns, from which high-order statistics, including the variogram, can be borrowed. For geostatistical simulation, high-order statistics are used to generate Multiple Point Simulations (MPS)

As a first approach, Guardiano and Srivastava (1993) incorporated this concept in an algorithm called *ENESIM*. In this approach, for each node to be simulated the method retrieves a conditioning neighbourhood considering multiple points at a once including hard data and previously simulated nodes. This methodology forces the whole TI to be scanned every time a node is simulated, requiring then potent computational resources. Because of this situation the methodology remained impractical for many years until Strebelle (2002) came up with the idea of computing the conditional probabilities before performing the simulation instead of scanning the whole TI for each conditioning data event. This new approach called *SNESIM* was also improved by the idea of storing all probabilities from the TI as conditional cumulative distribution function (*ccdf*) of the patterns conforming the TI in a search-tree structure. This idea allows fast retrieval of all required conditional probabilities. Therefore, the computational requirements are less demanding than in *ENESIM* but still big enough to be hard to implement. The main disadvantage of the *SNESIM* is that the method searches for an exact match of the conditioning data event with the TI. Consequently, when the probability of a data event is not found in the search-tree, the furthest node is dropped incurring in a loss of conditioning information. Due to this the method requires a training image that is large and sufficient enough to contain the majority of possible conditioning data events that could be found during simulation.

To take advantage of new computer technologies, Huang and Lu (2013) and Strebelle (2014), implemented a parallel implementation of SNESIM. However, for large three-dimensional TI with intricate patterns, the improved methodology requires large storage memory. To overcome this problem, simulation with patterns *SIMPAT* (Arpat and Caers, 2007) was introduced. The algorithm does not search for an exact match in the pattern database, but it rather searches for the best possible match to the conditioning data event. *SIMPAT*'s major limitation is that the entire pattern database has to be searched to find the best match at each simulating node. Therefore, the computational time is extensively high.

Zhang *et al*. (2006) proposes an algorithm to treat the TI as a collection of patterns, right before the simulation is performed. The pattern geometry is then, defined by a template (T) containing a set nodes describing the information in the so-called "pattern database". This algorithm is called *FILTERSIM* (Zhang *et al*., 2006; Wu *et al*., 2008) and treat the patterns of the database by a series of filters to obtain filter scores value. These values are then grouped into classes by means of a similarity criterion regarding their filter scores (e.g., k-means clustering). Then, the classes are represented by their prototype which is the average value of all patterns in a class and afterwards during the simulation the conditioning data event is compared with the class prototypes to find the closest matched class. One of the downsides of the methodology is the dependence on linear filters to perform the pattern classification. Different geological domains require the usage of different filters, because the filters to apply should be related to the structures and geometries of the patterns. Therefore, finding the right filters to use is not an arbitrary task. In the other hand, one of the major problems of *FILTERSIM* as other MPS methods is that a pattern is drawn randomly from a class; no conditional cumulative distribution function is generated for each class like *SNESIM* does. Therefore, the pattern obtained from a "best match" class is randomly selected and not statistics are involved in it.

Following the idea of *FILTERSIM* and to reduce the size of the pattern database and accelerate the pattern searching for the best matching with a data event, a method called *WAVESIM* based on wavelet analysis and pattern recognition was proposed by Chatterjee *et.al* (2012). The methodology works as similar to other MPSs. First, a complete image that represents the geometrical/geological features of the physical properties of interest are considered in the TI. The TI is scanned with a template to generate a pattern database. Then, the obtained database has its dimension reduced by applying a discrete wavelet transformation to obtain the approximate sub-band image of the patterns and the related sub-band coefficients. This information is used to group the patterns into classes as similar as *FILTERSIM* does, herein the patterns are divided into classes using k-means clustering algorithm and finally averaged to obtain a class prototype.

WAVESIM can be used to simulate categorical and continuous variables. For simulation of categorical data a *ccdf* of the individual class prototype is obtained using the probability of each individual category within the class. Then, the grid is simulated by comparing the conditioning data event in each node with the prototypes of the class, at that point, a random pattern is generated

from the developed *ccdf* of the "best match" class. In synthesis *WAVESIM* does not generate a random pattern from a class, but it rather generates a random pattern from a *ccdf* developed for each class.

In terms of continuous simulations, the most challenging task is the generation of a continuous TI because to build it some additional information is necessary. For example in the oil-gas field they use sedimentation models, seismic to distinguish geometric structures as channels or streams, etc. (Okabe and Blunt, 2004). For the construction of the categorical TI, a wireframe is built from the drillhole samples and it is based on a geological interpretation which is used as additional information. Unfortunately, for continuous variables this extra information is not always available. Therefore, a continuous TI would be very subjective. Some attempts have been made to obtain a continuous TI through the use of low rank tensor like the work of Teixera (2014). In his work, *WAVESIM* draws the patterns randomly and not ccdf is generated, he shows that given the continuous character of this type of variables, a continuous TI gives very small probability to find a matching pattern of a certain point neighborhood in the patter database even if a large TI is used. Therefore, this limited number of pattern replications does not allow obtaining representative MP statistics (Hu *et al*., 2008; Hu *et al*., 2014).

There are other ways to obtain information from the TI, for instance the work of Mariethoz *et al.* (2010). In their work, they propose a direct sampling (DS) method which does not count and does not store the configurations of the TI as *SNESIM* does. DS directly samples the TI in a random way conditioned to the data event, but in this methodology the geometry and size of the templates are not predefined, it rather obtains the neighbourhood information within a search radius. This neighbourhood defines a set of lag vectors that is used to randomly scan the TI to find similar patterns. A threshold is defined by the user to find the patterns whose dissimilarity falls below it; when a pattern is found the algorithm stop the search and the central node is simulated. If after a defined number of iterations a pattern is not found, the most similar pattern is selected to simulate the central node. To speed up the simulation process Rezaee *et al*. (2013) proposed an extension of DS to simulate a group of nodes simultaneously (patching) when the central node is simulated. One of the drawbacks of the method is that to perform simulations a large set of parameters has to be defined before the simulation in order to obtain logical realizations of the deposit.

Continuing with the idea of patching to obtain faster simulations with a good continuity of geological structures, Faucher et.al (2013) proposed a method called Patchwork Simulation Method (*PSM*). This approach has the advantage of the adjustment of the probabilities in order to attain the reproduction of the histogram during the simulation because from the list of most similar patterns to the data event, a pattern is drawn accordingly to a "transition probability", instead of having each one of the candidate patterns with an equal probability of being randomly drawn.

The concept of TI image is a subjective matter. For example, two training images with the same second order statistics (variograms) can have quite different connectivity properties, geological structures, and shapes. Therefore, is complicated the obtain of a TI that always describes the natural variability (uncertainty) and reproduce the spatial connectivity of extreme values, being this particularly important because in mining planning optimization, the geometry of the mine tends to extend toward the areas of highest grade and/or have a very low stripping ratio, because cash flows occurring early are discounted less, and thus contribute to the increase of the NPV(it pays more to bring income forward and to delay expenditure as long as possible).

2.3.3 High-order spatial cumulants simulation methods

Given the problems of working with training images and to reduce their use to obtain high-order statistics, Mustapha and Dimitrakopoulos (2010) introduced an MPS framework based on spatial cumulants to model and simulate continuous variables, the authors showed that high-order spatial cumulants, calculated through the definition of a spatial template, can be used to capture complex geological features and geometrical shapes of the natural phenomena. A method based on spatial cumulants called *HOSIM* (Mustapha and Dimitrakopoulos, 2010) uses the information from spatial cumulants as a combination of lower or equal order spatial moments. A first moment is the mean of the data, the second moment is the variance of the data and any higher moment can be computed from these two. Here, the authors showed that *HOSIM* accurately reproduce many orders spatial statistics of a set of sparse data. The simulation using high-order spatial cumulants is a data driven method, as opposed to the other high-order simulation methods which are training image driven. This is because *HOSIM* quantifies spatial interactions using maps of high-order statistics getting first the multiple-point statistics from the data and only relying on the TI when

few replicates are found. Then the use of high-order maps allows the characterization of non-linear and non-Gaussian spatial random fields.

2.4 Stochastic mine production scheduling

In the past sections of this chapter, the limitations of the use of a single smoothed representation of a deposit into the mine planning process were stated, as well as the advantages of modelling geological uncertainty. Then, the efforts have focused on the development of tools to incorporate such modelled geological uncertainty, to not only quantify it, but also to manage the associated risk to obtain mine production schedules that improve the mine value and reduce the deviation from production targets; providing then, an optimal production schedule. In general, the optimal production schedule is the mine sequence that provides the maximum achievable discounted value of the project given operational constraints. This goal is usually accomplished through the use of operation research methodologies used to deal with production prediction problems including mine planning.

One of these operation research techniques is the linear programming (LP) (Johnson, 1968). Unfortunately, LPs do not provide a truly optimal solution since it may generates fractional blocks results, and returns mine sequences that extract the blocks in a way that does not respect the precedence constraints. It means that in the solution a block deeper in the ground can be mined before all its overlying blocks are mined, this is practically infeasible.

Another operations research technique applied in mining studies is dynamic programming for optimising schedules and mine production with metal price uncertainty optimizing cut-off grade (Dowd, 1976). Cut-off grade (COG) is one of the most popular destination policies used in the mining industry, the destination of the blocks is bases on the metal content (grade) being above or below a threshold. Based on this policy, Dowd's work shows that an increase in the COG results in a faster reduction of the mineral resource. Therefore, the method attempts to find a single cut-off grade policy that balances this reduction rate accounting for uncertainty in metal prices. The method is limited because ignores geological uncertainty, and assume that the production of the mine can vary as the price of the commodity change. The method also assumes a specific, ordered

block extraction sequence. It means that if this sequence is altered, the cut-off grade policy needs to be re-optimized.

Dynamic programming has not a standard mathematical formulation. The equations are specifically developed for each individual problem. Seymour (1994) attempted to optimize mine schedules using maximum NPVs as the optimizing criteria, but the number of variables and constraints that can be optimized is limited. This limitation is a big drawback given that the modelling problem of a real mine operation comprises a large number of variables and constraints. Retaking Dowd's (1977) work, Barr (2012) proposes an alternative partial differential equation formulation for optimizing the dynamic cut-off grade (assigns a cut-off value to each block according to the status according to the stage in which it is found, each time the deposit is evaluate.) with commodity price uncertainty, but in this case the formulation includes the option to temporarily shut down the mining operation. Unfortunately, this method is limited in its ability to account for geological uncertainty.

Another operations research technique applied in the solution of mine scheduling problems is mixed-integer programming (MIP) (Gershon, 1983). This approach is a variation of integer programming (IP) for problems requiring only some integer variables in the formulation. The remaining continuous variables are allowed to be fractional in the solution. Therefore, unlike IP, the formulation of the mining scheduling problem as a MIP allows partial blocks to be mined only if all precedent blocks have been completely removed. Still, the number of variables required to formulate the scheduling problem for a real mine deposit as a MIP is too large to solve the formulation within a reasonable time.

Unfortunately, the mentioned approaches above do not account for geological uncertainty, and there has been no success in developing a scheduling method to give optimum results in maximising net present value of a mining project (Ramazan and Dimitrakopoulos, 2004). Aiming to include grade uncertainty, Smith and Dimitrakopoulos (1999) proposed an approach where for a set of simulations an optimal schedule was obtained. Then, the probability of a block belonging to certain extraction period can be retrieved. If a block was mined in the same period for all the different schedules it means that the block is "optimally" mined in that period because the probability of being extracted is 100% for that given period. Then, a block probability level can

be calculated and used to plan sequences on where the uncertainty is accounted, indicating the level of risk in not achieving yearly production targets. Following this idea, Ramazan and Dimitrakopoulos (2004) included the local uncertainty associated to each one of the blocks of a deposit to have a yearly production in between the range of the production targets. This was accomplished by including a set of constraints that limit the possible deviation from the desired production targets. In the same work a new concept related to geological risk was conceived as Geological Risk Discount (GRD). This GRD discount allows to put off the blocks with higher risks to the latest periods of the operation. The authors showed that this optimization approach produced a schedule with a 6% less risk of not meeting production targets when compared with the conventional mine schedule. Nevertheless, this approach only includes local uncertainty through summarized probabilities; therefore joint local uncertainty is still not included in the optimization process.

Menabde *et al*. (2007) develop a MIP model that accounts for a variable cut-off grade (COG) during the LOM and handles geological uncertainty through constraints to control the mining and production capacity. It means that the formulation enforces the mining operation to meet the desired targets, but unlike Ramazan and Dimitrakopoulos' work, this methodology does not minimize the deviations from production targets. Therefore, it does not return a robust mine schedule accounting for uncertainty. Later, Boland *et al*. (2008) propose a multistage model that simultaneously generates an adaptive production schedule and scenario-dependent cut-off grade decision. It means that for every orebody realization, the ore/waste classification assumes perfect geological knowledge and this fixed classification is not useful in another geological simulation. From there, the results yield an overly optimistic destination decisions, as it assumes that the grades of the mined materials are known at the beginning of each period and do not provide a long-term guide for mine operations.

2.4.1 Stochastic integer programming.

A more flexible approach to solving long term production scheduling is based in the so called Stochastic Integer Programming (SIP) (Birge and Louveaux, 1997). This type of mathematical programming is an extension of the mentioned MIP with uncertainty in one or more of the related coefficients (Escudero, 1993). SIP as a mathematical programming is able to

consider multiple equally probable realizations and generate an optimal solution for a set of defined objectives within a feasible solution space constrained by a set of restrictions.

SIP was first introduced in mining problems by Ramazan and Dimitrakopoulos (2004). They presented a framework that allows the management of geological risk in terms of not meeting planned targets during an actual operation; unlike the results from traditional scheduling methods that use a single orebody model and where risk is randomly distributed between production periods while there is no control over the magnitude of the risks on the schedule. SIP directly maximizes the NPV while minimizes the deviation from production targets. In this methodology instead of setting hard constraints the deviations are penalized within the objective function. This concept gives flexibility in the solution because when a set of different objectives and constrains are imposed the problem can become infeasible.

Later, Ramazan and Dimitrakopulos (2007) demonstrated the value of the stochastic solution in two different deposits. A 10% higher NPV was obtained when the methodology was applied to a gold deposit, in comparison with the conventional schedule optimization. The same good results were obtained when the methodology was in a copper deposit, achieving a 25% higher NPV. Both results have a greater chance of meeting production expectations than the mine schedule obtained through conventional methods. In a similar way, Leite (2008) presented the results of the application of the methodology in a copper deposit without the inclusion of stockpiles. The author reports an improvement of 29% in the NPV when compared to the results obtained with a conventional deterministic framework.

As was mentioned in a previous section, Albor and Dimitrakopoulos (2010) use a SIP and a heuristic algorithm to find the pit limits. In their work, the problem is reduced to the decision about the optimal number of pushbacks and for each one of the designs, a LOM production schedule is obtained through SIP in a way that the design leading to the best NPV maximization and risks minimization trade-off is chosen. Their results returned a 15% larger pit and an increased 30% the NPV when compared to the results of the conventional approach.

Dimitrakopoulos and Jewbali (2013) describe an application of a SIP model which integrates long and short-term mine planning. This is done in an operative gold mine in Australia where the grade

control data from mined areas can be obtained and analyzed in conjunction with the exploratory drillholes, serving as a basis for a joint-simulation to be used as future grade control data in unexploited areas of the deposit. The conditional simulation based on successive residuals is used to update existing simulations of the orebody, incorporating the future data gathered in the operation. Finally, the SIP approach is applied on the updated models, which now contain updated information available by the time of the mine operation. The case study showed an increase of $230M (AUD) in comparison to the values obtained through the conventional schedule obtained the same year.

Leite and Dimitrakopoulos (2014) use the SIP framework in an application at a copper deposit achieving not only a 29% higher NPV in comparison to the one obtained with the conventional method, but also shortened the LOM from eight years to seven years because the conventional schedule is based on a single orebody model which overestimates the amount of ore above the cut-off. Spleit (2014) applied a SIP in an Iron ore deposit showing that the expected production tonnages and qualities obtained using a single orebody model vary significantly when a set of simulation is used to quantify the uncertainty in these both items. From the application, a 5.8% higher NPV was obtained in comparison to the determinist model.

2.4.2 Efficient Solution Approaches for SIP

Despite the good results obtained using SIP mentioned above, the SIP formulations for optimizing production scheduling are usually too large to be solved with conventional solvers like CPLEX –IBM, because optimization of mining deposits usually requires the optimal solution for thousands to several millions of blocks. Therefore, models using exact methods for integer programing are not the most appropriate to solve large-scale mining production schedule models without applying specific constraints to reduce the number of required binary variables. A way around this problem is to apply solution approaches based on heuristics and metaheuristics, to provide solution for realistic size instances in a reasonable amount of time. (Lamghari et.al 2012; Lamghari et.al 2014).

Heuristic and metaheuristic algorithms can provide a faster solution than exact methods. In some cases, when exact methods fail to find any feasible solution, this is the only way to obtain an

approximate solution. To provide an efficient solution method for the mine schedule of large mineral deposit Lamghari and Dimitrakopoulos (2012) propose a metaheuristic method based on Tabu Search (TS). For the implementation of this methodology, an initial feasible solution is obtained by allowing a linear relaxation of binary variables associated to waste blocks to reduce the number of binary variables without affecting the integrality of the ore blocks. This initial solution is iteratively modified searching for different solutions in its neighbourhood. These new solutions are generated by shifting the period of some blocks, keeping the feasibility and improving the objective value. The TS stops, when a number of successive non-improving iterations is reached. After a diversification strategy is apply to generate a new set of starting solutions used for a further search. For the application of TS, the authors test two diversification strategies, one is a variable neighbourhood strategy where the best solution found so far is chosen and a period shifting to a set of different blocks is applied while maintaining the feasibility of the problem. The other one is a long-term memory diversification strategy, which moves blocks to periods that they have rarely been. The results show that the long-term memory diversification strategy outperforms the first strategy.

Later, Lamghari *et al.* (2013)propose a new heuristic methodology called Variable Neighbourhood Decent (VND). The methodology consists in fully explore a neighborhood before starting a new search in another structure to scape local optima (the relative best solutions within a neighbor solution set). The search stops when no move in any of the three neighbourhoods improves the value of the objective function. This method provides fast solutions (in the order of a few hours) and with a small gap of 3% in between the exact solution obtained for the corresponding linear relaxation and the heuristic solution.

As was mentioned in a previous section of this literature review, a more recent application of Heuristic algorithms in the process of solving large-scale mining production schedule models has been successfully applied. Explicitly using Simulated Annealing and Particle Swarm (Montiel, 2015; Goodfellow, 2016). Finally, the most recent application of heuristics is an approach proposed by Rimele (2016). In his work, as similar as Ramazan and Dimitrakopoulos (2013) the author solves the SIP model splitting the work in two. First, finding a linear relaxation of the problem by relaxing binary variables associated to waste blocks to reduce the number of binary variables without affecting the integrality of the ore blocks; this initial solution is used for the

second stage of the work, where the original problem is solved to obtain a fully binary solution. In Rimele (2016) work, he also solves the linear relaxation of a simplified model first, but then, the obtained fractional schedule is used as input for a heuristic method called Topological Sorting Algorithm (TSA) (Chicoisne *et al*., 2012). The methodology was applied to an iron ore deposit obtaining a solution within 2% of optimality in only 12 minutes vs. 21h53m solution time when a schedule close to the optimal solution with all the binary variables included is attempted.

CHAPTER 3

DESCRIPTION OF THE METHODS

Since geological uncertainty has a major impact on mine production and scheduling, this chapter focuses on a thorough explanation of the methodologies applied to model uncertainty through a set of simulations of spatially correlated categorical (e.g. rock types) and continuous variables (e.g. metal grades). These orebody realizations are later included for long term production scheduling.

To optimize mine profitability, the mine planning process relies on the creation of mine plans that are as accurate as possible to optimize production at all stages, from the mine to the market. From geological database (e.g. drillholes) a first step of the mine planning workflow is the creation of a representation to describe the deposit in ground as three-dimensional database, where the attributes of a deposit are stored in the form of a orebody model, in a way that each one of the values of interest is stored at the centroid of a block with the corresponding XYZ coordinate in space.

Conventional mine planning makes use of 3D wireframes (polygons) and solids to model the limits of geological units inherent to an orebody. These limits (boundaries) are obtained through a geological interpretation of available geological data (e.g. drillholes) and some interpolation process. In traditional orebody modelling these boundaries are assumed to be fixed and may not be able to adequately model the detailed structures of geological units. To overcome this problem, stochastic geostatistics make use of multiple point statistics methods to characterize spatial relationships of spaced data that cannot be inferred from drilling data alone.

Multiple Point Simulations MPS methods as *SNESIM, FILTERSIM,* and *WAVESIM* among others are options to model high-order spatial relations of categorical variables (lithological units, rock types). In this chapter, Section 3.1 describes in detail *WAVESIM,* which is used to obtain a set of simulations describing geological uncertainty of the boundaries describing the lithologies in the deposit.

Once the lithological units are modelled, they are stored as wireframes or group of blocks defining the limits. Conventional orebody modelling fills these wireframes with blocks with attribute values as continuous variables (e.g. grades, geometallurgy properties). Usually geological deposits

contain several variables of interest that are spatially correlated. Therefore, the conventional process involves detailed variogram analysis to estimate grade (grades) and tonnage of each block using estimation methods as Kriging to finally obtain a single realization of the deposit (see Figure 3) which is just a smooth representation of the reality given the average-weighting nature of the estimation method.

To simulate a set of correlated continuous variables and overcome the smoothing effect of the grade averaging of conventional approaches. Stochastic simulation addresses the joint-simulation by decorrelating variables to perform an independent simulation for each one of the decorrelated variables. The result is a set of simulations describing the uncertainty of the attributes of the orebody to quantify geological uncertainty. Section 3.2 describes in detail the decorrelation process of the variables through Maximum/Minimum autocorrelation factor (MAF) in combination with Direct Block Simulation *DBSIM* to obtain simulations directly at block support with a method called *DBMAFSIM*.

To obtain a realization of the deposit, each one of the simulated lithologies is used as boundaries to perform grade simulation. This process is done one time for each one of the elements of interest (see Figure 3 (right)). The process is repeated as many simulations of the boundaries are available usually no more than ten (Albor, 2009; Montiel, 2012).

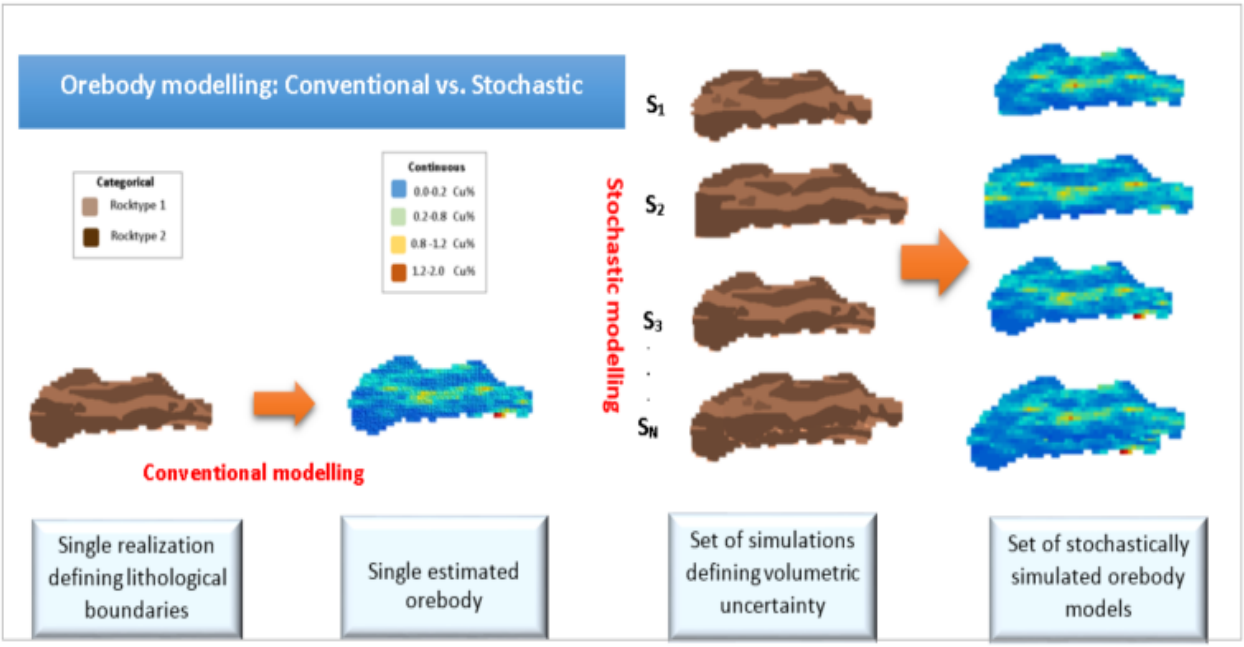

Figure 3. Orebody modelling: Conventional vs. Stochastic approach

To continue the mine planning process, conventional mine planning makes use of the single orebody block model obtained through conventional estimation methods to produce a production schedule respecting a set of mining and operational constraints. Inaccurate geological models introduce errors into the downstream mining plan processing, resulting in unexpected cost increases and revenue reductions. To overcome this problem stochastic mine planning framework makes use of a set of stochastically simulated orebodies to integrate geological uncertainty to the mine design and production planning. Section 3.3 describes in detail the mathematical model to mine production scheduling problem constrained to a set of operational restrictions and production targets.

3.1 Simulation of categorical variables –WAVESIM

The simulations of categorical variables as rock types, lithologies etc. can be modelled through MPS methods. As was described in Chapter 2, Section 2.3.2., a type of MPS based on pattern simulation is viewed as an image reconstruction problem (Arpat, 2004; Zhang *et al*., 2006; Arpat, 2007). It generally consists in two steps, first, a pattern database is generated by scanning a TI, using a given template, then, the pattern providing the best match to the conditioning data is

searched in the pattern database. One can consider the method to be similar to solving a jig-saw puzzle, in the sense that the TI provides the multi-scale puzzle pieces and the algorithm put the pieces together in a randomized way constrained to local data.

This section is dedicated to explaining in detail the following steps for categorical simulation with wavelet decomposition *WAVESIM* (Chatterjee *et al*., 2012).

Summary of *WAVESIM:*

1. Generate the pattern database by scanning the training image with a given template.

2. Decompose the patterns using wavelet analysis.

3. Group these patterns into classes using k-means algorithm.

4. Calculate the prototypes of each class.

5. Define random path visiting all nodes to be simulated.

6. For each node to be simulated, find the neighborhood (conditional data)

7. Compare data event to prototypes.

8. Choose a pattern from best matched.

9. Past it back onto simulation grid.

10. Repeat steps 6 to 8 until all nodes are simulated.

11. Repeat steps 5 to 9 to generate multiple realizations.

3.1.1 Notation

For clarity, this section introduces the required notation for explaining the *WAVESIM* algorithm. This notation is an adaptation of Arpat (2004) –Stochastic simulation with patterns.

3.1.1.1 Training Image

A training image (TI) is essentially a database of geological patterns from which multiple-point statistics (high-order statistics), and low order statistics including the variogram, can be borrowed. The TI can be obtained from actual data such as drilling information or other datasets considered representative of the area being modeled. The TI is usually discretized in a regular Cartesian grid G_{TI}.

Let be $u = (x, y, z) \in G_{TI}$ and $TI(u)$ be a value of the TI indicating a specific multiple-point event of values within a template T centered at u (see Figure 4). Then, $TI_T(u)$ is the vector:

$$TI_T(u) = \{TI(u + h_0), TI(u + h_1), \dots, TI(u + h_\alpha), \dots, TI(u + h_{n_T-1})\} \quad (1)$$

where $\{h_\alpha\}$ is a set of vectors defining the geometry of the n_T nodes of the template T, and

$\alpha = 0, \dots, n_T - 1$. The vector h_0=0 identifies the central location u.

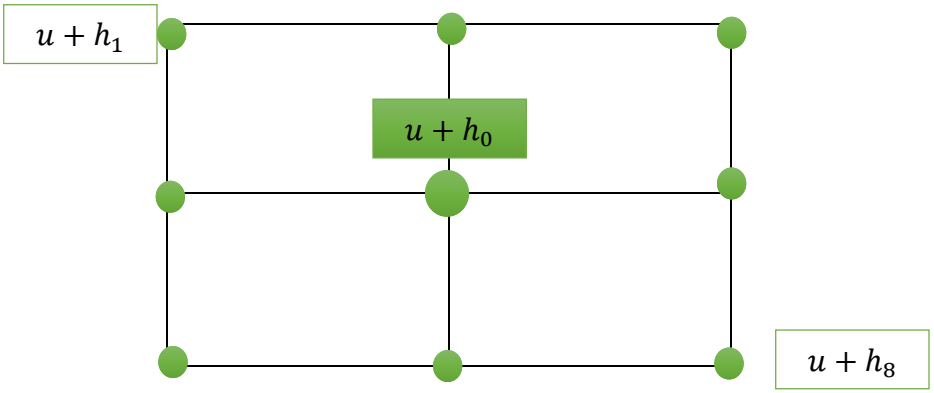

Figure 4. Example of a Template T of 3x3.

3.1.1.2 Patterns

A pattern geometry is defined by a template T containing $\boldsymbol{n_T}$ nodes. In any finite training image there is a finite maximum number of patterns that can be extracted defined over a template T. Then, a pattern $\boldsymbol{pat_T^k}$ is the particular $\boldsymbol{k^{th}}$configuration of a vector of values of the TI as described in (1), but now with each value now denoted by $\boldsymbol{pat_T^k(h_\alpha)}$.

$$pat_T^k = \{pat_T^k(h_0), pat_T^k(h_1), \dots, pat_T^k(h_\alpha), \dots, pat_T^k(h_{n_T-1})\} \quad (2)$$

where $k = 0,\ldots, n_{pat_T} - 1$, and pat_T the number of total available patterns in the pattern database associated with the TI and h_α a set of vectors defining the geometry of the n_T nodes of the template T, all n_{pat_T} are defined on the same template T. Note that $pat_T^k(h_\alpha)$ is location –independent, hence the definition of a *particular pattern is itself location-independent.*

3.1.1.3 Indicator variable

The simulation of categorical variables implies the simulation of different categories at once. For this, the categories inside the TI have to be tagged to differentiate them during the simulation process. The TI is transformed in a set of "indicator training images" using indicator variable transformation to obtain a vector of binary values for each category.

Let $\boldsymbol{M}$ be the number of categories to be simulated, then the indicator variable $\boldsymbol{I_m(u)}$ with $\boldsymbol{m = 1,..,M}$. This indicator is defined as:

$$\boldsymbol{I_m(u)} = \begin{Bmatrix} \mathbf{1, if\ } \boldsymbol{u} \mathbf{\ belongs\ to\ category\ } \boldsymbol{m} \\ \mathbf{0, otherwise} \end{Bmatrix} \quad (3)$$

From there each location $\boldsymbol{u}$ is flagged by category through a vector of binary values where the $\boldsymbol{m^{th}}$ element is 1 if a node in certain location $\boldsymbol{u}$ belongs to category $\boldsymbol{m}$, or 0 otherwise.

3.1.2 Generation of the pattern database

As was mentioned before, the first step to perform orebody simulation through *WAVESIM* as with other MPS is the generation of the pattern database. To achieve this the Training Image (see Section 3.1.1.1) is "scanned" using a given template T, then a pattern is generated by centering T on each one of the nodes in the TI as is shown in Figure 5(a). Afterwards, the obtained patterns are stored in the multiple-point set of vectors in the form of a readable database; this database is the so called pattern database, Figure 5(b).

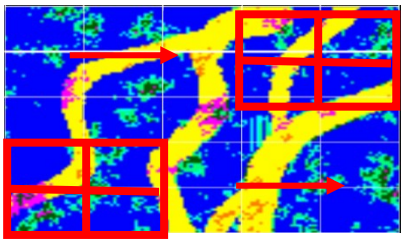

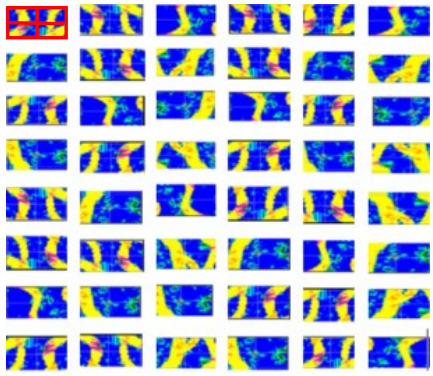

a) Training Image and Template (red rectangle) b) pattern database

Figure 5. Generation of a pattern database.

3.1.3 Dimensional reduction of the pattern database

After the generation of the pattern database, the stored patterns need to be classified and then divided into classes to allow a faster simulation process (see Section 2.3.2). Aiming for reduction of computational requirements in terms of CPU and RAM before the classification of the patterns, the whole pattern database has its dimension reduced using Wavelet decomposition.

Wavelet decomposition for image compression is a known method widely applied for image and data compression applied in fields like medicine where wavelet decomposition for image compression is used to compress electrocardiographs signals (Ramakrishnan and Saha, 1977) and computer science implementations where wavelet compression is the base of the popular format JPEG.

Wavelet decomposition applied to image compression decomposes an image in two type of information. The first one, is an average type information of the nearby pixels, this produces as many coefficients as there are pixels in the image. The average type information is called approximate sub-band of the image and is the one keeping the variability of the data. The second type is the information of how the pixels move off from local average.

To classify the patterns, *WAVESIM* obtains a wavelet based representation of the patterns through Wavelet decomposition aiming to provide an approximate sub-image of the patterns for data compression purposes. From the Wavelet decomposition the information of the approximate sub-band of the nearby pixels describing a pattern is used as a form of transform coding to break a signal (pattern information) into a number of frequency bands. Then, the signal is encoded independently to obtain a decomposition of an image, in this case a decomposition of the patterns. The approximate sub-band of an image is considered enough representation of the complete image because provides average type information about the patterns and preserves most its data variability. Then, the dimension of the pattern database can be reduced by selecting the scale of wavelet decomposition. (Chatterjee *et al*., 2012).

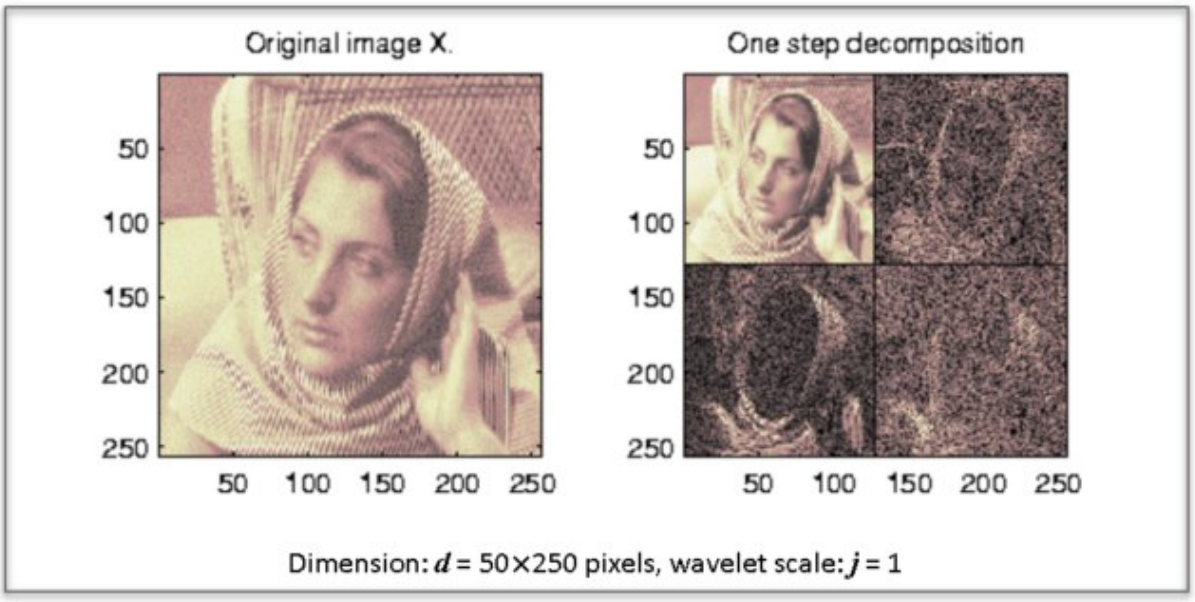

Figure 6. 2D Wavelet decomposition, image compression. Source: One-Dimensional Selection of Wavelet Coefficients Using the Graphical Interface - Matlab Webserver (http://matlab.izmiran.ru/)

Wavelet decomposition is effective for data compression because the dimension of the original image, denoted by ***d*** and the scale number in wavelet decomposition, in approximate sub-band is denoted by ***j,*** is 2^{jxd} times less in comparison with the amount of data in the training image (see Figure 6).

The decomposition of the pattern database is represented as summation from where a pattern of dimension: $\boldsymbol{d} = p \times p$ can be decomposed as follows:

$$pat_T^k = \sum_{i,l=0}^{N_{J-1}} a_{J,i,l}\, \emptyset_{J,i,l}^{LL} + \sum_{B\in D} \sum_{j=1}^{J} \sum_{i,l=0}^{N_{J-1}} w_{j,i,l}^{B} \psi_{j,i,l}^{B} \quad (4)$$

where:

$D = \{LH, HL, HH\}, L = Low - pass\ filter, H = High - pass\ filter$

$N_{J-1} = \frac{N}{2^j}, \quad J = \text{Number of scales}.$ If p is even $N = p$ otherwise $N = (p+1)$

$\emptyset_j = \text{scaling function}$

$\psi_j^B = \text{wavelet function}$

$k = 0,\ldots, n_{pat_T} - 1$, being pat_T the number of total available patterns in the pattern database associated with the TI.

The scaling coefficient is experimentally calculated by taking inner products between a pattern pat_T^k and scaling $\emptyset_j$ and wavelet functions ψ_j^B

$$a_{j-1} = \langle\, pat_T^k, \emptyset_j \rangle \quad (5)$$

The wavelet coefficient is experimentally calculated by taking inner products

$$w_{j-1}^B = \langle\, pat_T^k, \psi_j^B \rangle \quad (6)$$

At each node (pixel location) the template of neighborhood data values is convoluted by these functions to obtain the approximate template and wavelet sub-band data.

The original length of a pattern vector is N^d, after the wavelet decomposition the length of the of the approximated sub-band is:

$$LN = \left(\left(\frac{N}{2^j}\right)^d\right) \quad (7)$$

where ***d*** = dimension of the image and ***j*** = number of scales

For categorical TI, the length of the approximate sub-band for the M-categories will be:

$$LN = \left(\left(\frac{N}{2^j}\right)^d x\ M\right) \quad \text{M: Number of categories} \quad (8)$$

Therefore, depending of the value of the scales, the dimension of the original pattern vector can be reduced. The critical step of wavelet decomposition for image compression relies on the selection of the optimal scale ***j,*** given that the main goal of dimensional reduction is to retain maximum data variability by fewer dimensions. To calculate the best scale a calculation of the entropy value of each pattern at scale ***j*** needs to be estimated. From there, an optimal scale is obtained when no more decomposition is possible. This step is out of the scope of this thesis. For more details, read (Chatterjee, Dimitrakopoulos, and Mustapha 2012).

3.1.4 Pattern database classification

After the reduction of the dimensionality of the patterns, they need to be classified using the obtained approximated sub-bands of the patterns. *WAVESIM* classifies the patterns into classes using K-means clustering technique (MacQueen, 1967; Hartigan and Wong, 1979). In this technique the pattern database is classified in a (k) number of clusters, in a way that within a cluster the variance of the clustered information is minimized. The following description of the method is an adaptation from (Ding and He, 2004).

First, a number of patterns represented by approximated sub-band are randomly selected from the compressed pattern database to represent the initial centroids. Then, each pattern is compared to the initial centroids to assign it to a class which has the closest distance to the centroids as shown in Figure 7 (left). The distance is calculated as the squared Euclidian distance between a pattern and the centroid of one of the classes. The goal of K-means clustering technique is to minimize the distance in a way that at each iteration, the objective is to minimize the following function.

$$Z = \sum_{j=1}^{k} \sum_{i=1}^{n} \left\| T_i^{\,j} - C_j \right\|^2 \quad (9)$$

$T_i^{\,j}$: Pattern i classified in cluster j

C_j: Centroid of a class related to cluster j

$k =$ number of cluster $= n =$ number of classes

$\left\| T_i^{\,j} - C_j \right\|^2$ is the squared Euclidean distance between $T_i^{\,j}$ and C_j, then Z is the summing over all distances between the patterns and their respective class centroid. The process stops when the position of the centroids no longer change. Finally afterwards, the patterns are classified into classes.

3.1.5 Pattern based simulation

3.1.5.1 The concept of class prototype

Thus *WAVESIM* has generated the pattern database, and then through wavelet decomposition the pattern database was compressed in size and classified. These steps are the requirements of the methodology to perform the simulation. Then, following the idea of *FILTERSIM* (Zhang, 2006) and in order to reduce the simulation time *WAVESIM* performs an extra step right before the simulation. In this step, having the pattern database classified, the prototypes of the classes are calculated. The prototypes are obtained by averaging all the falling patterns in a particular class (see Figure 8).

These prototypes are used during the simulation process when the similarity measure between the conditional data event and the patterns is calculated in a way that instead of measuring the distance to each one of the patterns, the measure is done only in between the data event and the prototype of the classes aiming to reduce the processing time of the method.

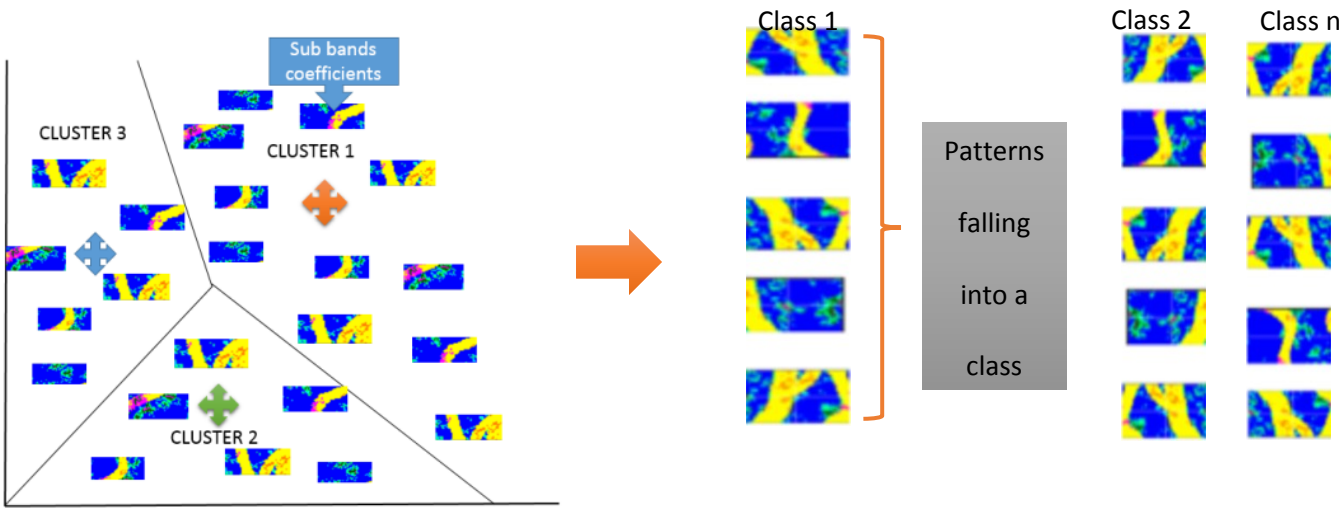

Figure 7. Representation of clustering classification.

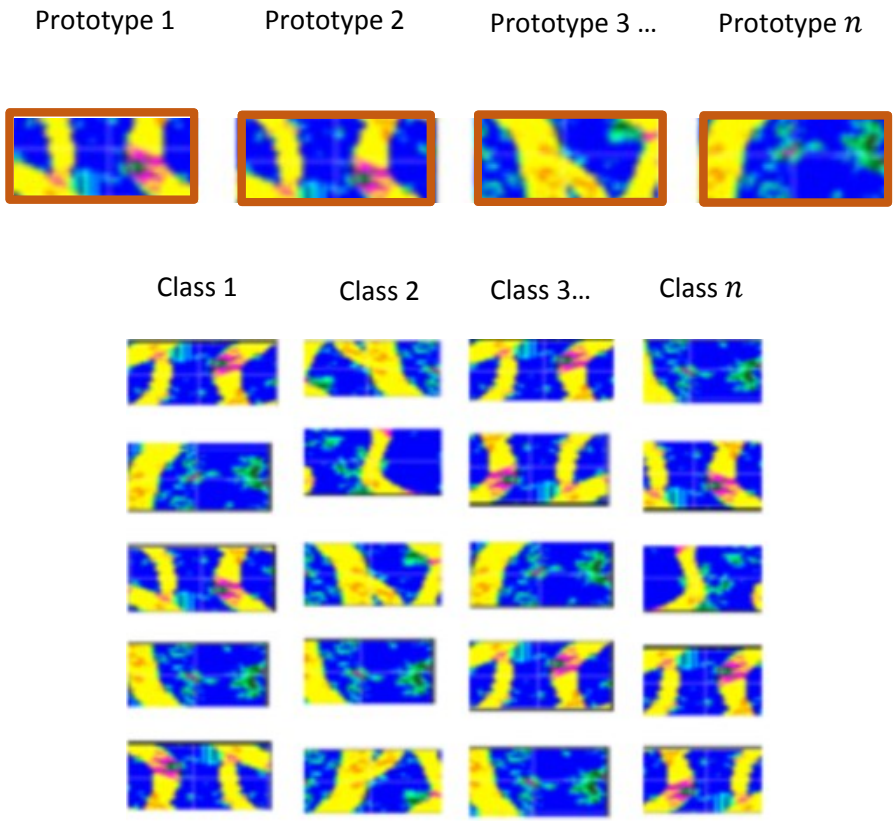

Figure 8. Representation of pattern averaging inside a class (prototypes).

3.1.5.2 Similarity measures

During the simulation, the similarity between the conditional data event and the prototypes of the class is measured by a distance function to calculate the distance from prototypes to the conditioning data event and choose the most similar one. The distance function used in this approach is L2-norm (the generalized term for the Euclidean norm).

$$d(x,y) = \sum_{i=1}^{3} w_i * \left(\frac{1}{n_{type}} \sum_{j=1}^{ntype} (x(j) - y(j))^2 \right) \quad (10)$$

where x is the conditioning data event, y is the prototype of class, n_{type} is the number of data from a particular data type, and w_i is the weight associated with data type i. Three data types are considered for distance calculation $i = 1,2,3$: 1= hard conditioning data, 2=previously simulated node inside inner patch and 3= pattern pasting node data.

Generally, "hard conditioning" data have higher weight than other data types and "pasting node" data the lowest (Chatterjee *et al*., 2012). The sum of the weights should be equal to one.

$$\sum_{i=1}^{3} w_i = 1 \quad (11)$$

If all nodes in a neighborhood are informed the distance between the data event and prototypes is calculated based on their sub-band coefficients obtained through Wavelet decomposition. For these cases a modified distance function is done as follows:

$$d(x,y) = \sum_{i=1}^{3} w_i * \left(\frac{1}{n_{approx}} \sum_{j=1}^{napprox} (x^{approx}(j) - y^{approx}(j))^2 \right) \quad (12)$$

where n_{approx} represents the number of approximate sub-band coefficients after wavelet decomposition, x^{approx} is an approximate sub-band coefficients of conditioning data event and y^{approx} is an approximate sub-band coefficient of the prototype class.

After the distance between a conditioning data event and each of the class's prototypes is calculated and the class with the lowest distance value is chosen. It is important to mention that if there are hard data events within the conditioning data events, only equation (10) will be used.

For categorical simulation, a *ccdf* relative to the central node is built for that class. Then a Monte-Carlo sampling is done over this *ccdf* in order to choose the category of the central node. After this step, a pattern is randomly selected from the ones which have the central nodes belonging to the same category drawn in the Monte-Carlo sampling.

3.1.5.3 Padding the grid.

When a pattern is pasted onto the simulation grid, the user can choose to freeze an innermost portion (inner patch) of the pattern. This set of innermost nodes will not be visited again during the simulation, and only the nodes outside this innermost portion will be revisited and consequently, re-simulated. After pasting the drawn pattern at a simulated node, the next node is visited following a random path.

There are three possible outcomes at this stage:

- Outcome 1: No hard data near the neighborhood of the node d (neighborhood is defined by template T). Then, any pattern of the pattern database works to simulate the node and is randomly selected. After this, each node in the in the inner patch becomes conditional information.
- Outcome 2: The hard data event is at least partially informed. It means that at least a pattern of the pattern database returns a Euclidian distance of zero. Then, the most approximate template will return only the exactly match of the hard data event. In a manner that this information is frozen and remain untainted during the simulation.
- Outcome 3: None of the patterns fulfill the condition. Then, the algorithm performs another search to find a most similar pattern to the hard data. In mining, this is not likely to happen because the training image, in general, reflects a geological scenario consistent with the hard data. The training image contains patterns that agree with the hard data patterns.

Finally, the same distance function and the pattern drawing process is performed until all nodes the grid are simulated. The algorithm stops when no nodes are left unvisited.

3.2 Simulation of continuous variables – DBMAFSIM

In general, a mineral deposit contains more than one element of interest. These elements are usually correlated to each other. Joint-geostatistical simulation techniques are thus required to generate models preserving the spatial relation of the elements to be simulated.

To jointly simulate multiple variables, an effective technique is to decorrelate the variables. These variables are then independently simulated in a transformed space and then back-transformed after the simulation to the original data space, keeping the original correlations between variables. A decorrelation method called Maximum/Minimum Autocorrelation Factors (MAF) is an approach based on Principal Component Analysis (PCA), where the transformed variables are decorrelated at all distances. MAF avoids the tedious modelling and fitting of a linear model of corregionalization since the transformation is directly derived from the experimental data.

The efficiency of joint simulation using MAF is enhanced when the simulations are done directly on a block support scale (*DBSIM*) (Godoy, 2003). To apply this method in a deposit with multiple correlated variables, Boucher and Dimitrakopoulos (2009) introduced the concept of MAF combined with DBSIM for geostatistical simulations *(DBMAFSIM).* The methodology transforms a set of correlated variables into uncorrelated factors which can be then independently simulated and then back transformed preserving the original correlation of the data.

This section is dedicated to explaining in detail the following steps for continuous simulation of correlated variables directly at block support.

Summary of *DBMAFSIM:*

1. Transform data $\boldsymbol{Z}(u)$ to normal scores $\boldsymbol{Y}(u)$
2. The normal scores $\boldsymbol{Y}(u)$ are transformed to MAF factors $\boldsymbol{M}(u)$
3. Define a random path visiting each block
4. The group of N points discretizing each block are sequentially simulated with the LU decomposition method.
5. The group of points for each MAF factor are averaged to obtain block support values. The obtained values are introduced to the data set as conditional data.

6. The simulated variables are back transformed from MAF-space to normal scores $\boldsymbol{M}(u) \rightarrow \boldsymbol{Y}(u)$.
7. Normal scores are back transformed to data space $\boldsymbol{Y}(u) \rightarrow \boldsymbol{Z}(u)$.
8. Repeat steps 4-7 until all blocks are simulated.

3.2.1 Notation

For clarity, this section introduces the required notation for explaining the *DBMAFSIM* algorithm.

3.2.1.1 Search neighborhood.

In general, a search neighborhood is considered a spatial context of a grid node, generally characterizing its local surroundings. The term search neighbrhhod is used as a generic term that does not have a formal definition.

In *DBMAFSIM* a search neighborhood is an ellipsoid that gathers a set of point values (drillholes) and preoviously simulated blocks to simutaneously simulate the points in each block (see Figure 9).

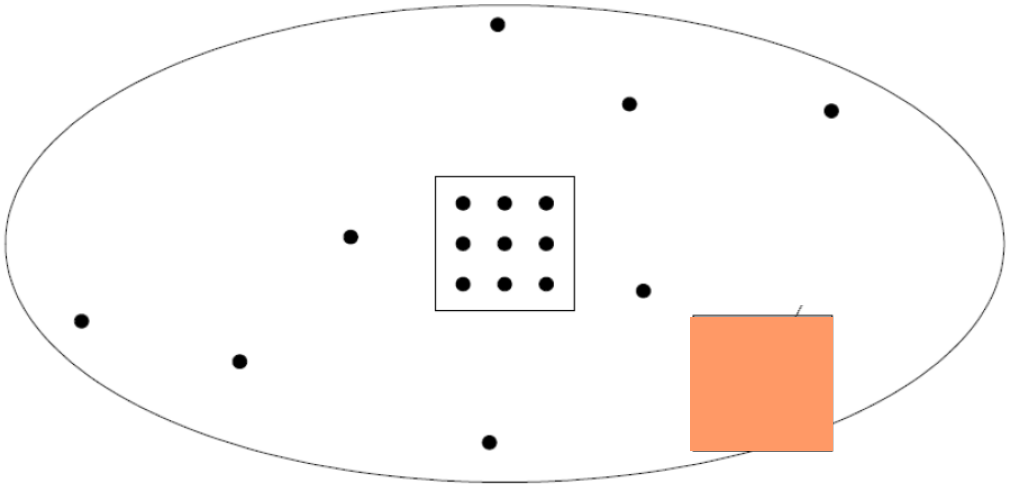

Figure 9. Search neighborhood (ellipsoid) and point values surrounding and previously simulated blocks (orange square). Modified from (Boucher and Dimitrakopoulos, 2009)

3.2.1.2 Variable decorrelation.

Decorrelation is a general term for any process that is used to reduce autocorrelation within a set of data, or cross-correlation within a set of variables while preserving other aspects of a signal (see Figure 10). Once the variables are decorrelated are also referenced as orthogonal variables.

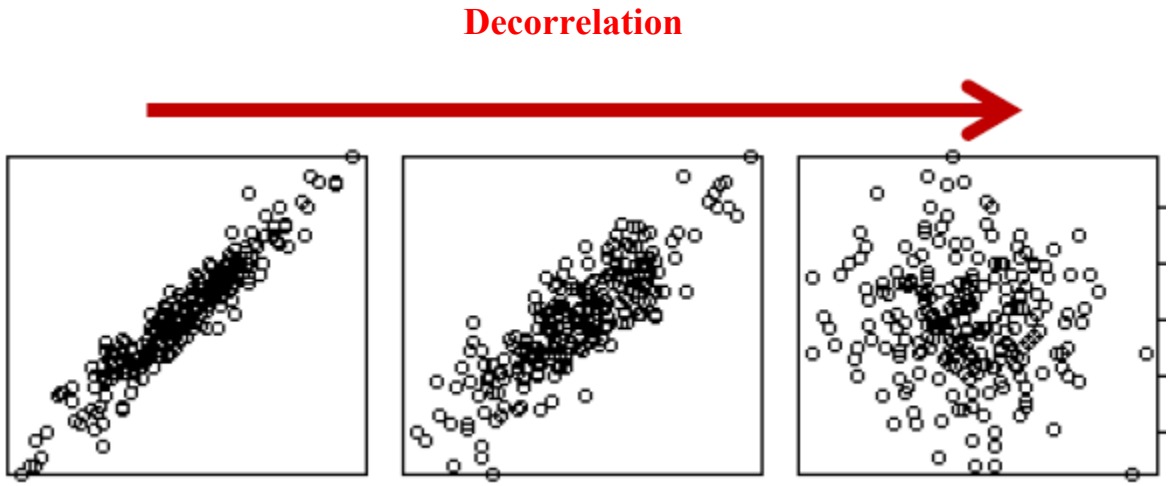

Figure 10. Data decorrelation process.

3.2.2 Orthogonalization with Minimum/Maximum Autocorrelation Factors MAF

MAF performs a linear transformation of a multivariate vector to a new set of variables, called "factors" of the original vector. Consider the stationary vector Random Function (RF) $\boldsymbol{Z}(u) = \{Z^1(u), \dots, Z^k(u)\}$ that is transformed into its Gaussian equivalent $\boldsymbol{Y}(u) = \{\phi_1(Z^1(u)), \dots, \phi_k(Z^k(u))\}$.

The resulting vector RF $Y(u)$ is composed of K Gaussian RFs assumed to be multi-Gaussian. Then the MAF of the variables are defined as a new vector RF $\boldsymbol{M}(u) = \{M^1(u), \dots, M^k(u)\}$ where the K RFs are independent and obtained from the multi-Gaussian vector RF $\boldsymbol{Y}(u)$ using the co-efficient $\boldsymbol{A}$ such that.

$$\boldsymbol{M}(u) = \boldsymbol{A}^T \boldsymbol{Y}(u) \tag{13}$$

Note that MAF variables $\boldsymbol{M}(u)$, are linear function of $\boldsymbol{Y}(u)$, which are a non-linear transformation of the original data $\boldsymbol{Z}(u)$ such that:

$$\boldsymbol{M}(u) = \boldsymbol{A}^T \boldsymbol{\phi}(\boldsymbol{Z}(u)) \tag{14}$$

Let $\boldsymbol{B} = cov[\boldsymbol{Y}(u), \boldsymbol{Y}(u)]$ be the variance/covariance matrix of $\boldsymbol{Y}(u)$ and $\boldsymbol{\Gamma}_Y(h)$ the variogram matrix at lag (distance) h. Then, the matrix of coefficients $\boldsymbol{A}$ that are used to decorrelate $\boldsymbol{Y}(u)$ and is generated from:

$$2\Gamma_Y(h)\boldsymbol{B}^{-1} = \boldsymbol{A}^T \Lambda \boldsymbol{A} \tag{15}$$

$$2\Gamma_Y(h) = cov[Y(u) - Y(u+h), Y(u) - Y(u+h)] \tag{16}$$

The derivation of $\boldsymbol{A}$ is equivalent to performing two successive PCA decompositions (Desbarast and Dimitrakopoulos 2000; Rondon 2012). One of the advantages of working with decorrelated (orthogonal) variables is that only the direct covariance models $C_1(h), \dots, C_k(h)$ is required. It is even more important to recognize that the orthogonal variables can be simulated independently.

3.2.3 Simulating variables at block support DBMAFSIM

Once the variables are decorrelated in MAF space, is time to perform the joint-simulation of the variables. Stochastic conditional simulation through *DBMAFSIM* considers conditional data influencing the block simulation as the data points within a search neighborhood (see Section 3.2.1) through LU decomposition (see Section 2.3.1):

Consider a block at location v discretized with a vector of N points of the k^{th} variable m_s^k=$\{m^k(u_1), \dots, m^k(u_N)\}$ with $u_i \subset v$, and $i = 1, .., k$ with a neighborhood of conditional hard data points and previously simulated points m_d^k. Then the vector m_s^k can be simulated through the Cholesky descomposition.

$$m_s^k = C_{sd}^k {C_d^k}^{-1} m_d^k + L_s^k w_s \tag{17}$$

where,

$$m_d^k = \left[m_p^k \;\; m_b^k\right]^T \tag{18}$$

$$\begin{bmatrix} C_d^k & C_{sd}^{k\,T} \\ C_{sd}^k & C_s^k \end{bmatrix} = \begin{bmatrix} L_d^k & 0 \\ L_{sd}^k & L_s^k \end{bmatrix} \begin{bmatrix} L_s^{k\,T} & L_{sd}^{k\,T} \\ 0 & L_s^{k\,T} \end{bmatrix} \tag{19}$$

The variables m_p^k and m_b^k are respectively, the hard data and the vector of previously simulated blocks within the search neighborhood.

L_s^k and w_s are vectors determined by a Cholesky decomposition using equation (19) (Boucher and Dimitrakopoulos, 2012).

C_d^k is the covariance matrix of conditioning data comprised of the hard data points (drillholes) and the previously simulated blocks.

C_s^k is the point support covariance matrix between the points discretizing the block and C_{sd}^k is the matrix of a point and point to block covariance between the discretizing points and the hard data points and previously simulated blocks.

When a block-support data is considered the submatrix of conditioning data becomes:

$$C_d^k = \begin{bmatrix} C_d^{k,pp} & C_d^{k,pb\,T} \\ C_d^{k,pb} & C_d^{k,bb} \end{bmatrix} \tag{20}$$

The pp index refers to the point to point covariance between hard data, pb is the point to block covariance between the hard data and the previously simulated blocks, and bb is the block to block covariance between previously simulated blocks.

Then the submatrix of conditioning data and the vector of point-support data discretizing the block is:

$$C_{sd}^k = \left[C_{sd}^{k,pp} \;\; C_{sd}^{k,pb}\right] \tag{21}$$

where $C_{sd}^{k,pp}$ and $C_{sd}^{k,pb}$ are the covariance matrix of the discretizing points with the point scale hard data and with the previously simulated blocks, respectively.

Subsequently, the simulated point values in MAF space are averaged at block support scale. These blocks with values in MAF space are introduced as conditioning data to the data set and used for further simulation, rather than using the discretized points. In the other hand, the block value to be outputted in original data space is obtained through a back transformation of the point support data and averaging them for each MAF factor using the following equation:

$$z_s^k = \frac{1}{N}\sum_N(\phi^{-1}(\boldsymbol{A}^{-T}m_s^k)) \tag{22}$$

where $\boldsymbol{A}$ is the matrix of MAF coefficients derived with equations (15) and (16). Then equation (22) allows extending the direct block simulation DBSIM of Godoy (2003) to the joint direct block simulation with *MAF*. The main steps of *DBMAFSIM* are graphically summarized in Figure 11.

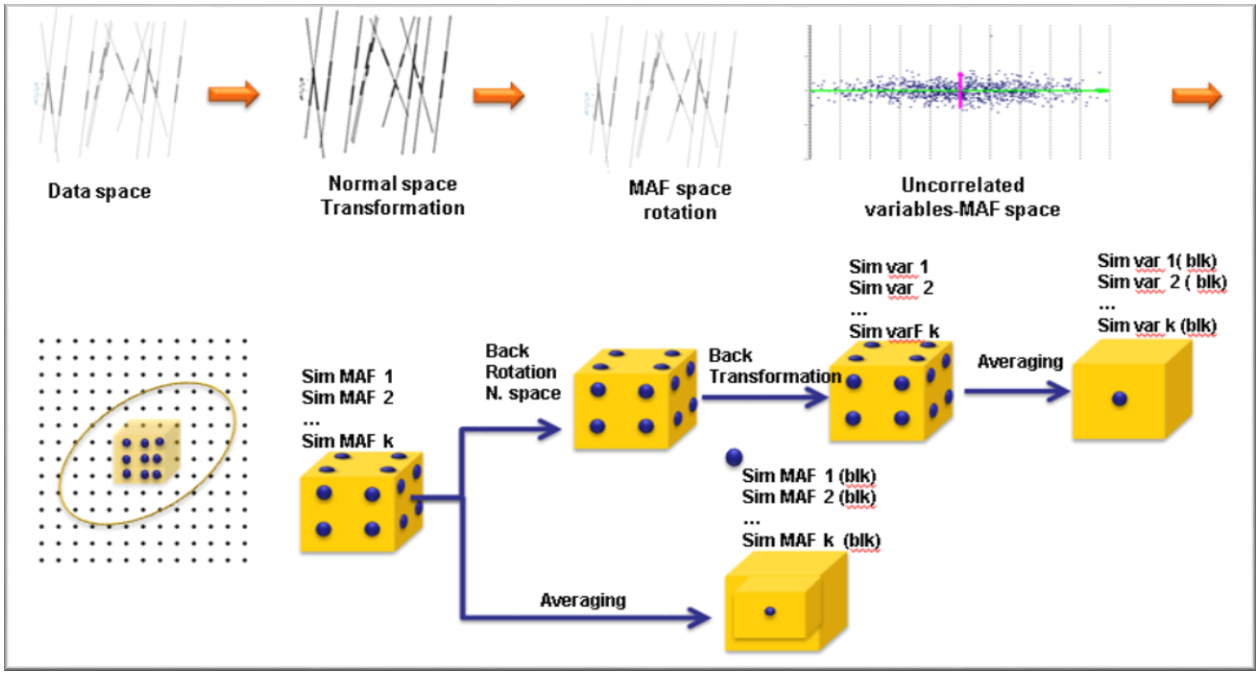

Figure 11.*DBMAFSIM* – workflow.

3.3. Stochastic integer programing- SIP- for long term production scheduling

As mentioned in previous sections a set of simulations is issued to not only quantify geological uncertainty but also this set of equally probable realizations is the key factor in the process of obtaining a mine production schedule optimized to manage geological risk.

This section presents the model of the Open-pit Mine Planning Integer Programming (OMPSIP) formulation based on Ramazan and Dimitrakopoulo (2007; 2013).

3.3.1 Notation

For a better understanding of the descriptions of the formulations herein present, the following notation adapted from Rimele (2016) is used.

$B = \{i = 1, \dots, N\}$ Set of blocks in the orebody,

$P = \{p = 1, \dots, P\}$ Set of considered periods for the schedule,

$D = \{d = 1, \dots, D\}$ Set of destinations available for the blocks,

$S = \{s = 1, \dots, S\}$ Set of scenarios, equiprobable orebody stochastic simulations,

$\mathcal{C} = C_1 \cup C_2$ Set of block's characteristics,

$\mathcal{C}_1 = \{C_1 = 1, \dots, C_1\}$ Linear metallurgical characteristics (e.g. tonnages),

$\mathcal{C}_2 = \{C_2 = 1, \dots, C_2\}$ Non-linear characteristics (grades),

$G(B, A)$ Oriented graph representing the precedence relationships between blocks, $(a, b) \in A$ if $a \in B$ is a predecessor of $b \in B$.

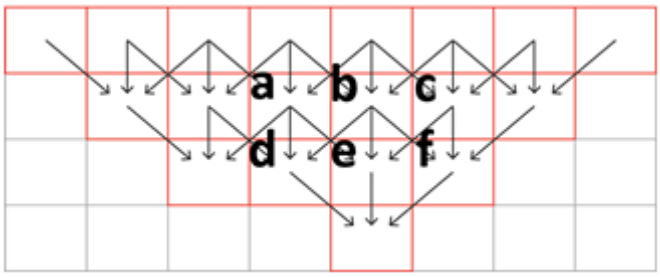

Figure 12. Precedence relationships between blocks (Rimele, 2016).

$\boldsymbol{\Gamma_i^+ = \{b \in B; (i,b) \in A\}}$ Set of direct successors of block$\boldsymbol{i}$. On Figure 12, $\boldsymbol{\Gamma_b^+ = \{d,e,f\}}$;

$\boldsymbol{\Gamma_i^- = \{a \in B; (a,i) \in A\}}$ Set of direct predecessors of block$i$. On Figure 12 , $\Gamma_e^- = \{a,b,c\}$

$\boldsymbol{\Gamma_i^{-Tot}}$ Set of all the predecessors of block**.**

On Figure 12, $\boldsymbol{\Gamma_e^{-Tot} = \{a,b,c\} \cup \Gamma_a^{-Tot} \cup \Gamma_b^{-Tot} \cup \Gamma_c^{-Tot}}$;

$\mathcal{N}(i)$ is a set of neighbours of block i : typically blocks at the North, East, South and West on the same level and one block below.

3.3.2 Parameters

$\boldsymbol{v_{i,d,s}}$ Economic value of block $\boldsymbol{i}$ in scenario $\boldsymbol{s}$ if it is sent to destination $\boldsymbol{d}$;

This economic value depends on several parameters:

$$\boldsymbol{v_{i,d,s}} = \begin{cases} -\boldsymbol{E_{waste}^{cost} * t_{i,s} - TH^{cost} * TH_{i,d}} & \textbf{if } \boldsymbol{d = 0} \Leftrightarrow \textbf{waste dump} \\ \boldsymbol{R_{i,s} - P_{conc}^{cost} * conc_{i,s} - E_{ore}^{cost} * t_{i,s} - TH^{cost} * TH_{i,d}} & \textbf{if } \boldsymbol{d = 1} \Leftrightarrow \textbf{mill} \end{cases}$$

where:

$\boldsymbol{R_{i,s}}$ Revenue from selling the metal content of block $\boldsymbol{i}$ in scenario $\boldsymbol{s}$;

$\boldsymbol{conc_{i,s}}$ Concentrate tonnes of block $\boldsymbol{i}$ in scenario $\boldsymbol{s}$, $\boldsymbol{conc_{i,s} \in C_1}$;

$$\boldsymbol{conc_{i,s} = t_{i,s} * Rec_{i,s}}$$

$\boldsymbol{Rec_{i,s}}$ Weight recovery of block $\boldsymbol{i}$ in scenario $\boldsymbol{s}$, obtained from the simulation of the Davis Tube Weight Recovery (used in the case study);

$\boldsymbol{P_{conc}^{cost}}$ Processing cost of concentrate material per tonne;

$\boldsymbol{E_{ore}^{cost}}$ Extraction cost of ore material per tonne;

$\boldsymbol{E_{waste}^{cost}}$ Extraction cost of waste material per tonne;

$\boldsymbol{TH_{i,d}}$ Truck hours needed to send block $\boldsymbol{i}$ to destination $\boldsymbol{d}$;

$\boldsymbol{TH^{cost}}$ Cost per truck hour;

$\boldsymbol{t_{i,s}}$ Tonnage of block $\boldsymbol{i}$ in scenario $\boldsymbol{s}$;

$\boldsymbol{q_{c_1,i,s}}$ Quantity of characteristic $\boldsymbol{c_1}$ of block $\boldsymbol{i}$ in scenario $\boldsymbol{s}$;

$\boldsymbol{g_{c_2,i,s}}$ Grade $\boldsymbol{c_2}$ of block $\boldsymbol{i}$ in scenario $\boldsymbol{s}$;

$\boldsymbol{target_{c,p}^{\pm}}$ Minimum (-) and maximum (+) targets of quantity or grade $\boldsymbol{c}$ in period $\boldsymbol{p}$;

$\boldsymbol{pen_{c,p}^{dev\pm}}$ Penalty cost of deviation from the targets of quantity or grade $\boldsymbol{c}$ in period $\boldsymbol{p}$ (excess +, shortage -);

$\boldsymbol{r}$ Discount rate taking into account the time value of money and the uncertainty of the future streams of cash flows;

$\boldsymbol{d_p} = \frac{1}{(1+r)^{p-1}}$ Discount factor

3.3.3 Variables

Binary variables:

$$x_{i,d,p} = \begin{cases} 1, \text{if block } i \in B \text{ is sent to destination } d \in D \text{ by period } p \in P \\ 0, Otherwise \end{cases}$$

To simplify the notation, $x_{i,d,p=0}$ =0, $\forall i \in B, \forall d \in D$

Note that the binary value of the variable is defined by period "by period $p \in \mathcal{P}$" . It means that block i was extracted prior period p or exactly at that period. This definition is used to facilitate the branching when the model is solving (Caccetta and Hill, 2003).

Continuous variables:

$dev^{\pm}_{c,p,s} \in \mathbb{R}^{+}$ Deviation from the targets in terms of characteristics c for scenario $s \in S$, during period $p \in P$ (excess +, shortage -).

3.3.4 General OMPSIP

This section describes the OMPSIP formulation which will be used in the rest of the study.

Objective function:

$$\max \boldsymbol{Z} = \overbrace{\frac{\mathbf{1}}{\boldsymbol{S}}\sum_{\boldsymbol{i}\in\mathcal{B}}\sum_{\boldsymbol{d}\in\mathcal{D}}\sum_{\boldsymbol{p}\in\mathcal{P}}\sum_{\boldsymbol{s}\in\mathcal{S}}\boldsymbol{d_p} * \boldsymbol{v_{i,d,s}} * \left(\boldsymbol{x_{i,d,p}} - \boldsymbol{x_{i,d,p-1}}\right)}^{\boldsymbol{Part\ 1}} - \overbrace{\frac{\mathbf{1}}{\boldsymbol{S}}\sum_{\boldsymbol{c}\in\mathcal{C}}\sum_{\boldsymbol{p}\in\mathcal{P}}\sum_{\boldsymbol{s}\in\mathcal{S}}\boldsymbol{d_p} * \left(\boldsymbol{pen}^{\boldsymbol{dev+}}_{\boldsymbol{c,p}} * \boldsymbol{dev}^{+}_{\boldsymbol{c,p,s}} + \boldsymbol{pen}^{\boldsymbol{dev-}}_{\boldsymbol{c,p}} * \boldsymbol{dev}^{-}_{\boldsymbol{c,p,s}}\right)}^{\boldsymbol{Part\ 2}} \quad (23)$$

The objective function comprises two parts: $Part\ 1$ aims to maximising the expected profit, Discounted Cash Flow (DCF), while $Part\ 2$ minimizes the expecting cost of deviating from the production targets; that is, the risk associated with geological uncertainty. Using this formulation, the expected result is a schedule robust to the set of simulations (Ramazan and Dimitrakopoulos, 2007).The application of a discount factor delays the risk and favors the extraction of the most valuable blocks in the early periods. This discount factor is a key point for mining companies as they usually expect a fast return on their investment.

Constraints

- **Reserve constraints**

$$x_{i,d,p} - x_{i,d,p-1} \geq 0 \qquad \forall i \in \mathcal{B}, \forall d \in \mathcal{D}, \forall p \in \mathcal{P} \qquad (24)$$

$$\sum_{d \in \mathcal{D}} x_{i,d,p} \leq 1 \qquad \forall i \in \mathcal{B}, \forall p \in \mathcal{P} \qquad (25)$$

Constraint (24) specifies that a block extracted at a certain period is also defined as already extracted in the following periods It means that the block is only extracted once. Constraint (25) states that a block can be sent to only one destination.

- **Slope constraints**

$$\sum_{d \in \mathcal{D}} x_{i,d,p} \leq \sum_{d \in \mathcal{D}} x_{j,d,p} \qquad \forall i \in \mathcal{B}, \forall j \in \Gamma_i^-, \forall p \in \mathcal{P} \qquad (26)$$

A block i is available for extraction only if all of its direct predecessors Γ_i^- have already been extracted or are extracted within the same period. This means that the block is reachable; i.e., without blocks above it and that the slope constraints for the stability of the walls are satisfied.

- **Quantity constraints**

Upper bound (27)

$$\sum_{i \in \mathcal{B}} \left(q_{c_1,i,s} * \left(x_{i,d,p} - x_{i,d,p-1} \right) \right) - dev^+_{c_1,p,s} \leq target^+_{c_1,p} \qquad \forall c_1 \in \mathcal{C}_1, \forall d \in \mathcal{D}, \forall p \in \mathcal{P}, \forall s \in \mathcal{S}$$

Lower bound (28)

$$\sum_{\boldsymbol{i \in \mathcal{B}}} \left(\boldsymbol{q_{c_1,i,s}} * \left(\boldsymbol{x_{i,d,p} - x_{i,d,p-1}} \right) \right) + \boldsymbol{dev^-_{c_1,p,s}} \geq \boldsymbol{target^-_{c_1,p}} \qquad \forall \boldsymbol{c_1 \in \mathcal{C}_1}, \forall \boldsymbol{d \in \mathcal{D}}, \forall \boldsymbol{p \in \mathcal{P}}, \forall \boldsymbol{s \in \mathcal{S}}$$

These two sets of constraints define soft constraints for the upper and lower bound (27-28) respectively, on the quantities targets at each period and in each scenario.

The variables $dev^{\pm}_{c_1,p,s}$ are used as buffers to allow deviations but these deviations are penalized in the objective function.

- **Grade quality constraints**

Upper bound (29)

$$\sum_{i\in\mathcal{B}}\left(g_{c_2,i,s} * t_{i,s} * \left(x_{i,d,p} - x_{i,d,p-1}\right)\right) - dev^{+}_{c_2,p,s} \leq target^{+}_{c_2,p} * \sum_{i\in\mathcal{B}}\left(t_{i,s} * \left(x_{i,d,p} - x_{i,d,p-1}\right)\right) \quad \forall c_2 \in \mathcal{C}_2, d = 1, \forall p \in \mathcal{P}, \forall s \in \mathcal{S}$$

Lower bound (30)

$$\sum_{\boldsymbol{i\in\mathcal{B}}}\left(\boldsymbol{g_{c_2,i,s}.\, t_{i,s}} * \left(\boldsymbol{x_{i,d,p} - x_{i,d,p-1}}\right)\right) + \boldsymbol{dev^{-}_{c_2,p,s}} \geq \boldsymbol{target^{-}_{c_2,p}} * \sum_{\boldsymbol{i\in\mathcal{B}}}\left(\boldsymbol{t_{i,s}} * \left(\boldsymbol{x_{i,d,p} - x_{i,d,p-1}}\right)\right) \quad \forall \boldsymbol{c_2 \in \mathcal{C}_2, d = 1, \forall p \in \mathcal{P}, \forall s \in \mathcal{S}}$$

Similar to the capacity constraints, constraints (29) and (30) penalize excess and shortage of the average grade c_2 at each period and for each scenario.

- **Extraction smoothing constraints**

$$\sum_{d\in\mathcal{D}} x_{i,d,p} \leq \sum_{d\in\mathcal{D}} x_{j,d,p} \qquad \forall i \in \mathcal{B}^{1/2}, \forall j \in \mathcal{N}(i), \forall p \in \mathcal{P} \quad (31)$$

These operational constraints impose a continuous sequence of extraction in a way that the extracted blocks, at least within the same period, should be close to each other.

- **Earliest period of extraction constraints**

$$x_{i,d,p} = 0 \tag{32}$$

$$\forall i \in \mathcal{B}, \forall d \in \mathcal{D}, \forall p \in \left\{ \bigcup_{c_1 \in \mathcal{C}_1} \left(t \in \mathcal{P};\ \forall s \in \mathcal{S}, \sum_{t'=1}^{t} target^{+}_{c_1,t'} - \Delta_{c_1,t'} \leq \sum_{j \in \Gamma_i^{-Tot} \cup \{i\}} q_{c_1,j,s} \right) \right\}$$

These last constraints, equivalent to an earliest start of a job, are optional. They eliminate variables to make the model easier to solve. The idea is that to reach a block i by period p, at least all its full cone of predecessors Γ_i^{-Tot} must be extracted. This cone plus the block i represent a certain tonnage or quantity which can be compared to the sum of the quantity targets from the first period to period p. If this last tonnage is less than the one of the cone, it is impossible to reach i by p, even in the most optimistic situation in which only the cone is mined. As a consequence, in such a case, the corresponding variables $x_{i,d,p}$ can be set to 0, which says that block i will not be extracted at period p, without any loss of optimality and making the problem easier to solve. The parameters $\forall c_1 \in \mathcal{C}_1, \forall t' \in \mathcal{P}, \Delta_{c_1,t'} \in \mathbb{R}^+$ are used to keep the flexibility of the stochastic formulation which allows deviations from the production targets. Typically one can take $\Delta_{c_1,t'} \cong \frac{1}{4} * target^{+}_{c_1,t'}$.

3.3.5 Partial Relaxation

From the formulation presented in the last section and from Section 2.4.2. It can be seen that the main issue when solving this kind of OMPSIPs with commercial solvers is that the computational requirements are enormous. The larger the number of variables and constraints is, the more complicated it is to achieve an optimal solution for the model. The problem is even more complex to solve when is mandatory respect integrality constraints to obtain binary solutions (e.g. a block fully mined in a certain period p) (see Figure 13).

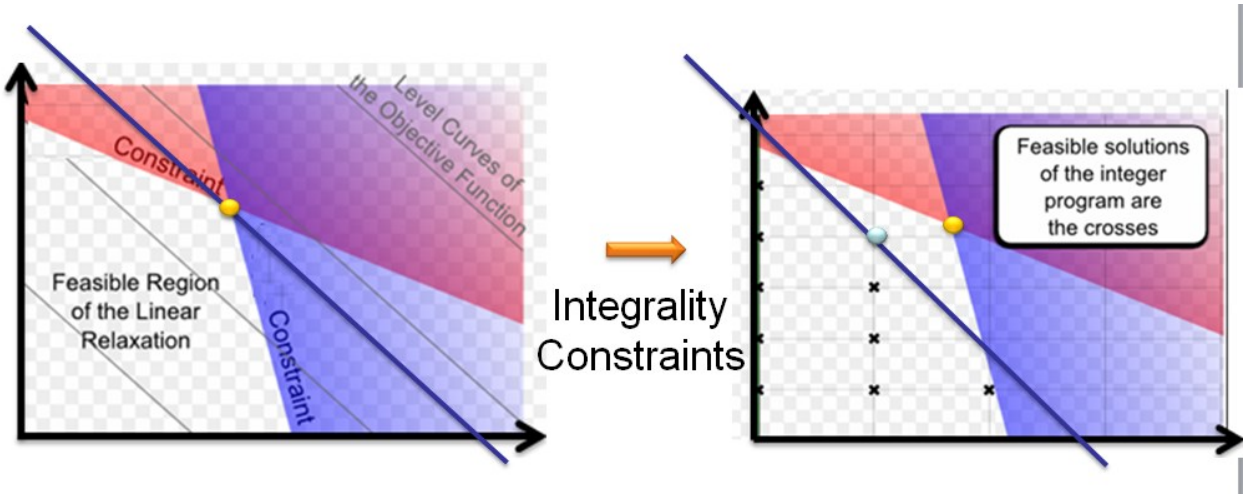

Figure 13. Loss of value in objective function due to Integrality constraints.

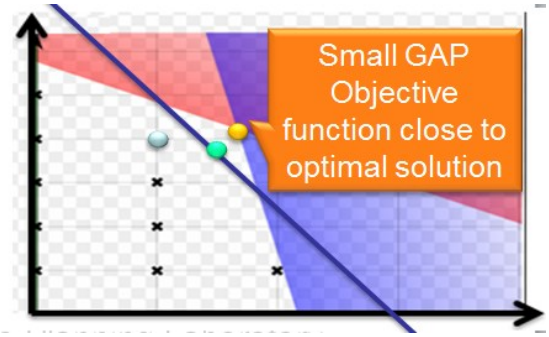

Figure 14. Relaxed solution – reduced binary variables.

The idea here is then; reduce the number of binary variables in order to accelerate the solution process. First, an initial feasible solution of the OMPSIP is obtained by allowing a linear relaxation of binary variables associated to waste blocks to reduce the number of binary variables without affecting the integrality of the ore blocks. The partial relaxation returns a fractional schedule which is used as an input for a heuristic algorithm to obtain a final result close to the initial formulation. i.e., extraction variables which must be binary (see Figure 14).

As the work develops by Ramazan and Dimitrakopoulos (2013). This methodology solves the OMPSIP by splitting the procedure into two steps. The first step is to solve the non-fully binary (relaxed) model described in this section. This initial solution returns a fractional schedule, which is used for the second step where the original problem described in Section 3.3.4 is solved.

For the solution of the relaxed OMPSIP, additional notation for the general OMPSIP algorithm (Section 3.3.4) is required:

Note 1: $x^*_{i,d,p}$ and $dev^*_{c_1,p,s}$ replace respectively $x_{i,d,p}$ and $dev^{\pm}_{c,p,s}$ in the formulation stated in Section 3.3.4. Affecting equations (23 to 31) of the general OMPSIP model.

$\boldsymbol{x^*_{i,d,p}}$ Fractional value obtained from the relaxed model representing the percentage of block $\boldsymbol{i} \in \boldsymbol{\mathcal{B}}$ sent to destination $\boldsymbol{d} \in \boldsymbol{\mathcal{D}}$ at period $\boldsymbol{p} \in \boldsymbol{\mathcal{P}} \cup \{\boldsymbol{0}\}$;

$\boldsymbol{dev^*_{c_1,p,s}}$ Value of the deviation of $\boldsymbol{c_1} \in \boldsymbol{\mathcal{C}_1}$ from the quantity target in period $\mathbf{p} \in \boldsymbol{\mathcal{P}}$, for scenario $\boldsymbol{s} \in \boldsymbol{\mathcal{S}}$, obtained from the relaxed model;

Note 2: $(\boldsymbol{p_i}, \boldsymbol{d_i})$ and $\boldsymbol{rcap_{c_1,p,s}}$ are added to the general OMPSIP model.

$(\boldsymbol{p_i}, \boldsymbol{d_i})$ Pair of variables used to store the period of extraction and destination assigned to the block $\boldsymbol{i} \in \boldsymbol{\mathcal{B}}$;

$\boldsymbol{rcap_{c_1,p,s}}$ Residual capacity of quantity $\boldsymbol{c_1} \in \boldsymbol{\mathcal{C}_1}$ in period $\boldsymbol{p} \in \boldsymbol{\mathcal{P}}$ for scenario $\boldsymbol{s} \in \boldsymbol{\mathcal{S}}$; i.e., the quantity that can still fit into period $\boldsymbol{p}$ without exceeding the upper bound target.

Definition of the weights

From the relaxed or partially relaxed solution, two sets of weights $\{\boldsymbol{w1_i}, \forall \boldsymbol{i} \in \boldsymbol{\mathcal{B}}\}$ and $\{\boldsymbol{w2_{i,d}}, \forall \boldsymbol{i} \in \boldsymbol{\mathcal{B}}, \forall \boldsymbol{d} \in \boldsymbol{\mathcal{D}}\}$ are defined and will be used in the TopoSort algorithm.

$$\boldsymbol{E1_i = \sum_{p \in \mathcal{P}} p * \sum_{d \in \mathcal{D}} \left(x^*_{i,d,p} - x^*_{i,d,p-1}\right) + (P+1)\left(1 - \sum_{d \in \mathcal{D}} x^*_{i,d,P}\right)} \qquad \forall \boldsymbol{i} \in \boldsymbol{\mathcal{B}} \qquad (33)$$

$$\boldsymbol{w1_i = -E1_i} \qquad \forall \boldsymbol{i} \in \boldsymbol{\mathcal{B}} \qquad (34)$$

$$\boldsymbol{w2_{i,d} = \sum_{p=1}^{P} \left(x^*_{i,d,p} - x^*_{i,d,p-1}\right)} \qquad \forall \boldsymbol{i} \in \boldsymbol{\mathcal{B}}, \forall \boldsymbol{d} \in \boldsymbol{\mathcal{D}} \qquad (35)$$

$E1_i$ can be defined as the expected value of the extraction period of block i. Since the weight $w1_i$ is the opposite of $E1_i$, the higher the weight is the sooner the block is extracted. The weight $w2_{i,d}$ represents the percentage of block i sent to destination d from which the most likely destination

of the block can be directly determined. The objective of both sets of weights is to give to the heuristic algorithm (see Section 3.3.6) an input that allows it to be as close as possible to the relaxed solution while respecting the various constraints.

3.3.6 Heuristic Method

The relaxed model with reduced binary variables provides a fractional solution. Now, the objective is to make this solution fully binary with the use a heuristic method that can provide a faster solution than exact methods. Rimele (2016) proposed the application of a heuristic method to solve the mine schedule problem inspired by the work developed by Chicoisne and Espinoza (2012). The main idea of the algorithm called Topological Sort Algorithm (TSA) is to sort the blocks in a topological order based on pre-defined weights obtained from the relaxed solution as result of the assignment of a certain block to a certain period to obtain a fully binary solution.

Once the relaxed OMPSIP is solved, the result is used as an initial solution to solve the general OMPSIP model defined in Section 3.3.4. The relaxation of the problem gives information of the most probable destination for every block. For each realization and each period, the initial residual capacity of quantity c_1 is set as the upper target. Then, if for a certain period exist at least one block from to the list of predecessors, that has to be send to the waste dump or have a capacity of quantity of c_1 less than the remaining capacity. The block is removed from graph G and assigned to the current period. In case where no block can fit anymore in the current period, the next period is considered. Then, from the application of TopoSort Algorithm, a satisfactory binary schedule is expected to be obtained respecting the general OMPSIP model where models often require thousands to millions of decision variables.

CHAPTER 4

CASE STUDY: APPLICATION AT AN IRON ORE DEPOSIT IN NORTHERN QUEBEC, CANADA

The methods for strategic mine planning described in chapter 3, were applied to the KéMag iron deposit a property of New Millennium Iron Corp (NML). The deposit is located on the extreme western margin of the Labrador Trough (see Figure 15). The Trough, known as the Labrador-Québec Fold Belt extends for more than 1,000 km along the eastern margin of the Superior craton from Ungava Bay to Lac Pletipi, Québec. The belt is about 100 km wide in its central part and narrows considerably towards the north and south.

The KéMag deposit is an iron formation of the Lake Superior type, consisting of banded sedimentary rocks composed principally of bands of iron oxides, magnetite and hematite within quartz (chert)-rich rock with variable amounts of silicate, carbonate and sulphide lithofacies. Lithofacies that are not highly metamorphosed or altered by weathering are referred as "Taconite". These type of deposits are suitable to produce fine iron concentrate which is pelletized. The selling price of iron pellets is higher compared to the selling price of iron concentrate.

4.1 Study area and data

The simulation of the KéMag deposit is perform conditioned to a set of information provided by NML, consisting of the drilling data from a total of 264 drillholes that constitutes 6,295 assays, later composited over every 15m and discretized into nine (9) different lithologies within an extension of 14.5 km long, 8.5 km wide and 480m in vertical depth. The average drill spacing is 300m which is quite sparse, but common for taconite orebodies given its inherent low variability over large distances. Each drillhole log consists of a set of intervals coded by lithology and with associated qualities (laboratory determined).

Table 1 shows the categorical codification of the iron formation. The lithological code represents the seam or strata intersected by the drillholes. The economic lithologies comprise of strata 3 to 9 and are identified on the basis of chert colour and oxide texture. These are the lithologies that are simulated using *WAVESIM* method.

Table 1. Codes by lithology.

Strata	Lithology	Code	Iron Formation
1	Overburden	OB	N/A
2	Menihek Shale	MS	N/A
3	Lean Chert	LC	Upper
4	Jaspen Upper Iron Formation	JUIF	
5	Green Chert	GC	
6	Upper Red Cherty	URC	Middle
7	Pink-Grey Cherty	PGC	
8	Lower Red Cherty	LRC	
9	Lower Red-Green Cherty	LRGC	

4.1.1 Notes on the data

The KéMag deposit for mine production is under "Feasibility stage", it means that the project is being evaluated in terms of its practical and financial viability. Given this early stage of the project, not much information about the deposit is available. NML is the owner of another iron ore deposit in the same area where KéMag is located. This deposit is called LabMag and is located 18km to the south of the KéMag deposit. Both deposits share practically the same geology, this assumption is confirmed by the fact that the drilling has intersected the same iron formations in both deposits. Therefore, the KéMag deposit is interpreted as being identical to the LabMag deposit. Also, geological interpretation of the KéMag deposit relies on the knowledge gained in the exploration of the neighboring LabMag deposit, since most of the areas of the KéMag deposit only contain 1 drillhole, and only a limited area where a cross-section contains 4 drillholes allowed for a detailed interpretation of the seams, confirming a general dip of 6° to the southeast, just like the LabMag deposit. This level of geological knowledge is considered sufficient to classify the mineral resources to the Indicated level.

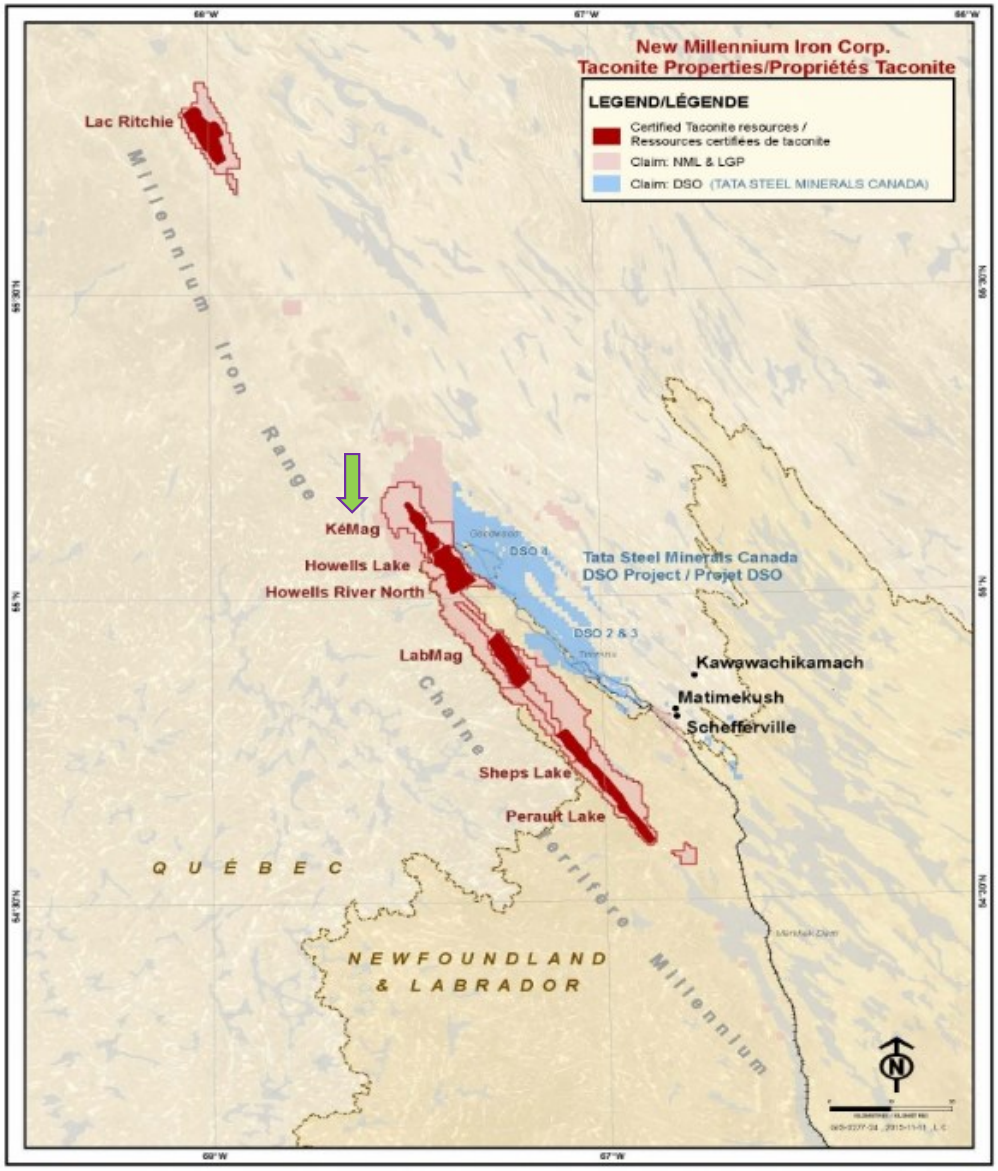

Figure 15. Iron Range- New Millennium Limited.

The KéMag deposit has four highly correlated qualities of interest: Head iron grade (FeH), The Davis Tube Weight Recovery (DTWR), The David Tube concentrate grade (FeC), and the Davis Tube concentrate silica grade (SiO_2); disseminated over 7 stratigraphic units of magnetite, plus two overlying waste-type units.

The geological unit of the deposit that contains the highest consistent concentration of magnetite is PGC. In the other hand, LC and JUIF also contain high concentrations of magnetite, while

hematite is most common in LRC, URC, and JUIF units. Silicate iron minerals are most prevalent in LIF and LC, just beneath the Menihek formation.

The planned mining method for the project is open pit mining with 15 meter bench height and operated with the conventional truck and shovel combination. The financial model (costs) used for this case study are the same set of costs estimated by NML for the operation of LabMag deposit. Given confidentiality agreements, this information is not disclosed in this thesis.

In terms of operational constraints, to solve the mathematical model of the mine production scheduling only two continuous variables are considered to control the production process: the average DTWR grade and the average silica per period. Silica concentration in the input feed material represents the main pollutant for iron ore processing and is crucial for maintaining the quality of the metal production. The lower the silica the better the selling price of the pellets in the market. The production scheduling is done over a Life of Mine (LOM) of 10 years and only two destinations are considered: the "mill" for processing the ore and the "waste dump" for disposal of waste material.

4.2 Stochastic mine planning of the KéMag deposit

As was outlined in chapter 3, the stochastic mine planning workflow starts with generating a set of orebody realizations that captures geological uncertainty of the limits of the nine geological units (lithologies) of the KéMag deposit. In this thesis, a set of 15 realizations is generated using *WAVESIM* (see Section 3.1). Afterwards the boundaries of the lithologies described by the 15 realizations of categorical variables (lithologies) are used as limits for the simulation of the jointly-correlated continuous variables (grades). The simulation of the grades is performed using *DBMAFSIM* (see Section 3.2). Here, the four grades of the KéMag deposit (DTWR, FeC, FeH, and SiO2) are decorrelated first and then, fifteen (15) simulated realizations of continuous variables are generated directly at block support scale.

Finally, the set of generated simulations were used in the general Open-pit Mine Planning Stochastic Integer Programming (OMPSIP) (see Section 3.3). The OMPSIP allows the integration of geological uncertainty in the mine design and production scheduling process. However, considering the computationally expensive nature of such integer programming models an

application of an acceleration method is also applied to reduce the solution time for the optimization model.

4.2.1 Simulation of lithological units using *WAVESIM*

To simulate the boundaries of the lithologies, the main goal is to simulate the geometry of each stratigraphic layer in order to capture their spatial uncertainty. From the initial information outlined in Section 4.1.1. A Training Image (TI) (see Figure 16) is created through a geological interpretation using a set of wireframes provided by NML. The wireframes are discretized in a Cartesian grid of 70x100x26 with cell size of 100mx100x15m. From there, a total of 182,000 nodes are used to perform the simulation of ore lithologies (see Section 3.1.1).

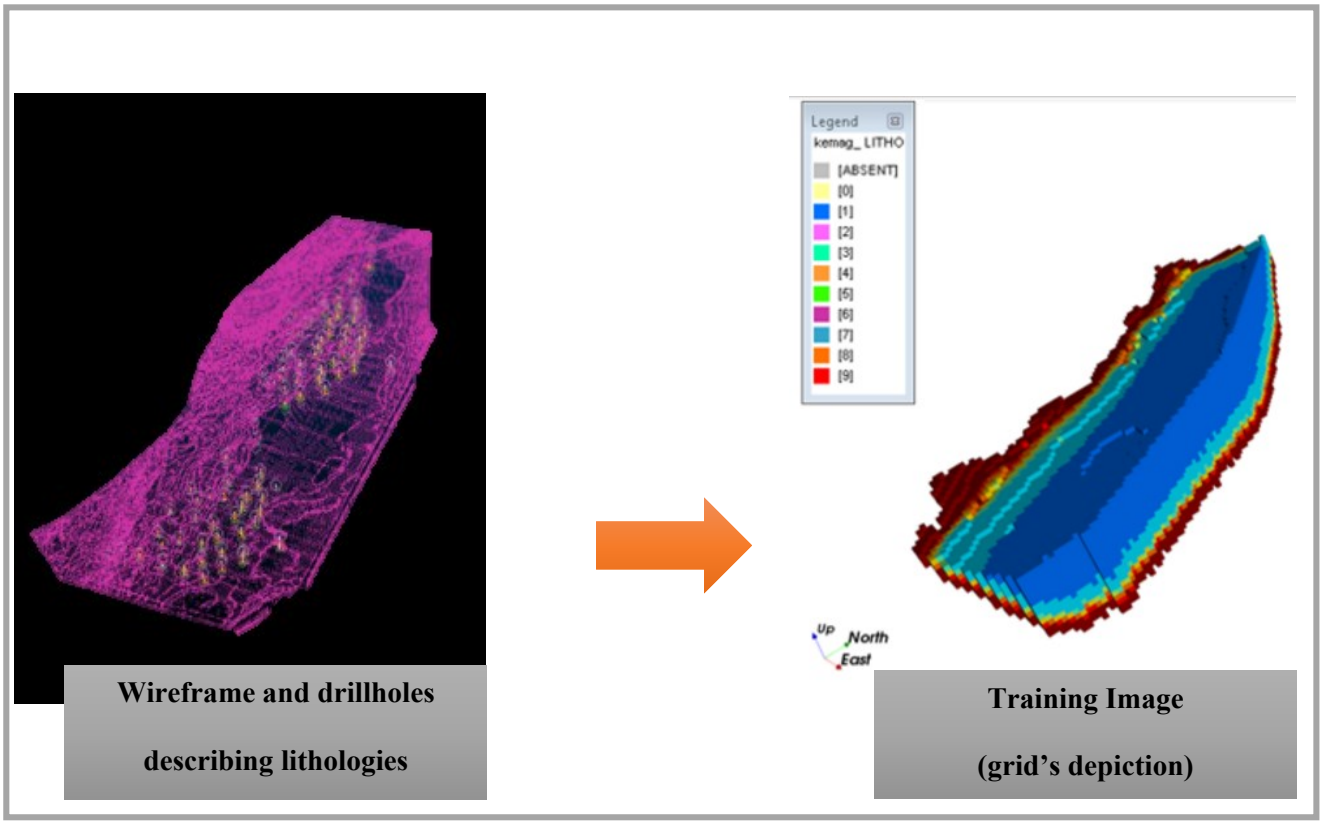

Figure 16. KéMag deposit Training Image.

For the simulation of the waste lithologies, a different process is perform taking advantage of the fact that in the KéMag deposit these lithologies are not correlated with the ore layers. The simulation of these layers is complex because the waste layers are extremely thin (less than 7m)

in some regions of the deposit, recall that the block discretization in this study is of size 100mx100x15m. Therefore, its thickness is extremely thin to be modelled in conjunction with the seven ore lithologies. Thus, in order to save time and computational resources, waste layers were simulated separately.

The waste lithologies (MS and OB), need to be simulated because they are required for the OMPSIP model outlined in Section 3.3. To simulate them, the MS lithology was simulated through *WAVESIM* using as hard data each one of the obtained simulations of the ore lithologies and a very simple 3D training image. On the other hand, the OB lithology is simply overburden, thus, its volume was obtained by intersecting the topographic surface with the contact of the layers for each simulation obtained using *WAVESIM*. It is important to note that these 2 layers are considered waste therefore have no iron content and were not included for generating simulation of continuous variables (grades).

4.2.2 *WAVESIM* Parameters

One of the advantages of the *WAVESIM* is that the set of input parameters required to perform simulation is reduced to only three main factors: Template size, Inner patch and Number of clusters. All of them are defined in Section 3.1.

The number of clusters and template size are defined through trial and error approach. Hence, the values in table 2 are the ones showing the best trade-off between quality of the results and computational time for the simulation of 7 ore lithologies.

Table 2. WAVESIM parameters.

Parameter:	**Value:**
Template size	13x13x5
Inner Patch	9x9x3
Number of Clusters	30

4.2.3 Validation of the simulated boundaries

The obtained simulations are validated in terms of histograms, variograms, and high-order statistics compared to the training image and the hard data (e.g. drillholes). High-order statistics are validated through High-Order Spatial Cumulants (HOSC) (Dimitrakopoulos et. al., 2010) (see Section 2.3.3). Spatial cumulants are an extension of the covariance function, and it is able to describe non-Gaussian stationary and ergodic random fields since they can capture complex spatial patterns and their connectivity in geological fields (De Iaco and Maggio, 2011).

4.2.3.1 Visual inspection of the simulation of the boundaries

Figure 17 shows the results obtained from simulation of the KéMag's lithological boundaries. The training image (left) and two simulations randomly selected from the fifteen available (right). From the comparison of the sections of the training image and simulations, it can be clearly perceived that the simulations respect the same spatial configuration, as the TI, given that each lithology tends to appear in the same region. However, as expected, the simulated realizations are "patchy" and present more variable patterns in comparison to the TI.

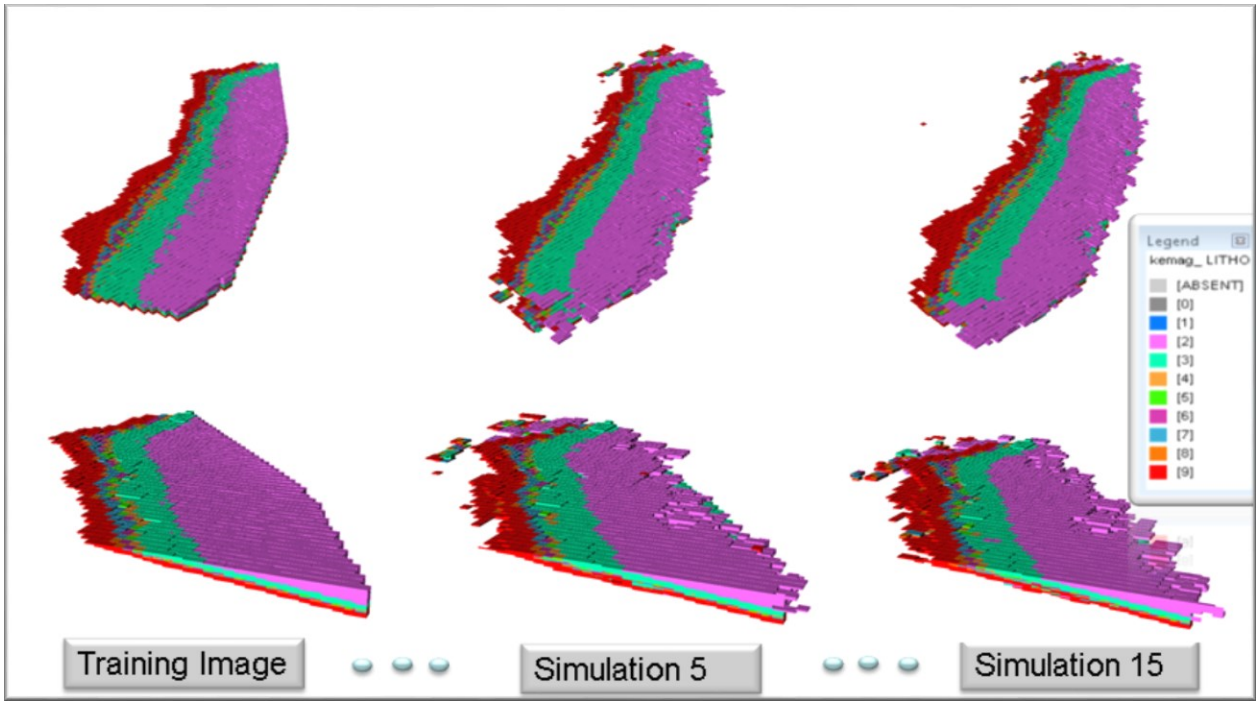

Figure 17. Cross sections (right Training Image, left simulations).

4.2.3.2 Histogram of the simulations

In addition to visual inspection, the simulations are subsequently validated by histogram comparison between data and simulated values. Figure 18 shows that the fifteen simulations reproduce relatively well the proportion of the ore deposit when compared with the TI and the hard data (HD).

Lithology 3 –LC and Lithology 9-LRGC (see table 1), are the lithologies with higher proportions in volume for the KéMag deposit. The reason why the proportions of the simulations for lithology 3-LC are bigger than the TI and HD proportions is due to the fact that *WAVESIM* reproduces the simulation in a cubic 3D grid. Thus, as lithology 3–LC is closer to the surface, has more "empty space" in the cubic grid to paste patterns belonging to this category, some post-processing methodologies can be applied to constraint the simulation grid and avoid this situations, however, this post-processing is out of the scope of this thesis. In the other hand Lithologies 4 to 9 proportions are perfectly in between the hard data and training image proportions.

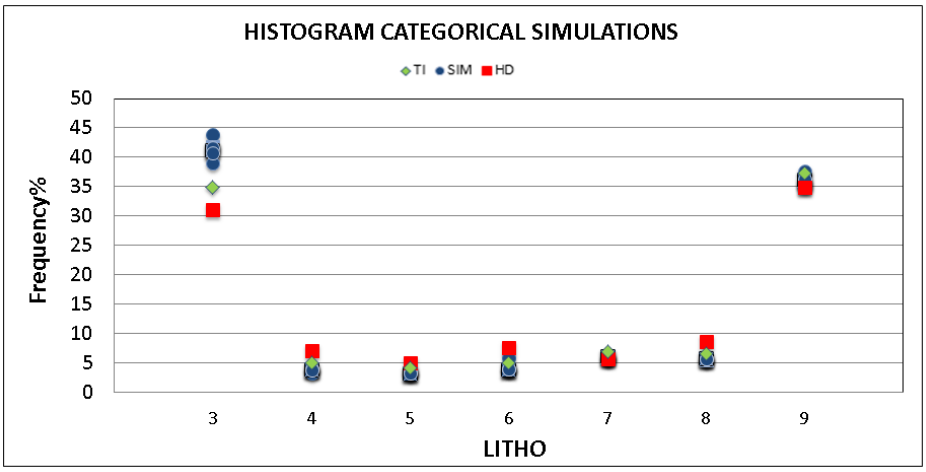

Figure 18. Histogram of categorical simulations compared to hard data and training image.

4.2.3.3 Variograms of the simulations

In geostatistics it is common to plot a variogram in a specific direction, to this, the distance relaxation and angular tolerance are necessary to account for the samples that are not regularly spaced when calculating the variograms for different directions.

Given the numerical difference of the codes describing the lithologies, an indicator variogram for each lithology was obtained. Indicators are binary transforms of a variable, having values of either 1 or 0. Indicator variograms can be used for a similar range of geostatistical estimation techniques as standard variograms. (Western and Blöschl, 1998).

Figure 19 and 20, shows the indicator variogram for lithology 03-LC and 09-JUIF respectively in two directions for the 15 simulations along with, HD and TI. The variograms are obtained using a distance (lag) separation of 150m and a tolerance of 100m. All the results suggest a reasonable reproduction of the variogram for the simulations compared to the training image and hard data. Also the cross-variogram from Figure 21, between the two main ore layers shows that the simulations are following the same behavior and relation as the HD and TI.

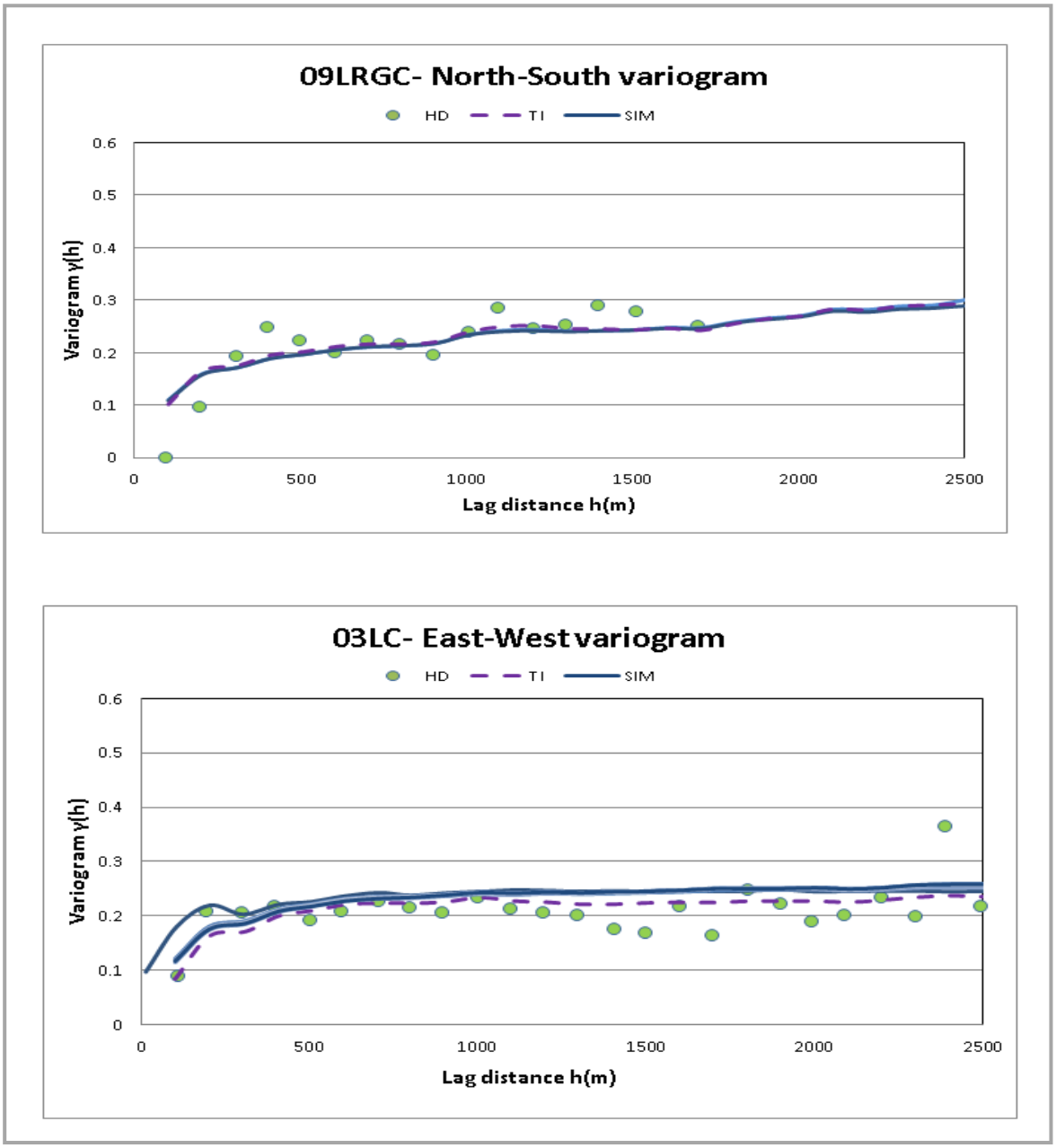

Figure 19. Variogram of categorical simulation for lithology 3-LC in two different directions, compared to hard data and Training Image

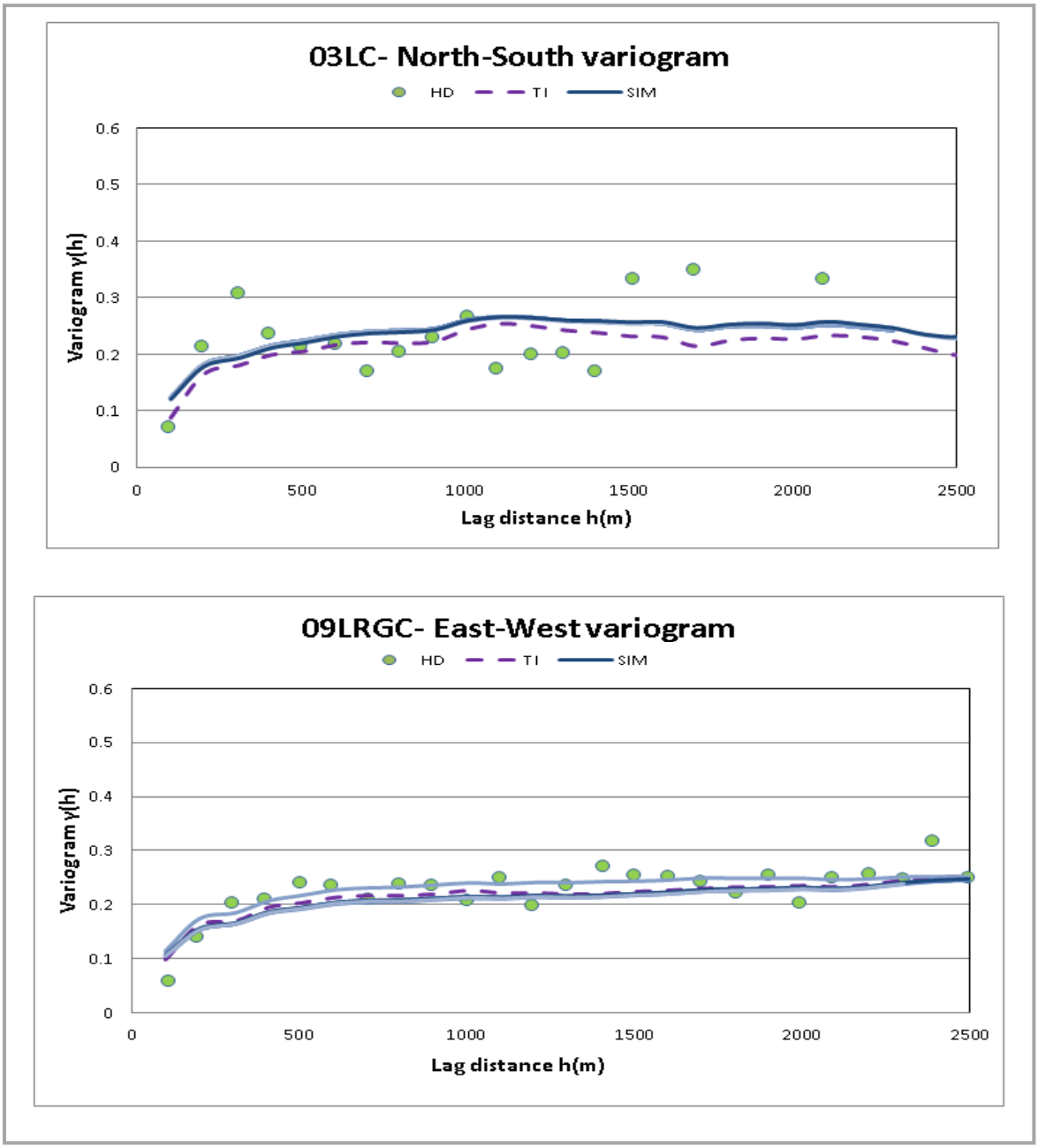

Figure 20. Variogram of categorical simulations for lithology 9-LRGC in two different directions, compared to hard data and Training Image.

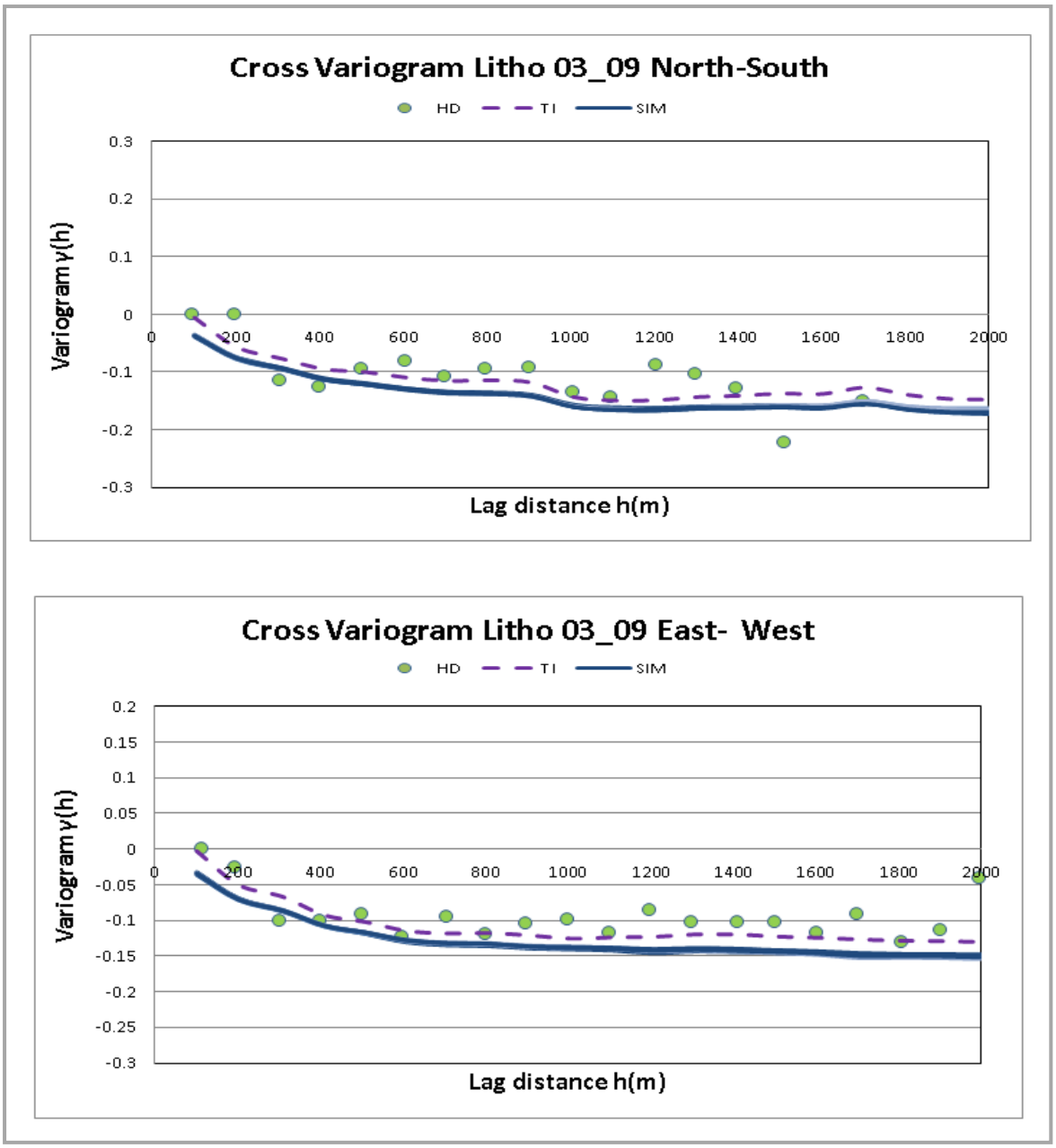

Figure 21. Cross-variogram of categorical simulations for 2 different lithologies in two different directions, compared to hard data and Training Image.

4.2.3.4 High-Order cumulant maps of the simulations

Given that *WAVESIM* is a multiple-point simulation method, the high-order relations should also be reproduced by the simulations. Therefore, validations are also performed in terms of high-order statistics, which are obtained through cumulant maps. In order to calculate the cumulant describing the cumulant map, spatial templates have to be defined, an L-Shape template was used to calculate the 3rd order cumulant as {(1, 0, 0) ;(0, 1, 0)}.

Figure 22 shows the cumulant map calculated for a single material type 03 –LC for the TI and the two randomly selected simulations. From the figure it can be seen that the cumulant map of the simulations shows a similar pattern as the TI for the first 2 km in north direction and the first 500 m along east direction. The lithologies have a strong correlation in this area as represented by the highest absolute values (red area in Figure 22). Also, as the orebody has high north-south strike length, thus the high cumulant values show more correlation in north-south direction. It can be also seen that the extension of the orebody in the north-south direction is well reproduced by the simulations in terms of their cumulant maps. However, after 500m, the north direction shows smaller correlations. This is related to the sparse location of the drillholes.

Recall that *WAVESIM* retrieves statistics from the TI and the hard data (drillholes), and as was mentioned in the beginning of this section, the distance in between drillholes for KéMag deposit is large and have sparse drillhole density thus, this it was impossible to obtain a cumulant map for the hard data.

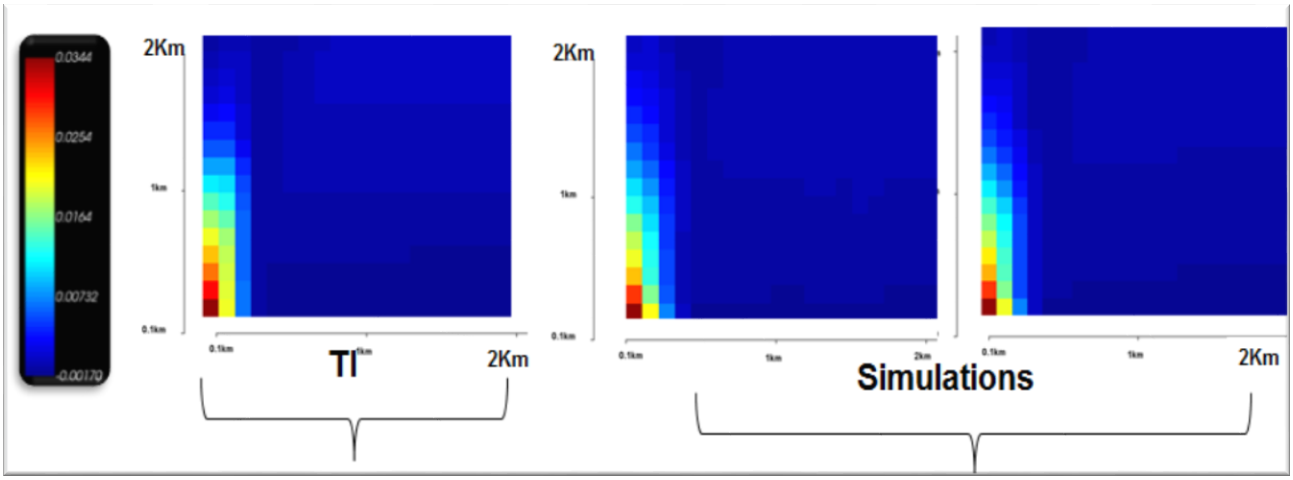

Figure 22. Third-order cumulant map for Training Image and simulations.

Results for validation of the lithological boundaries simulation in terms of low-order statistics (histogram and variograms) and high-order statistics (cumulant maps), indicates that in general, all fifteen simulations reproduce the spatial features of the drillhole information and training image very well.

4.3 Simulation of continuous variables (grades)

4.3.1 Data

Having defined the lithological boundaries through multiple point simulation (*WAVESIM*). The grades attributes of interest: Head iron grade (FeH), The Davis Tube Weight Recovery (DTWR), The David Tube concentrate grade (FeC), and the Davis Tube concentrate silica grade (SiO_2), were simulated within these boundaries using Gaussian conditional simulation method called *DBMAFSIM* that generates the simulations directly at the block support scale, which for the present case study was 100mx100mx15m (same discretization for categorical simulation).

To evaluate the degree of correlation between different grade attributes (DTWR, FeC, FeH and SiO_2), some correlation coefficient denoted by ρ or r, are used. The most common correlation coefficient is the so-called Pearson's correlation coefficient, which is only sensitive to a linear relationship between two variables (which may exist even for non-linearly correlated variables). The Pearson's correlation coefficient ranges from −1 to 1. A value of 1 implies positive linear

correlation, a value of −1 implies negative correlation and a value of 0 implies no linear correlation between the variables.

Other correlation coefficient for a more robust measurement of the degree of correlation is the Spearman's correlation. This correlation coefficient is more sensitive to non-linear relationships. Spearman's correlation is a rank correlation, which is important because the normal score transformation is foremost requirement to perform *DBMAFSIM* (see Section 3.2) which only preserve the rank correlation. Spearman's coefficient is appropriate for both categorical and continuous variables and is considered a non-parametric factor.

A Spearman's correlation of zero indicates that there is no correlation between variables. If the variables are perfectly monotonically related, the Spearman's correlation coefficient is equal to 1. The sign of the Spearman correlation indicates the direction of the association between variables; it means that positive correlations are indicated by a positive Spearman's correlation coefficient.

Both correlation measurement criteria are used to evaluate the correlation of the four variables in the drillholes database: DTWR,Feh,FeC and SiO_2. Table 3 and Table 4 indicate the Pearson's and Spearman's correlations coefficient for the drillhole information for different grade attributes respectively.

Table 3. Pearson's correlation for different grade attributes.

	FeH	**DTWR**	**FeC**	**SiO_2**
FeH	1.00	0.53	0.52	-0.13
DTWR	0.53	1.00	0.44	0.10
FeC	0.52	0.44	1.00	-0.09
SiO_2	-0.13	0.10	-0.09	1.00

Table 4. Spearman's correlation for different grade attributes

	FeH	**DTWR**	**FeC**	**SiO_2**
FeH	1.00	0.40	0.41	-0.23
DTWR	0.40	1.00	0.04	0.16
FeC	0.41	0.04	1.00	-0.77
SiO_2	-0.23	0.16	-0.77	1.00

From table 3, it can be seen that SiO_2 has a negative correlation with FeC and FeH, however are not strongly correlated since the Pearson's correlation coefficients are close to zero, and a similar weak positive relation could be observed between Silica and DTWR.

From table 4, it can be seen that the Spearman's correlation between DTWR and FeC is close to zero, which indicates no correlation between the variables. From this table, it can also be confirmed that the correlation between SiO_2 and FeC, SiO_2 and FeH is negative. Also, from tables 3 and 4 can be deducted that strong correlations exist between some of the grade attributes; this rationalizes the need to keep their correlations in the simulated realizations for the grade attributes.

4.3.2 Minimum and maximum autocorrelation factors (MAF)

Since, the simulated lithologies serve as boundaries or domains for the simulations of the grades attributed. It was noted that not all of them are sufficiently thick to perform individual variogram analysis. *DBMAFSIM* utilizes the variogram information for generating the simulations. Therefore, for this case study it is more appropriate to model the spatial continuity using a on one structure variogram model. The variograms that need to be modeled are based on the MAF factors. The modelled variograms for each one of the four grades in the form of MAF factors are then used to simulate the grades inside each lithology. Only the composites of the drillholes belonging to each respective lithology are used during the simulation.

As mentioned in Section 3.2, each of the simulated variables modeled herein needs first be transformed to normal scores and then using a lag distance of 150m in Eq. (15) to define the matrix of MAF factors. Specified lag distance is derived by trial and error technique to ensure suitable decorrelation of the MAF factors given the uneven spacing between drillholes.

After the data decorrelation is performed, a cross-variogram is generated to ensure the orthogonality of the different variables. Figure 23, describes the cross-variogram of the variables after MAF. It shows that there are no spatial cross-correlations between the four different factors for different lithologies, suggesting that variables are successfully decorrelated using MAF technique. The decorrelated variables are termed as MAF factors for further references.

I, the Pearson's and Spearman's correlation coefficients were calculated for the MAF factors. The results are presented in tables 5 and 6 respectively. Both correlation coefficients tends to zero ($\rho \sim 0$), ($r \sim 0$) for all the MAF factors, confirming that the MAF factors were successfully decorrelated.

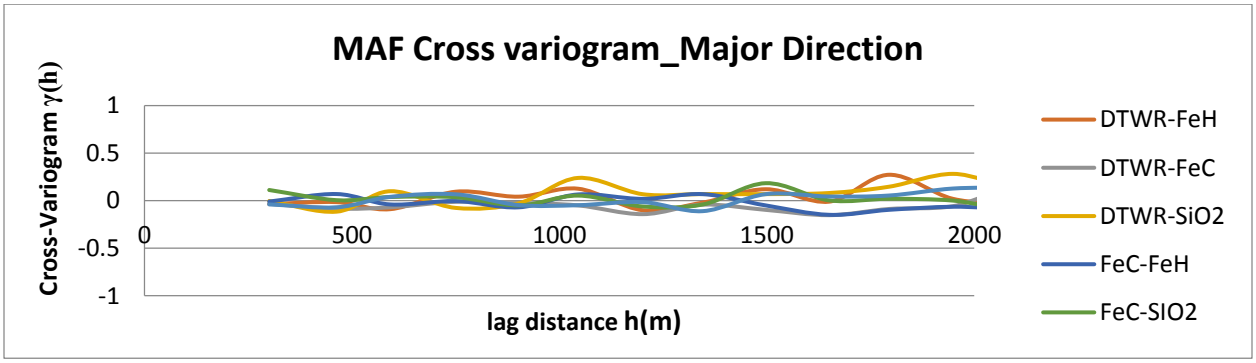

Figure 23. Correlogram between MAF factors– Major direction.

Table 5. Pearson's correlation coefficient for the MAF factors.

	FeH	**DTWR**	**FeC**	**SiO_2**
FeH	1.00	0.00	0.00	0.00
DTWR	0.00	1.00	0.00	0.00
FeC	0.00	0.00	1.00	0.01
SiO_2	0.00	0.00	0.01	1.00

Table 6. Spearman's correlation coefficient for the MAF factors.

	FeH	**DTWR**	**FeC**	**SiO_2**
FeH	1.00	0.00	0.00	0.00
DTWR	0.00	1.00	0.00	0.00
FeC	0.00	0.00	1.00	-0.009
SiO_2	0.00	0.00	-0.009	1.00

4.3.3 Conditional simulation of MAF factors

Further, after decorrelation of the variables, conditional simulations for different MAF factors within different lithologies (simulated previously) can be performed independently using Eq. (17) and averaged into blocks using Eq. (22).

Fifteen simulations are generated for each lithology (total of 15 x 7 = 105 simulations) using blocks of 100mx100mx15m discretized by 5x5x2 points per block. The modelled area of the deposit is 70 by 100 by 26 blocks along strike, dip and vertical direction that constitutes a total of 182,000 blocks.

4.3.4 Validation of the simulated grades

For validation of simulation generated using *DBMAFSIM*, the point-scale simulated values for some simulations in all the lithologies are retrieved and validated in data space.

4.3.4.1 Visual inspection of the simulations

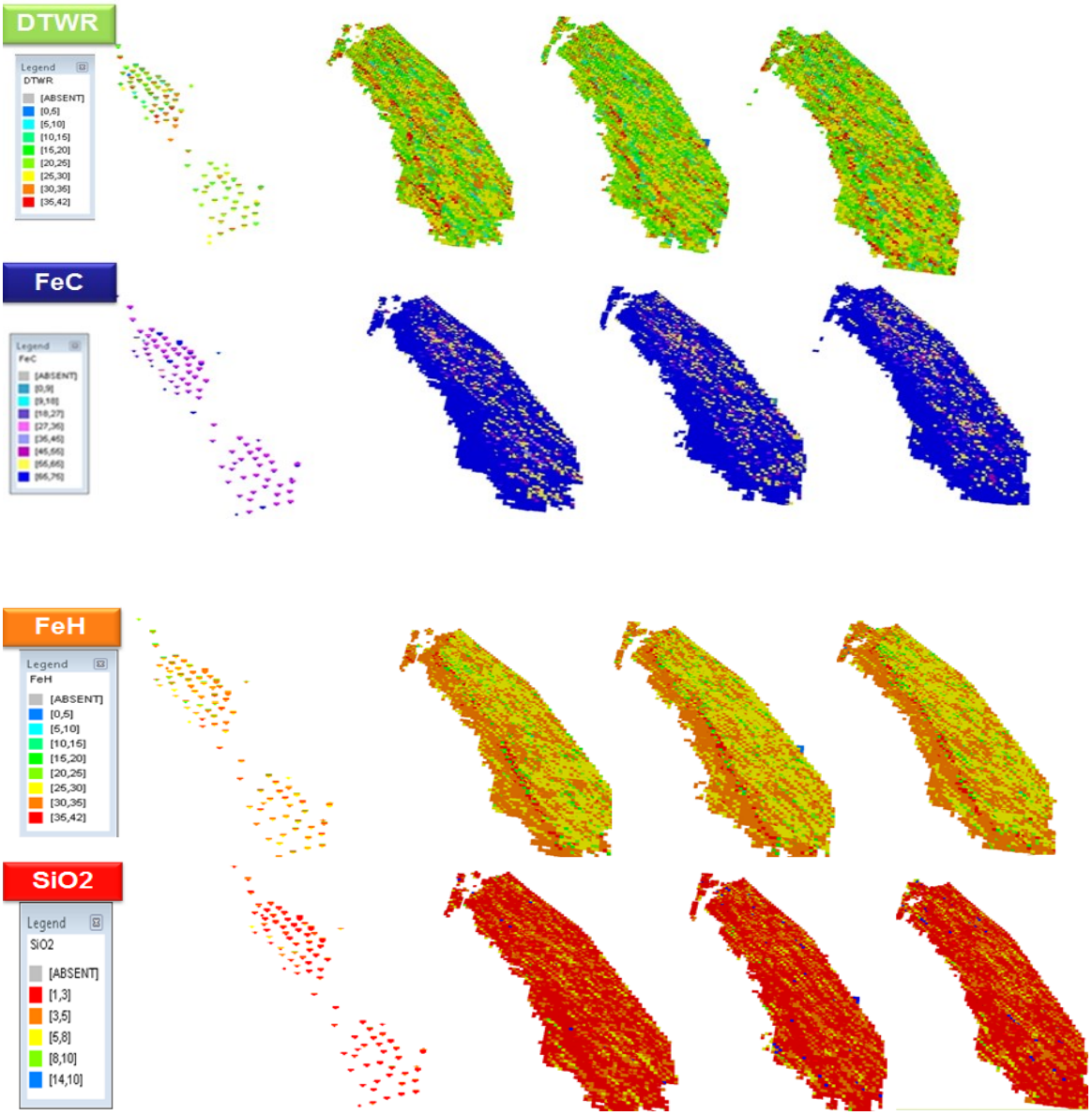

Figure 24. Plan view of hard data (drillholes) and some simulations for each grade simulated.

Figure 24 shows the plan view of the four simulated elements within simulated boundaries of the lithologies, highlighting that despite presenting different boundaries (because they are simulated inside different categorical orebody simulations) the simulations of grade attributes tend to reproduce the same spatial pattern of the drillhole information i.e. coinciding high grade and low grade areas between simulations.

4.3.4.2 Histograms of the simulations

The results of two lithologies 9LRGC and 5GC lithology are posted in Figures 25 and 26. Lithology 9LRGC is the one containing more hematite, and although lithology 5GC is not considered important because its iron content is low, this lithology is one of the thinnest layers of the set of lithologies. Therefore, this lithologies were chosen to represent the results in this thesis, but the validation is done for all of them. Figures 25 and 26 show that the distribution of each simulated attribute within one of the lithologies, and honours the declustered statistics inferred from the hard data.

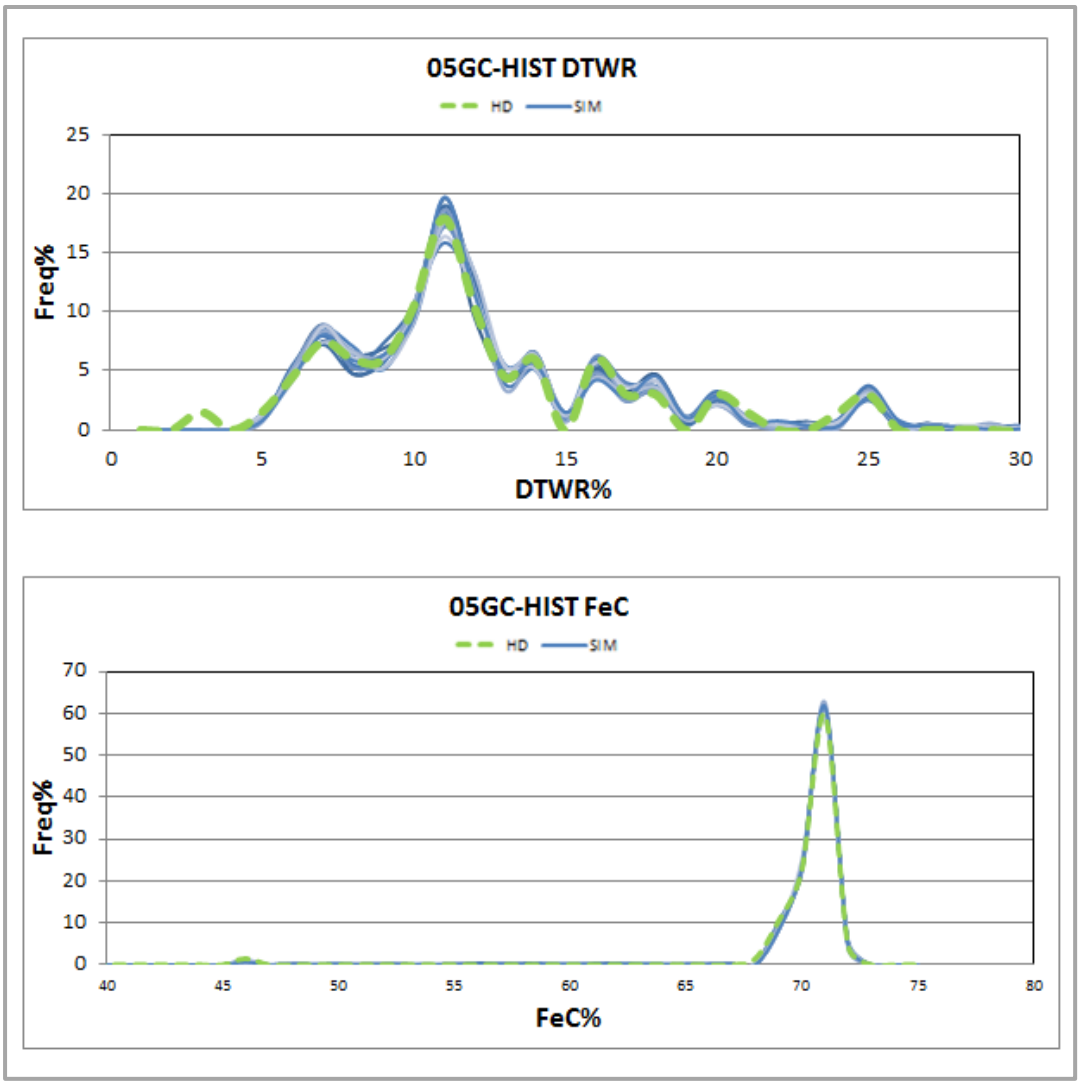

Figure 25. DTWR and FeC histogram for a single lithology 5-GC.

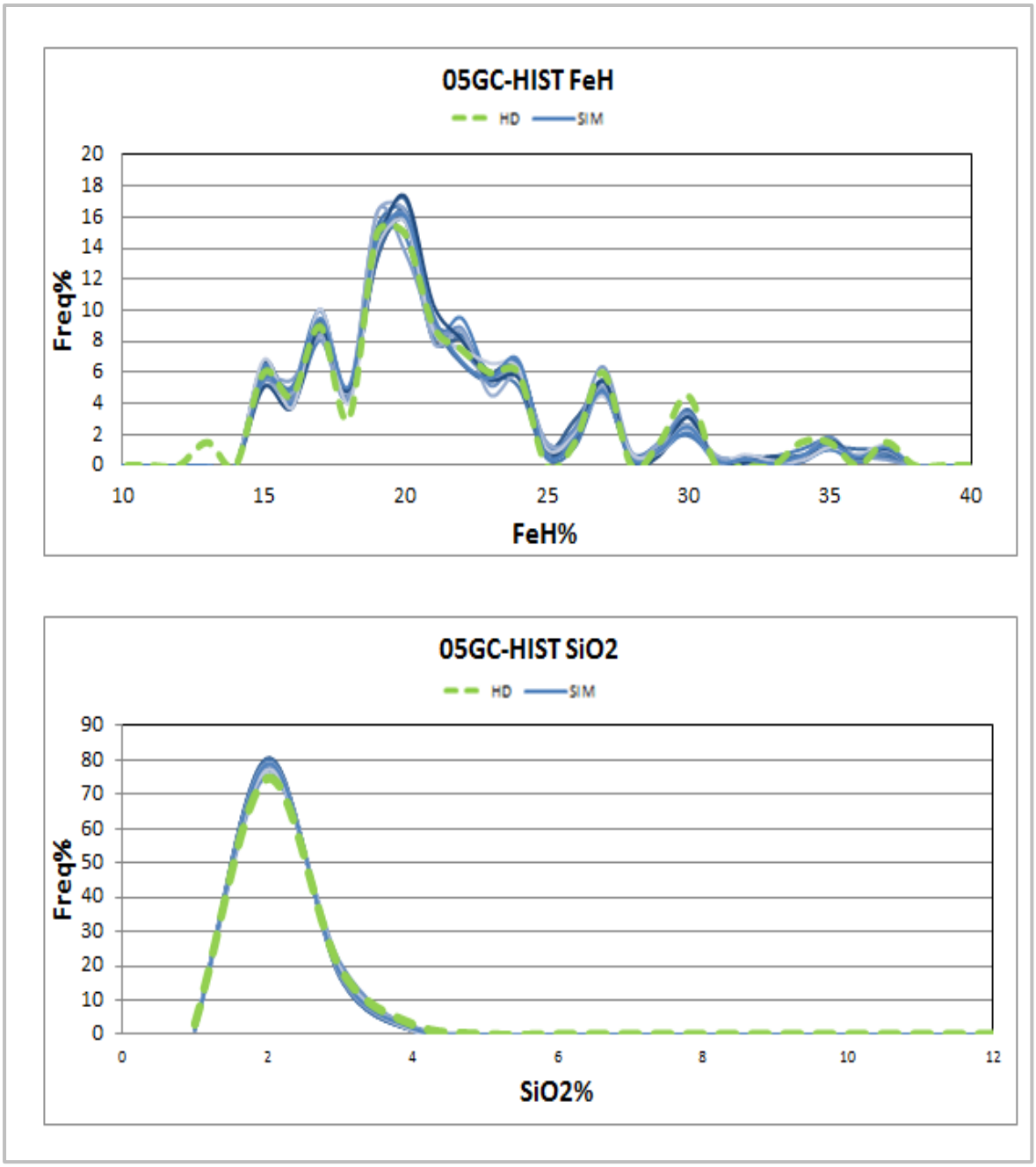

Figure 26. FeH AND SiO2 histogram for a single lithology 5-GC**.**

4.3.4.3 Variograms of the simulations

Figures 27, 28, 29, 30 and 31 show some variograms and cross-variograms for the hard data and the simulations in point support scale, within lithology 5GC and 9LRGC respectively for validations purposes. Overall, the simulations reproduce the spatial features of the hard data. The simulation variograms are reasonably consistent with the hard data for a range of 2km.

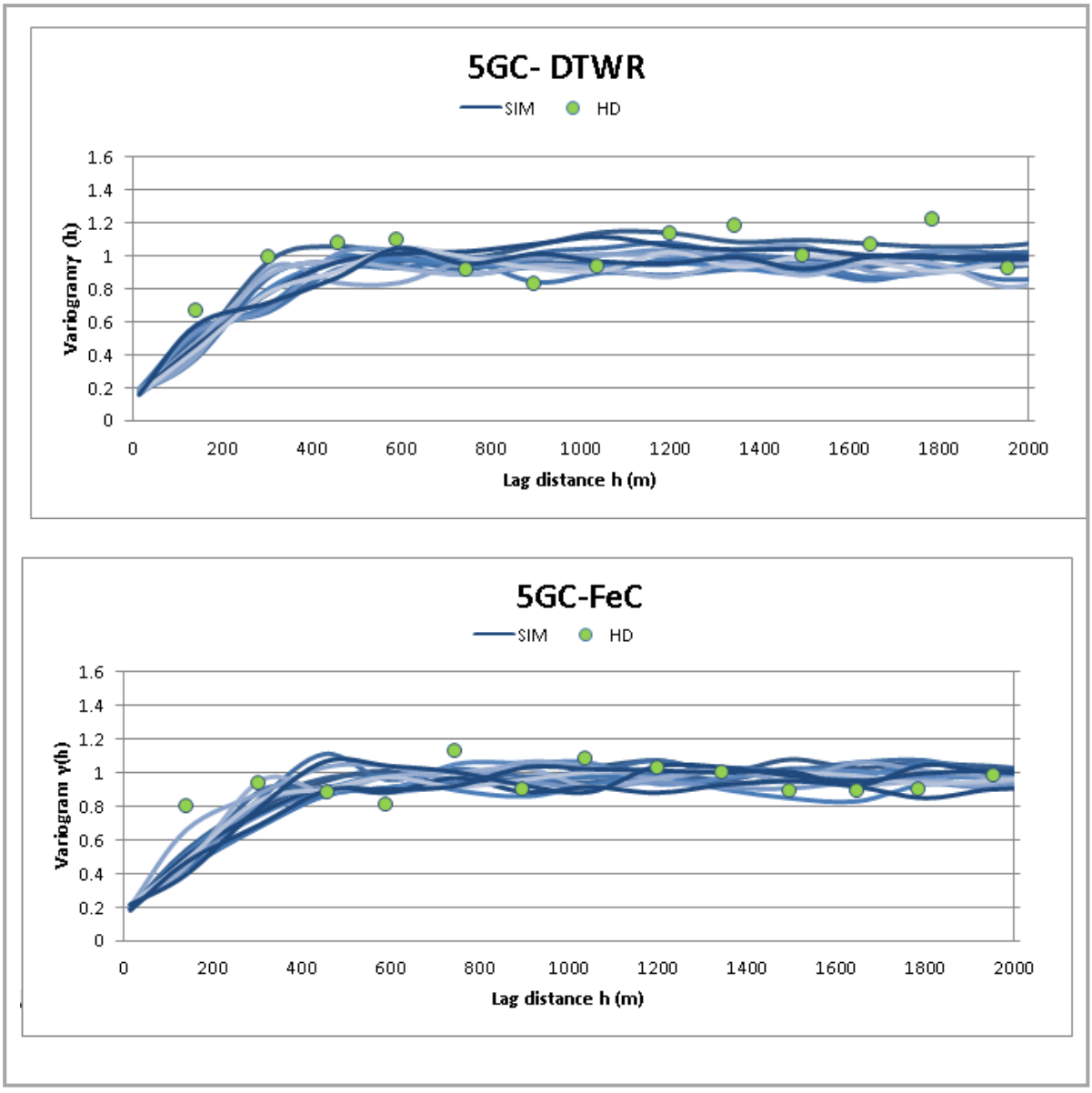

Figure 27. Variogram of DTWR and FeC in lithology 5-GC (point support scale).

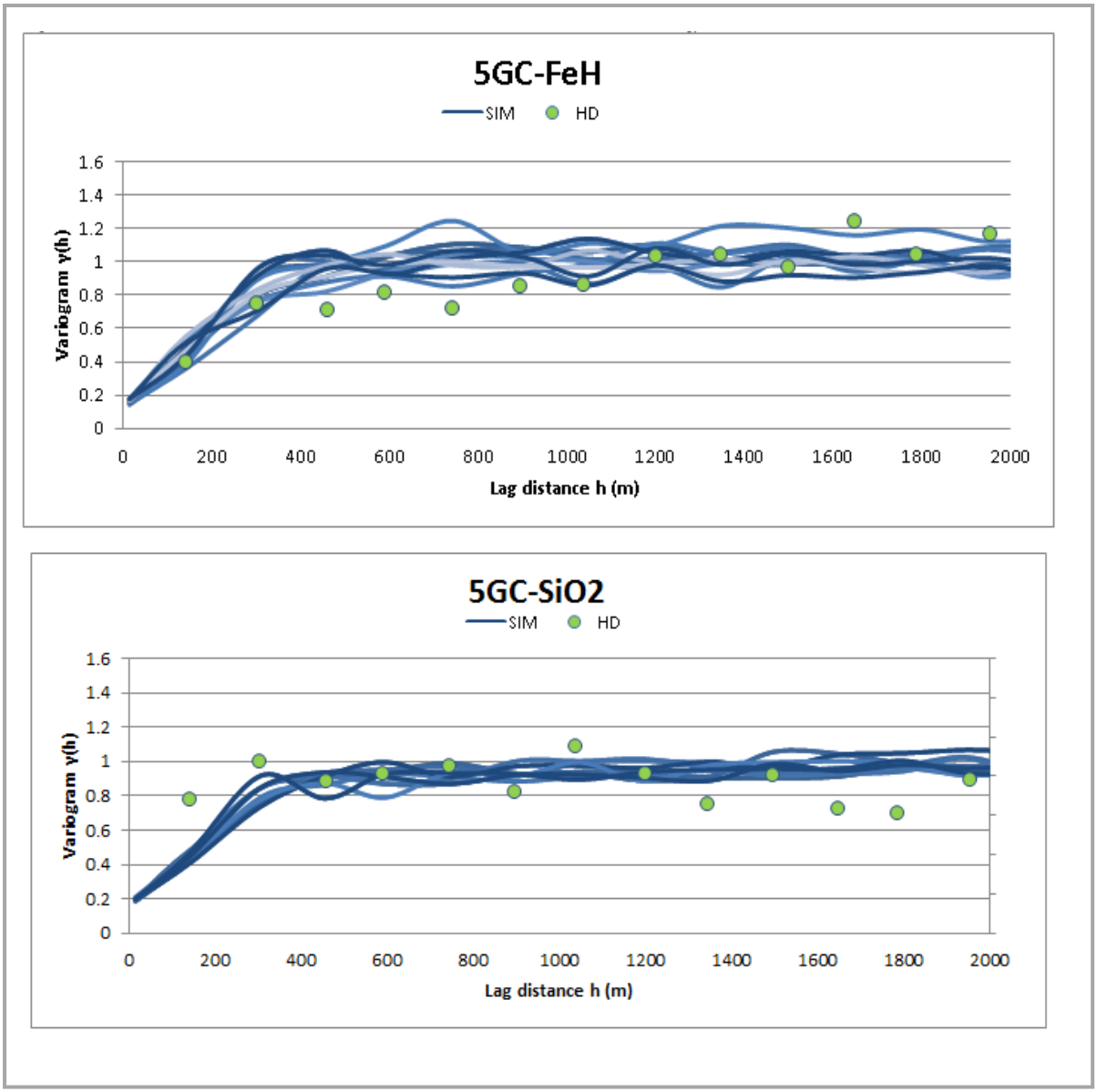

Figure 28. Variogram of FeH and SiO_2 in lithology 5-GC (point support scale).

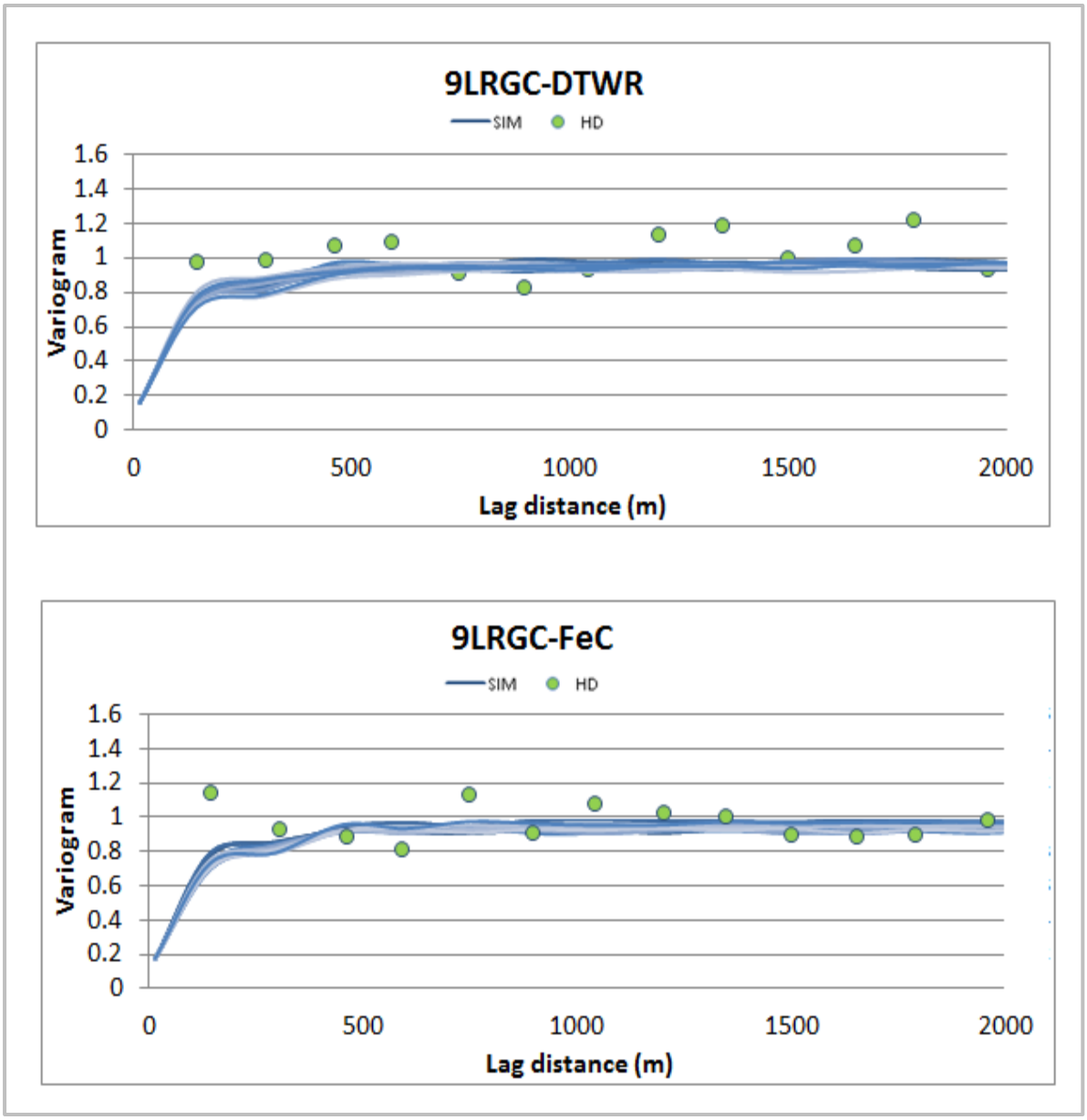

Figure 29. Variogram of DTWR and FeC in lithology 9-LRGC (point support scale).

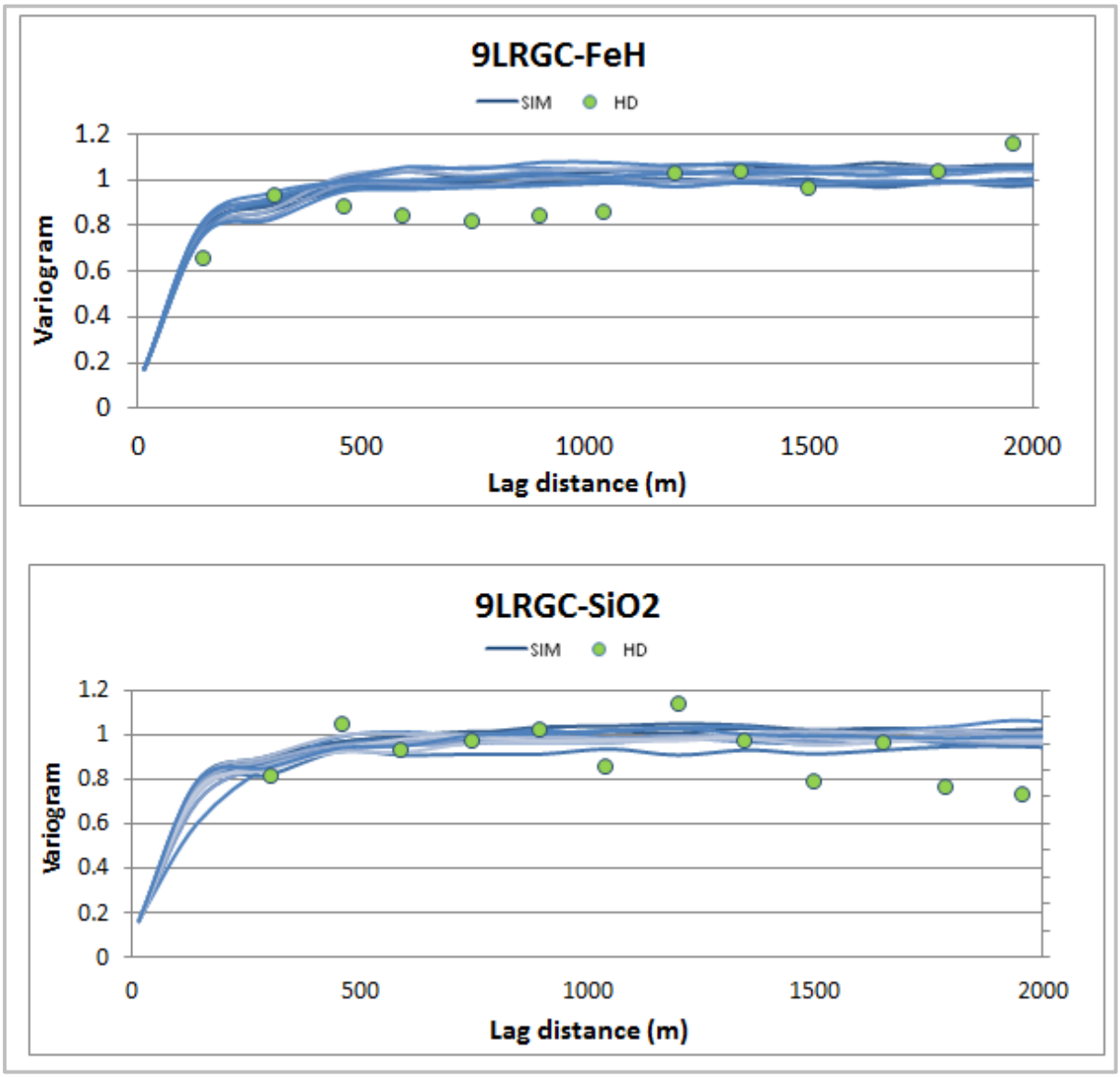

Figure 30. Variogram of FeH and SiO2 in lithology 9-LRGC (point support scale).

From Figure 31, the cross-variogram for Fe-SiO_2 within lithology 9-LRGC, shows that the simulations respect and emulate the trends of the hard data in MAF space and data space. Indicating that *DBMAFSIM* keeps the spatial relations, given its ability to generate simulations directly at block support scale thus, preserves better the connectivity of the extreme values compared to other Gaussian simulation method that generates simulations in point support scale.

The arguments can be further justified with the explanations that *DBMAFSIM* method averages the points to generate block values and uses the block values as conditional information for further

simulation. Considering that profitability of mining projects is driven by high grade values, the importance of connectivity of extreme values is further emphasized and outlines the significance of *DBMAFSIM* method which preserves such connectivity of high grade values

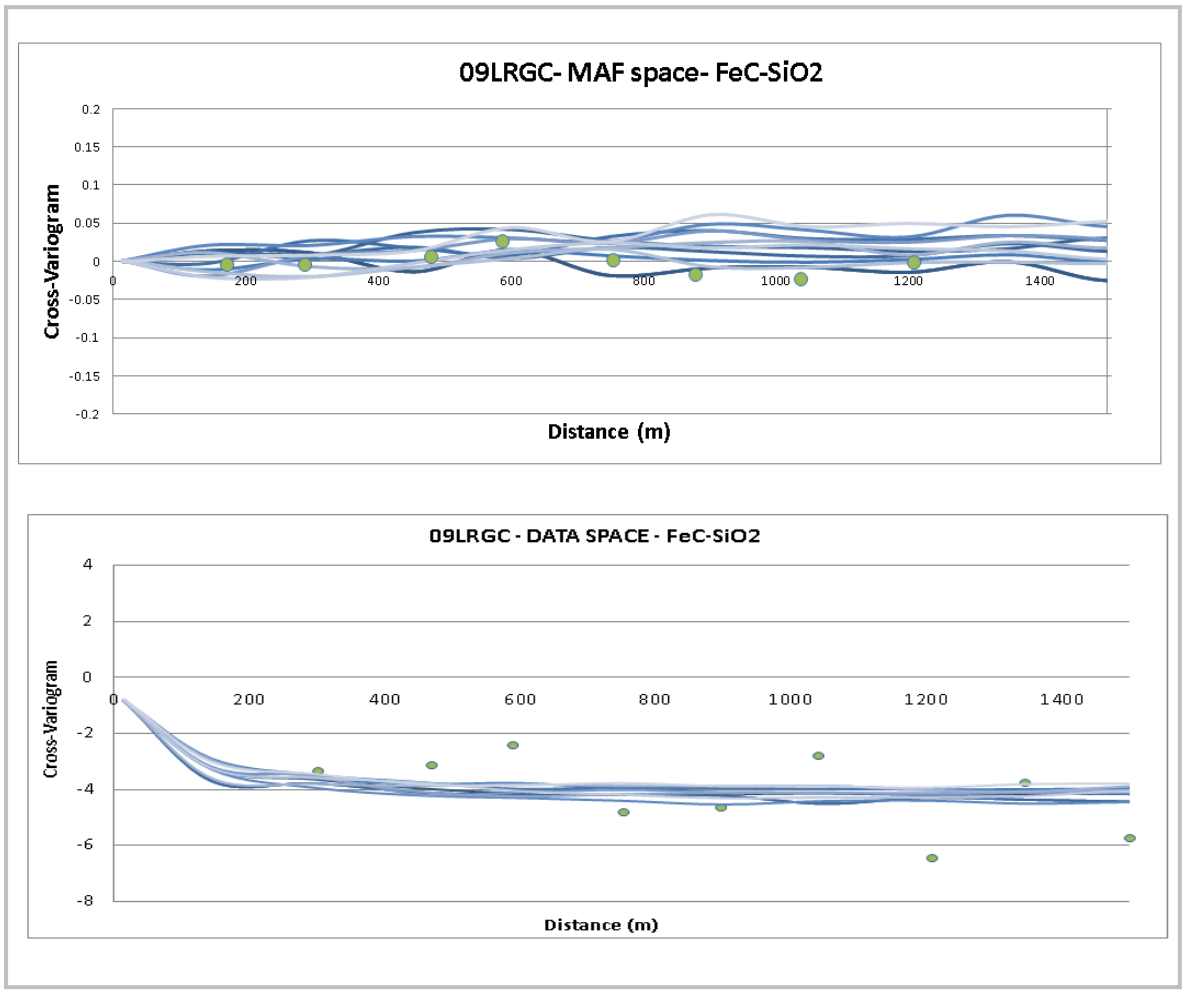

Figure 31. Cross-Variogram for simulation of two grades in a single lithology in MAF space (upper graph) and Data Space (lower graph), compared to hard data (green dots).

Validation of the simulated grade attributes generated using *DBMAFSIM* suggest that the simulations are following the same trend and behaviour as the hard data information (data space).

4.4 SIP-mining schedule: quantification of variability

In chapter 3 it was outlined that a realistic forecast of the long term mine production scheduling, is obtained using stochastic integer programming (SIP).The intensive investments associated with iron projects highlights the importance of assessing the risk, which can be modelled through the use of the jointly simulated geological scenarios in order to ensure the viability of the project.

As mentioned in Section 4.1, the deposit considered in this case study does not s have strictly defined information regarding the mining and production rates, owing to the feasibility stage of the project. Therefore, for the purposes of this thesis and viability of the application, most of the constraints for the SIP model are procured from the production estimations for the LabMag deposit, also a property of NML (Spleit, 2014; Rimele, 2016).

For taconite deposits, a control of FeC and, SiO_2 the only deleterious material is required. The production of fine iron concentrate is generated through beneficiation and can be sold as a final product. However, due to the characteristics of the deposit, the extracted material is preferably pelletized because the selling price of iron pellets is higher in comparison to the selling price of iron concentrate.

For the purposes of this thesis a 10 years mine production schedule is generated, with a yearly production target of 10 Mt of iron ore concentrate. To produce pellets, LabMag's metallurgical plant was designed and optimized for a concentrator with an average input of a DTWR of 27%. The performance of the metallurgical plant might be affected by the silica content which for this kind of operation is expected to be in between 2.3% and 2.9%.The above parameters were originally designed form LabMag deposit, and are the parameters used to define the constraints of the SIP model for the KéMag deposit.

4.4.1 Stochastic mine production scheduling

The results of the stochastic mine production scheduling using the 15 simulations obtained through the processes described in Sections 3.1 and 3.2 are shown in Figures 32 to 36. Note that the presented results represents the fully binary solution of the relaxed model obtained through the use of a Topological Search Algorithm (TSA) (see Section 3.3.6).

Figure 32 shows the obtained mine and destination schedule per block, we can see that the areas (destination and production period) are well defined describing a practical mining sequence considering the layered strata type nature of the deposit and the size of the blocks. This is the result of the implementation of the smoothing constraints (eq. (31)) in the general OMPSIP. The plan view of Figure 32 also shows that the first period is where the waste lithologies (layers) are extracted, this is due to the fact the waste lithologies (OB and MS) are mostly overlying the ore material. It can be also appreciated that some artifacts still exists as isolated blocks to be mined in some periods. This can be further improved using some pre-processing algorithms. However, is not discussed in the current work and it is out of the scope of this thesis.

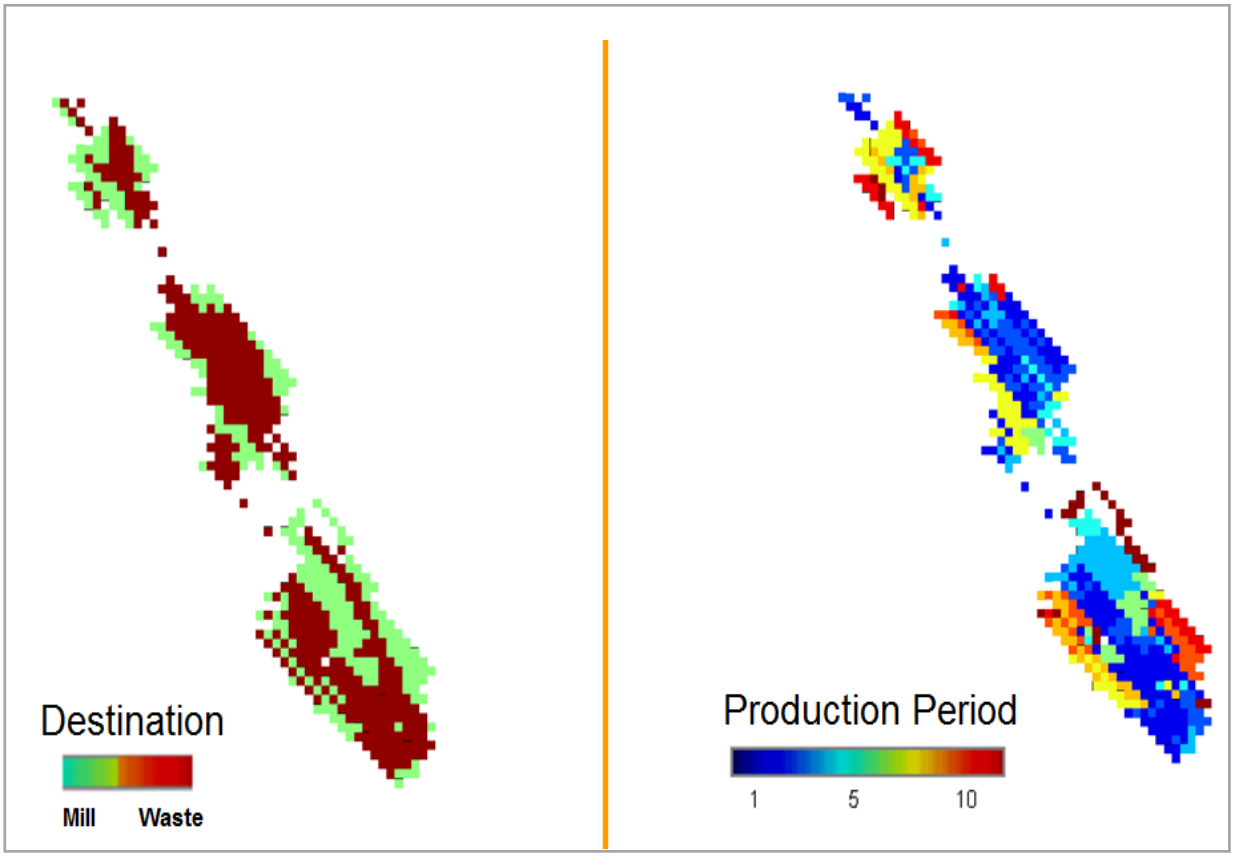

Figure 32. Destination (right) and Mine schedule (left) plan view

As was outlined in Section 3.3.5, solution of the relaxed model is considered as the upper theoretical limit for the solution of the general OMPSIP model. The tonnage, and qualities for each period are evaluated for each simulation in order to analyze the variability per period in terms of tonnage and quality targets for a LOM of ten years. From Figure 33 we can see that the estimated

target production of 10 million tonnes per year is hardly achieved over all simulations and even the expected (average type) realization fails to achieve the concentrate target.

The run of mine (material sent to the mill), which was not constrained, is plotted in figure it can be seen that the differences between scenarios are not significant. This is important in terms of mine equipment selection (trucks and shovels). However the implications related to the ROM are out of the scope of this thesis and are not considerable given the early stage of the project.

In terms of production, achieving the targeted concentrate tonnage is usually one of the main goals of the production scheduling. Nevertheless, from Figure 36, a steady behaviour of DTWR production can be seen, varying within the expected ranges and averagely around 27% as is desired for the concentrator. It is important to mention that the annual fluctuations of concentrate production are balanced by the DTWR production. For instance a year with less concentrate production has a greater average weight recovery implying that less ore must be mined to produce the same tonnage of concentrate.

On the other hand from Figure 35, it can be seen that Silica production deviates from production targets in the last periods. The average amount of Silica must be kept beneath a certain level when pellet production is desired, given that Silica is considered as an impurity and affects the selling price.

This is definitely not bad news for the project, given the key production targets and project indicators used to obtain the mine sequence are borrowed from another deposit of similar conditions, thus the results are not the finest. This project is under feasibility stage it means that the project is being evaluated in terms of its practical and financial viability. Then, these results are useful for the company and provide valuable information such as planed concentrate iron production of 10 Million tonnes per year might not be achievable in KéMag and that the average % SiO_2 is higher in KéMag than in LabMag deposit. Therefore, controlling the silica production becomes a new target for subsequent optimizations, since a consistent silica blend is desired across all periods. Changes in the input parameters and production targets for the SIP model can be studied and could result in better solutions but are outside of the scope of this thesis.

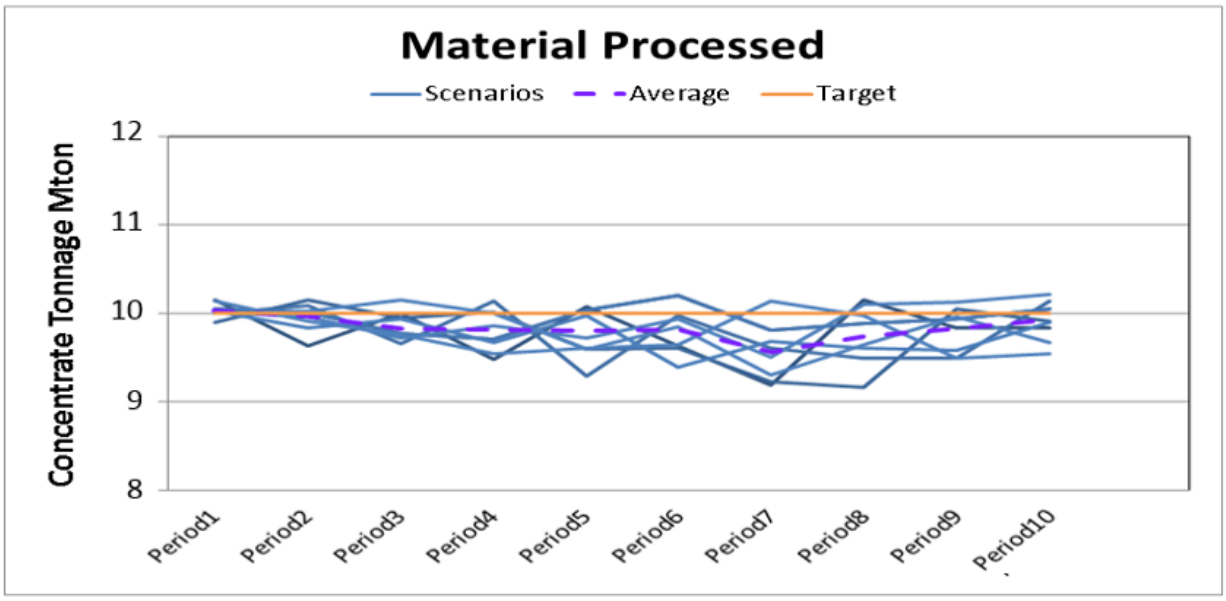

Figure 33. Yearly iron ore concentrate tonnes.

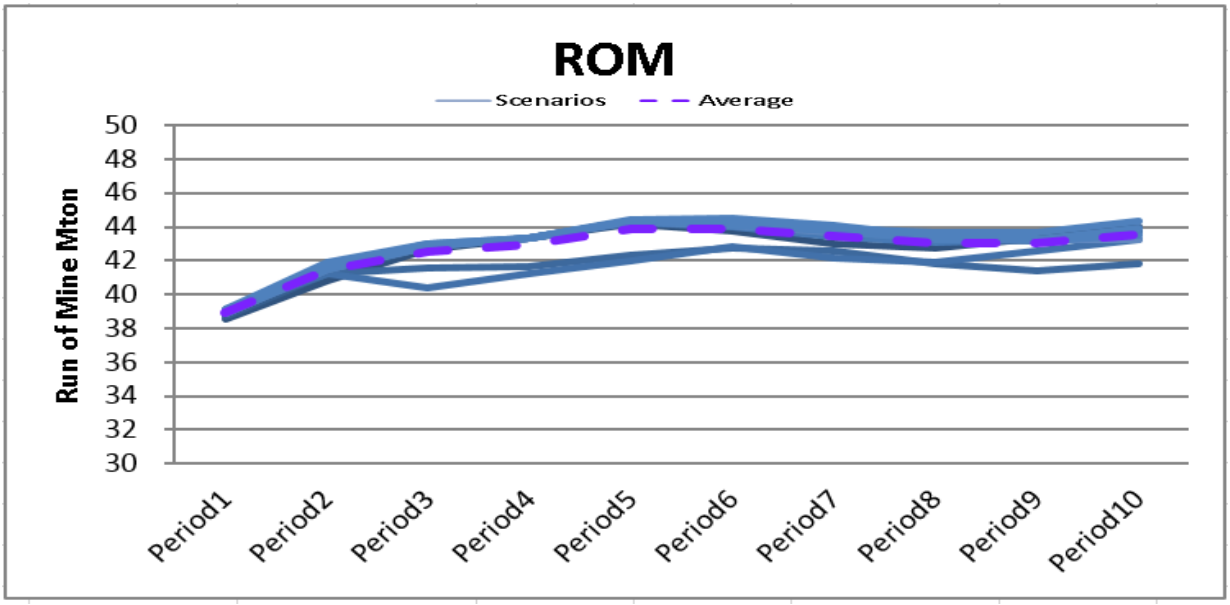

Figure 34. Yearly ROM

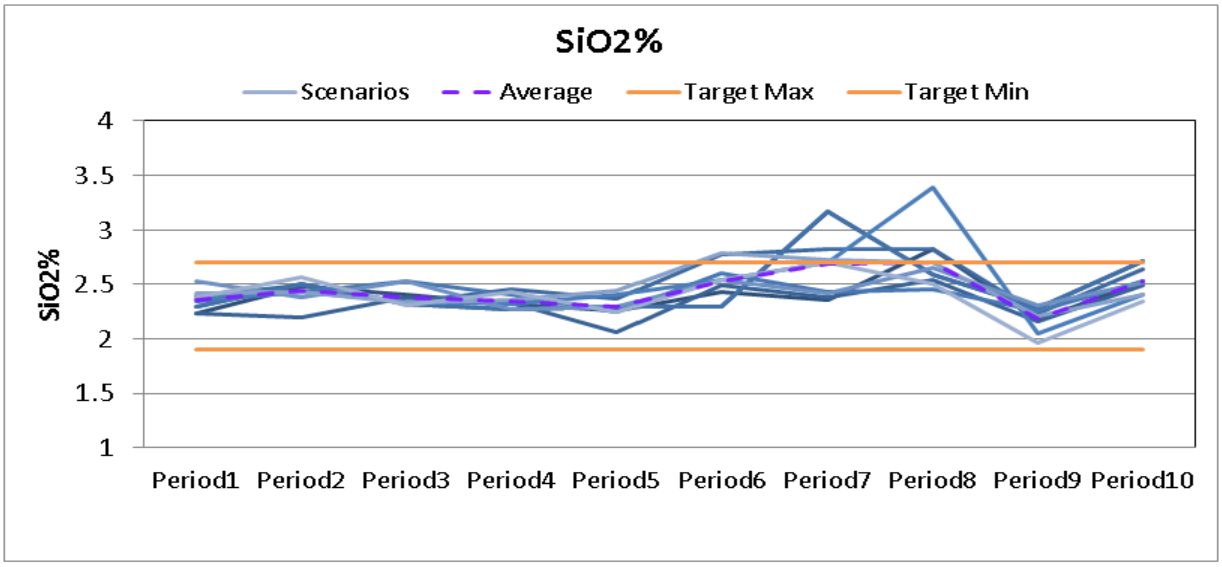

Figure 35. Yearly Silica production

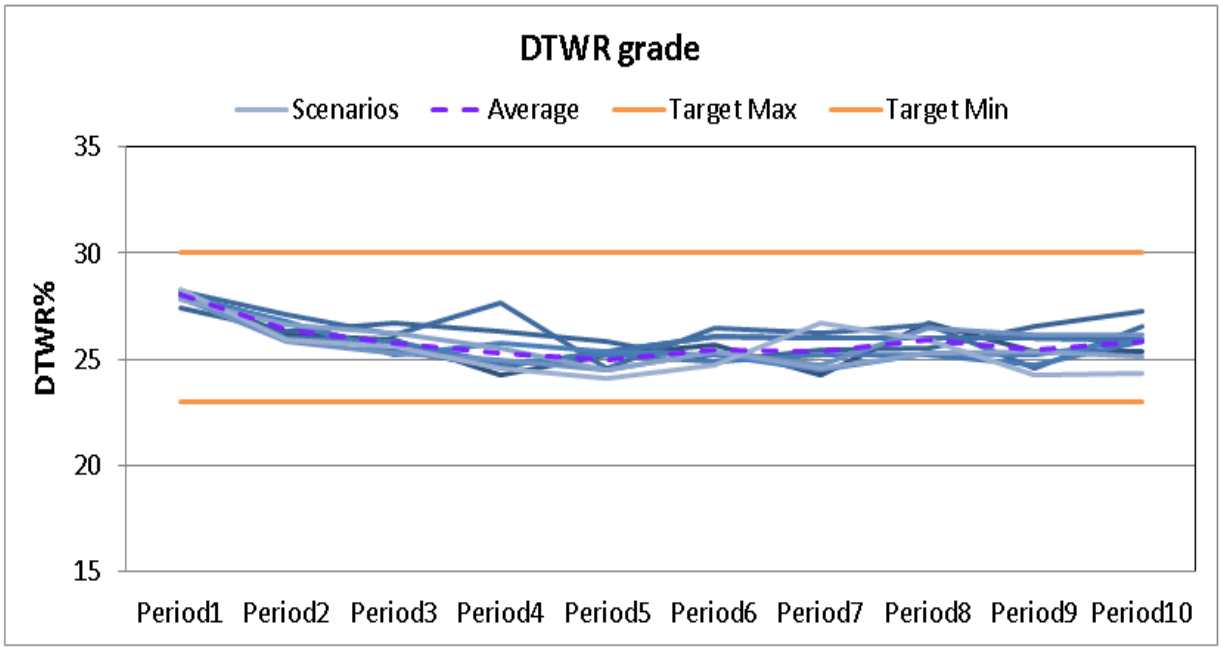

Figure 36. Yearly DTWR% production

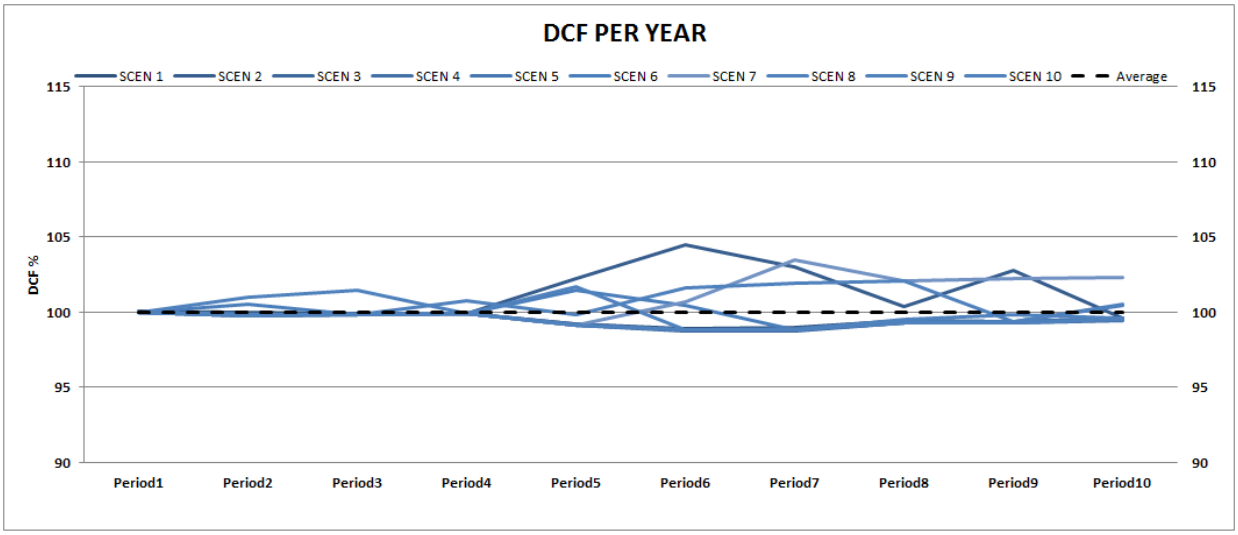

Figure 37.Yearly discounted cash flow (DCF %).

Figure 37 shows the DCF profiles for all the scenarios and their average. It can be observed that the scenarios do not present significant deviations from the average, except for period 6 and 7 where the DCF deviates in the order of 4%. This is because when the SiO_2 % goes higher in these periods (see Figure 35) the penalties applied over deviation from production target affects the revenue. This result might be considered acceptable because the risk is deffered to later periods with the applied risk discounting factor and is same as the economic discount factor.

CHAPTER 5

CONCLUSIONS AND RECOMMENDATIONS

5.1 Conclusions

This thesis addresses a complete stochastic mine planning framework in an application at an iron ore deposit in feasibility stage. In this stage of a project it is crucial to have mine plans and production schedules that provide a high degree of profitability and an overall understanding of all risks involved in the development of the project. The deposit used in this case study is the KéMag iron ore deposit, property of New Millennium Iron Corp (NML) and the full case study comprises the generation of a set of equally probable realizations of the deposit and the optimization of long term mine production schedule while considering the inherent geological uncertainty of the deposit.

Methods for stochastic geological simulation of categorical and continuous variables were described in the technical literature review. From the application of *WAVESIM* and *DBMAFSIM* in the KéMag deposit, a set of equally probable geological scenarios which capture the inherent uncertainty of the deposit were generated and then, used as input to stochastically optimize the mine production schedule in order to manage risk while seeking for a better revenue.

For this case study *WAVESIM* was chosen to model uncertainty of the seven iron –bearing layers and two overlying layers considered as waste material. This method was chosen because *WAVESIM* is a multiple point simulation method that captures the high-order statistics from training image and hard data. For the simulation of continuous variables, given the correlation of the grades in the KéMag deposit, a method called *DBMAFSIM* which is a combination of Direct Block Simulation method (DBSIM) and Minimum/Maximum Autocorrelation Factor (MAF), was chosen to model the grade uncertainty concurrently keeping the original correlation of the variables of interest. In this case study head iron, Davis Tube weight recovery, Davis Tube concentrate iron and silica grade were successfully modelled.

The generated set of simulations (realizations) were validated in terms of lower order statistics (variograms and histograms) and also for the simulations of the iron layers a third order cumulants

map was built to validate that the high-order relations were reproduced in the simulations. The statistics of the realizations were compared to both training images and drillhole samples statistics. This comparison showed as was mentioned in the literature review that all multiple point simulation methods are training image driven. It means that the statistics of the realizations tend to be in between the statistics of the training image and of the hard data. Thus, the training image has to be a representative of the deposit in order to obtain valid simulations.

Further, the validated simulations of the KéMag deposit were used as input for the stochastic optimization of the production schedule through a SIP framework coupled with a heuristic solution technique in order to acquire fast and efficient solution to the production scheduling problem that maximizes the expected value of the discounted cash flows by managing geological risk. Geological risk management for the outlined production schedule problem was incorporated by strictly reducing risk in the earlier years i.e., minimizing the risk of deviation from concentrate tonnage targets and produced silica target. It was shown that realized production tonnages and grade qualities could significantly vary (mostly for the last years of the life of mine, specifically for the Silica production) compared to the planned targets for quality and quantity attributes. In a sense, this was expected because given the feasibility stage of the KéMag mine project, the ideal operational parameters are not available yet. Therefore, for the purpose of the work presented in this thesis, the parameters modelled for other deposit of similar characteristics were utilized.

5.2 Recommendations

For multiple point simulation methods one of the challenges associated with their practical application is related to their lack of mathematical formality and their inability to guarantee that lower order statistics from the drillholes (hard data) information are reproduced during the simulation procedure. Multiple point simulation methods often tend to treat any point within a data event with equal importance and given that the TI contains more data points than the hard data, the simulations tends to reproduce more the statistics of the TI, rather than the statistics of the hard data. Given that MPS methods rely on scanning a training image to obtain a set of patterns, if there is a difference between the hard data information coming from the drillholes and the patterns in the training image any MPS method will tend to reproduce the statistics of the training image better than of the hard data. Therefore the results of the simulations tend to be training-image driven. The

argument was confirmed when the histogram and variograms of the simulations of the geological lithologies of the KéMag deposit where compared to the statistics of the drillholes and Training Image.

Thus, new methodologies to obtain data-driven high-order characterization of spatial uncertainty of lithological units, material types, and multi-element deposit simulations are required. Hopefully, a general framework for simulation of both categorical and continuous variables will be formulated in the future. Development of high-order approaches to simulate multiple correlated elements is also required. The data-driven spatial simulation of correlated random fields can be approached through a decorrelation framework, similar to past work for multivariate Gaussian random fields as shown for Minimum/Maximum Autocorrelation Factors. Utilizing the MAF technique, each one of the uncorrelated factors can be simulated independently using high-order simulation methods on the basis of high-order spatial cumulants.

In the last years, some high-order sequential simulation techniques for non-Gaussian spatially distributed variables has been developed based on concepts of high-order spatial cumulants. Limitations of this work include the case-dependent numerical instabilities in the approximation of probability density functions during the sequential simulation process. Moreover, high-order spatial statistics techniques are computationally demanding.

The extension of the KéMag deposit comprises a vast area of 14.5 km long and 8.5 km wide, therefore, a small block discretization might result in a huge amount of binary variables for the mathematical model limiting the use of conventional solvers like CPLEX –IBM. The block size for the geological simulations in this study was 100 m x 100m x 15 m in order to compare with a future conventional schedule that NML is preparing using this same level of selectivity. This block size is appropriate for an estimated model but for simulations, a smaller block size could be potentially important for capturing variability at the scale of equipment selectivity (SMU) and other features of interest.

The selected block size for simulation of continuous variables of interest (grades) seems to produce good results in terms of histogram and variogram reproduction. Also, it is worth to mention that the selected block size results in fewer binary variables for the SIP model and thus faster solution

can be acquired given that the amount of blocks to be processed is considerably less than using a smaller SMU.

The stochastic models described in the previous sections are characterized by a large number of binary variables and non-linear constraints and are required to simultaneously optimize the different components of the downstream process of the mineral value chain. Use of heuristics and metaheuristics algorithms combined with recent developments in open pit production scheduling is prevailing to obtain a "near-optimal" solution considering the large size of the problem for mineral value chain optimization which simultaneously optimizes the extraction sequencing, destination policies and processing stream decisions.

Finally, an optimization strategy can be applied to the KéMag deposit, aiming to optimize multiple aspects of the mining project. This could include managing (but not limited) the tonnage and qualities of ore, control of silica production, inclusion of a variable processing cost dependant on the quality of the ore being processed, as well as the inclusion of variable plant efficiency and the use of different operating modes.

REFERENCES

Albor Consuegra, F., & Dimitrakopoulos, R. (2009). Stochastic mine design optimisation based on simulated annealing: pit limits, production schedules, multiple orebody scenarios and sensitivity analysis. *Mining Technology: IMM Transactions Section A, 118*(2): 79-90.

Albor Consuegra, F., & Dimitrakopoulos, R. (2010). Algorithmic approach to pushback design based on stochastic programming: method, application and comparisons. *Mining Technology: IMM Transactions Section A 119*(2), 88-101.

Arpat, G. (2004). *Stochastic simulation with patterns. PhD thesis, Stanford University. CA 94305-2220.*

Arpat, G. B., & Caers, J. (2007). Conditional simulation with patterns. *Mathematical Geology, 39*(2): 177-203.

Barr, D. (2012).*Stochastic dynamic optimization of cut-off grade in open pit mines. Master's thesis, Queen's University, Kingston, Ontario, Canada*.

Benndorf, J., & Dimitrakopoulos, R. (2013). Stochastic long-term production scheduling of iron ore deposits: Integrating joint multi-element geological uncertainty. *Journal of Mining Science, 49*(1):68-81.

Birge, J., & F. Louveaux (1997). Introduction to Stochastic Programming. *Springer series in operations research and financial engineering*. 2nd edition, New York.

Boucher, A., & Dimitrakopoulos, R. (2007). A new efficient joint simulation framework and application in a multivariable deposit. *Orebody Modelling and Strategic Mine Planning*, (1), 319-328.

Boucher, A., & Dimitrakopoulos, R. (2009). Block simulation of multiple correlated variables. *Mathematical Geosciences,* 41(2):215-237.

Boucher, A., & Dimitrakopoulos, R. (2012). Multivariate block-support simulation of the Yandi iron ore deposit, Western Australia. *Mathematical Geosciences,* 44(4): 449-468.

Chatterjee, S., Dimitrakopoulos, R., & Mustapha, H. (2012). Dimensional reduction of pattern-based simulation using wavelet analysis. *Mathematical Geosciences, 44*(3): 343-374.

Chicoisne, R., Espinoza, D., Goycoolea, M., Moreno, E., & Rubio, E. (2012). A new algorithm for the open-pit mine production scheduling problem. *Operations Research, 60*(3): 517-528.

CRIRSCO (2006). International reporting template for the public reporting of exploration results, mineral resources and mineral reserves. Retrieved from website: http://www.crirsco.com/crirsco_template_v2.pdf

David, M. (1988). Handbook of applied advanced geostatistical ore reserve estimation. *Developments in Geomathematics*. Elsevier, Amsterdam.

De Freitas, M., & R. Dimitrakopoulos (2014). Simulation of Weathered Profiles Coupled with Multivariate Block-support Simulation of the Puma Nickel Laterite Deposit, Brazil. *COSMO Stochastic Mine Planning Laboratory: Technical Report* (1): 214-246.

Desbarats, A., & Dimitrakopoulos, R. (2000). Geostatistical simulation of regionalized pore-size distributions using min/max autocorrelation factors. *Mathematical Geology, 32*(8): 919-942.

Dimitrakopoulos, R. (2011). Stochastic optimization for strategic mine planning: a decade of developments. *Journal of Mining Science,* 47(2):138-150.

Dimitrakopoulos, R., Farrelly, C., & Godoy, M. (2002). Moving forward from traditional optimization: grade uncertainty and risk effects in open-pit design. *Mining Technology: IMM Transactions Section A,* 111(1): 82-88.

Dimitrakopoulos, R., & Jewbali, A. (2013). Joint stochastic optimisation of short and long term mine production planning: method and application in a large operating gold mine. *Mining Technology: IMM Transactions Section A,* 122(2): 110-123.

Ding, C., & He, X. (2004). K-means clustering via principal component analysis. *Proceedings of the twenty-first international conference on Machine learning*. ACM.

Dowd, P. (1976). Application of dynamic and stochastic programming to optimize cutoff grades and production rates. *Transactions of the Institute of Mining and Metallurgy. Section A. Mining Industry,* 85(1): 22-31.

Escudero, L. F., Kamesam, P. V., King, A. J., & Wets, R. J. (1993). Production planning via scenario modelling. *Annals of Operations research,* 43(6): 309-335.

Faucher, C., Saucier, A., & Marcotte, D. (2013). A new patchwork simulation method with control of the local-mean histogram. *Stochastic environmental research and risk assessment,* 27(1):253-273.

Geman, S., & Geman, D. (1984). Stochastic relaxation, Gibbs distributions, and the Bayesian restoration of images. *IEEE Transactions on pattern analysis and machine intelligence,* (6):721-741.

Gershon, M. E. (1983). Optimal mine production scheduling: evaluation of large scale mathematical programming approaches. *International Journal of Mining Engineering,* 1(4):315-329.

Godoy, M. (2002). *The effective management of geological risk in long-term production scheduling of open pit mines. PhD thesis, University of Queensland, Brisbane, Australia.*

Godoy, M., & Dimitrakopoulos, R. (2004). Managing risk and waste mining in long-term production scheduling of open-pit mines. *Society for mining metallurgy and exploration, volume* 36: 43-50.

Godoy, M., & Dimitrakopoulos, R. (2010). A risk analysis based framework for strategic mine planning and design method and application. *Journal of Mining Science*, 47(2).

Goodfellow, R. (2014).a) *Unified Modelling and Simultaneous Optimization of Open Pit Mining Complexes with Supply Uncertainty* (Doctoral dissertation, McGill University).

Goodfellow, R., Albor, F., & Dimitrakopoulos, R. (2012). Quantifying multi-element and volumetric uncertainty Coleman McCreedy deposit, Ontario, Canada. *Computers & Geosciences*, 42(1): 71-78.

Goodfellow, R., & Dimitrakopoulos, R. (2013). Algorithmic integration of geological uncertainty in pushback designs for *complex multiprocess open pit mines. Mining Technology: IMM Transactions Section A, 122*(2): 67-77.

Goodfellow, R., & Dimitrakopoulos, R. (2014). b). Stochastic Global Optimization of Open Pit Mining Complexes with Capital Expenditures: Application at a Copper Mining Complex. *COSMO Stochastic Mine Planning Laboratory: Technical Report* (1): 224-256

Goodfellow, R., & Dimitrakopoulos, R. (2016). Global Asset Optimization of Open Pit Mining Complexes under Uncertainty. *Applied Soft Computing, 40* (1): 292-330.

Goovaerts, P. (1997). *Geostatistics for Natural Resources Evaluation (Applied Geostatistics Series). Oxford University Press, Oxford*.

Guardiano, F., & Srivastava, R. (1993). Multivariate geostatistics: beyond bivariate moments. *In Geostatistics Kluwer Academic Publications volume 1,* (1):133-144.

Hu, L., & Chugunova, T. (2008). Multiple-point geostatistics for modelling subsurface heterogeneity: a comprehensive review. *Water Resources W11413,* 44(1): 34-54.

Hu, L., Liu, Y., & Scheepens, C. (2014). Multiple-Point Simulation with an Existing reservoir Model as Training Image. *Math Geoscience 227,* 46(1): 94-106.

Huang, T., & Lu, D. E. (2013). GPU-based SNESIM implementation for multiple-point statistical simulation. *Computers & Geosciences*, 5*4*(1):75-87.

Isaaks, E. (1990). *The Application of Monte Carlo methods to the analysis of spatially correlated data, Ph.D. Thesis, Standford University.*

Johnson, T. (1968). Optimum production scheduling. *In Proceedings of the 8th international symposium on computers and operations research Salt Lake City press*.

Journel, A. (1989). Non-Gaussian data expansion in the Earth sciences. *Terra Nova,* 1(2):123-134.

Journel, A. (1994). Modelling Uncertainty: some conceptual thoughts. *Geostatistics for the next century Kluwer Dordrecht Holland,* (1): 30-43

Journel, A. (1989). Fundamentals of geostatistics in five lessons. *Short course in geology: American Geophysical Union*. volume 8, Washington, DC.

Kirkpatrick, S., Gelatt, C., & Vecchi, M. (1983). Optimization by simulated annealing. *Science,* 220(4598): 671-680.

Lamghari, A., & Dimitrakopoulos, R. (2012). A diversified Tabu search approach for the open-pit mine production scheduling problem with metal uncertainty. *European Journal of Operational Research, 222*(3): 642-652.

Lamghari, A., Dimitrakopoulos, R., & Ferland, J. (2013). A variable neighborhood descent algorithm for the open-pit mine production scheduling problem with metal uncertainty. *Journal of Operational Research Society*, (1):1-28.

Lamghari, A., Dimitrakopoulos, R., & Ferland, J. (2014). A hybrid method based on linear programming and variable neighborhood descent for scheduling production in open-pit mines. *Journal of Global Optimization,* (1):1-28

Lane, K. (1988). The Economic Definition of Ore: Cut-off Grades in Theory and Practice. *Mining Journal Books Limited*.

Leite, A. (2008). *Stochastic optimization approaches to open pit mine planning: Applications for the value of stochastic approaches. Master Thesis, Department of Mining and Materials McGill University. Montreal, QC- Canada.*

Leite, A., & Dimitrakopoulos, R. (2007). Stochastic optimization model for open pit mine planning: application and risk analysis at copper deposit. *Mining Technology: IMM Transactions Section A*, 116 (1):109-118.

Leite, A., & Dimitrakopoulos, R. (2014). Stochastic optimization of mine production scheduling with uncertain ore/metal/waste supply. *International Journal of Mining Science and Technology 24*(1):755-762

Leite, A., & Dimitrakopoulos, R. (2010). Production Scheduling Under Metal Uncertainty-Application of Stochastic Mathematical Programming at an Open Pit Copper Mine and Comparison to Conventional Scheduling. *Advances in Orebody Modelling and Strategic Mine Planning Series Volume 17*.

Lopes, J., Rosas, C., Fernandez, J., & Vanesa, G. (2011). Risk quantification in grade-tonnage curves, and resource categorization in a lateritic nickel deposit using geologically constrained Joint conditional simulation. *Journal of Mining Science and Technology,* (2): 166-176.

Mariethoz, G., Renard, P., & Straubhaar, J. (2010). The direct sampling method to perform multiple-point geostatistical simulations. *Water Resources Research 46*(11): 1-14

Menabde, M., Froyland, G., Stone, P., & Yeates, G. (2007). Mining schedule optimization for conditionally simulated orebodies. *Orebody modelling and strategic mine planning uncertainty and risk management international symposium Spectrum series AusIMM,* (1):379-384

Metropolis, A., Rosenbluth, A., Rosenbluth, M., Teller, A., & Teller, E. (1953). Equation of state calculations by fast computing machines. *The Journal of Chemical Physics, 21*(6): 1087-1092.

Montiel, L., & Dimitrakopoulos, R. (2013). An extended stochastic optimization method for multi-process mining complexes. Retrieved from Les Cahiers du GERAD website http://www.gerad.ca/fichiers/cahiers/G-2013-56.pdf.

Montiel, L., & Dimitrakopoulos, R. (2014). Optimizing mining complexes with multiple processing, and transportation alternatives: An uncertainty-based approach. *European Journal of Operational Research volume 1*, 240(1): 79-84

Montiel, L., & Dimitrakopoulos, R. (2015). Optimizing mining complexes with multiple processing, and transportation alternatives: An uncertainty-based approach. *European Journal of Operational Research Volume 1,* 247(1):166-178.

Mustapha, H., & Dimitrakopoulos, R. (2010). High-order stochastic simulations for complex non-Gaussian, and non-linear geological patterns, Mathematical Geosciences, 42(5):457-485.

Okabe, H., & Blunt, M. (2004). Prediction of permeability for porous reconstruction using multiple-point statistics. *Physical Review E, 70(1):*197-216.

Ramazan, S., & Dimitrakopoulos, R. (2007). Stochastic Integer Programming for Optimizing of long term production scheduling for open pit mines with a new integer programming formulation. *Orebody Modelling and Strategic Mine Planning Melbourne Spectrum Series volume 2, 14* (1):385-391.

Ramazan, S., & Dimitrakopoulos, R. (2013). Production scheduling with uncertain supply: A new solution to the open pit mining problem. *Optimization and Engineering, 14*(2): 361-380.

Ramazan, S., Dimitrakopoulos, R. (2004). Traditional and new MIP models for production scheduling with in-situ grade variability. *International Journal of Surface Mining, Reclamation and Environment*, 18(2):85-98).

Rendu, J. (2013). An Introduction to Cut-off Grade Estimation. *Society for Mining Metallurgy and Exploration 2 edition*.

Rezaee, H., Mariethoz, G., Koneshloo, M., & Asghari, O. (2013). Multiple-point geostatistical simulation using the bunch-pasting direct sampling method. *Computers Geosciences,* 54 (1) : 293-308.

Rimele, A. (2016). *Méthode heuristique d'optimization stochastique de la planification minière et positionnement des résidus miniers dans la fosse. Master Thesis, Universite de Montreal département de mathématiques et de génie industriel École Polytechnique de Montréal. Montreal, QC-Canada.*

Rondon, O. (2012). Teaching aid: minimum/maximum autocorrelation factors for joint simulation of attributes. *Mathematical Geosciences,* 44 (4):469-504.

Seymour, F., & Inc, E. (1994). Finding the mining sequence, and cut-off grade schedule that maximizes net present value. *Transactions-society for mining metallurgy and exploration incorporated, 298: 1880-1884.*

Smith, M., & Dimitrakopoulos, R. (1999). Influence of deposit modelling on mine production scheduling. *International Journal of Surface Mining Reclamation and Environment Volume, 13* (1): 173-178.

Spleit, M., & Perth, W. A. (2014). Production schedule optimization-meeting targets by geological risk while addressing environmental and Equipment concerns. *Orebody modelling and strategic mine planning symposium,* (1): 397-403

Strebelle, S. (2002). Conditional simulation of complex geological structures using multiple-point geostatistics. *Mathematical Geology, 34* (1): 1-22.

Strebelle, S., & Cavelius, C. (2014). Solving speed and memory issues in multiple-point statistics simulation program SNESIM. *Mathematical Geosciences*, 46(2): 171-186.

Switzer, P., Green, A. (1984). Min/Max autocorrelation factors for multivariate spatial imaging, *Technical Report No 6, department of statistics*, Stanford University.

Switzer, P., & Parker, H. (1975). The statistics of selective mining unit. *Technical report No 75*, *Department of statistics,* Stanford University.

Teixera, M. (2014). *Multiple-point Simulation of Olympic Dam Copper Deposit, Analysis. Master Thesis, Department of Mining and Materials McGill University, Montreal, QC-Canada.*

Western, A. W., Blöschl, G. (1998). Geostatistical characterisation of soil moisture patterns in the Tarrawarra catchment. *Journal of Hydrology*, 205(1): 20-37.

Whittle, J., & Rozman, L. (1991). Open pit design in the 90's. *Proceedings Mining Industry Optimization Conference*. Vancouver, BC- Canada.

Wu, J., Zhang, T., Journel, A., & Fast, F. (2008). Simulation with score-based distance. *Mathematical Geosciences*, *40*(7): 773-788.

Zhang, T. (2006). *Multiple-point and pattern simulation using filter scores: the FILTERSIM algorithm. PhD Thesis, Stanford University, California.*

Zhang, T., Switzer, P., & Journel, A. (2006). Filter-based classification of training image patterns for spatial simulation. *Mathematical Geology, 38*(1): 63-80.